

**Mononuclear and Dinuclear Complexes of  
Allylated  $\alpha$ -Diimines as Catalysts for the  
Polymerization of Ethylene**

**Dissertation**

zur Erlangung des akademischen Grades eines  
Doktors der Naturwissenschaften (Dr. rer. nat.)  
der Fakultät für Biologie, Chemie und Geowissenschaften  
der  
Universität Bayreuth

vorgelegt von  
**Haif Alshammari**  
aus Riad, Saudi Arabien

Bayreuth 2008

This thesis fulfills the requirements of the doctoral degree of the Faculty of Biology, Chemistry and Geological Sciences at the Universität of Bayreuth.

Vollständiger Abdruck der von der Fakultät für Chemie, Biologie und Geowissenschaften der Universität Bayreuth genehmigten Dissertation zur Erlangung des akademischen Grades eines Doktors der Naturwissenschaften (Dr. rer. nat.).

Thesis submitted: 11. November 2008

Date of Scientific Colloquium: 13. February 2009

Examination Committee:

Chairman: Prof. Dr. Peter Strohriegl

1. Referee: Prof. Dr. Helmut G. Alt

2. Referee: Prof. Dr. Jürgen Senker

Prof. Dr. Karlheinz Seifert

The following work was undertaken during the period January 2004 to May 2008 under the supervision of Prof. Dr. Helmut G. Alt at the Lehrstuhl für Anorganische Chemie II der Universität Bayreuth.

My sincere acknowledgement to my supervisor

**Herrn Professor Dr. Helmut G. Alt**

for his guidance, encouragement and enthusiastic support during the course of this research program.

I am grateful to Saudi Basic Industries Corporation (SABIC) for the financial support and the measurement of Gel permeation chromatography (GPC).

## **Acknowledgement**

I would like to thank Prof. Dr. Rhett Kempe and Germund Glatz for the X-ray diffraction measurement.

Special thanks are due to Awal Noor and Ezzat Khan for their help in the NMR measurement and the determination of the molecular structure of several new compounds.

I'm thankful to Dr. Christian Görl for reading and correcting the manuscript and to Julian Lang for his help in translating.

I'm greatly indebted to my past and present labmates: Dr. Christine Denner, Dr. Ingrid Böhmer, Dr. Alexandra Kestel-Jakob, Dr. Katharina Schneider, Dr. Silke Taubmann, Dr. Sandra Taubmann, Hamdi Elagab, Rimkus Andrea, Khalil Ahmad, Frank Lüdel, Matthias Dötterl, Tanja Englmann, and Mohamed Abdelbagi for providing a pleasant and fruitful working atmosphere.

I would like to thank Walter Kremnitz for his technical support in the laboratory work while the administrative help by Frau Marlies Schilling and Frau Fakhera Heinrich is highly appreciated.

I would like to express my cordial thanks to all members in AC II for their friendly and cooperative behavior.

I'm very grateful to Dr. Markus Seitz and his wife, Steffi for the enjoyable time I spent with them at their house when I was newcomer in Bayreuth.

At last I would like to express my deepest sense of gratitude to my family members in Saudi Arabia for their constant moral support during the course of my studying here in Germany.

**To**

*My parents*

**&**

*My wife*

## Abbreviations

[1-3,4,6]	Reference number
$\alpha$ -	alpha-
Å	Angström
ax	axial
$\beta$ -	beta-
n-Bu	normal-Butyl
°C	Degree Celsius
Cat.	Catalyst
CDCl <sub>3</sub>	Deuterated chloroform
CD <sub>2</sub> Cl <sub>2</sub>	Deuterated methylene chloride
Cp	Cyclopentadienyl
$\delta$	chemical shift in ppm
Et	Ethyl
Eq	Equatorial
$\nu$	frequency
g	gram
GC	Gas Chromatography
GPC	Gel Permeation Chromatography
h	hour
Hz	Hertz
i-Pr	iso-Propyl
Kg	kilogram
M	Metal
M <sup>+</sup>	Metal ion
M <sup>•+</sup>	Molecular ion
MAO	Methylaluminoxane
Me	Methyl
mg	milligram
min	minute
ml	milliliter
mol	mole

mmol	millimole
m/e	mass/elemental electric charge
Mn	number average molar mass
Mw	weight average molar mass
Mw/Mn(PD)	polydispersity
MS	Mass Spectroscopy
μl	microliter
n	number of atoms
NMR	Nuclear Magnetic Resonance
PE	Polyethylene
Ph	Phenyl
PP	Polypropylene
ppm	parts per million
r.t.	room temperature
s	second
THF	Tetrahydrofuran
TMA	Trimethylaluminum
X	Halide
λ	wave length

# Contents

<b>1</b>	<b>Introduction</b>	<b>1</b>
1.1	General	1
1.2	Aim of the work	11
<b>2</b>	<b>General Part</b>	<b>12</b>
2.1	$\alpha$ -Diimine compounds bearing allyl groups and their complexes	12
2.1.1	General	12
2.1.2	Synthesis and characterization of ligands	13
2.1.2.1	Synthesis and characterization of compounds 1-3	13
2.1.2.2	Synthesis and characterization of compounds 4-6	16
2.1.2.3	Synthesis and characterization of compound 7	20
2.1.3	Synthesis and characterization of the complexes	23
2.1.3.1	Synthesis and characterization of the complexes 4a-g, 5a-g, and 6a-g	23
2.1.3.2	Synthesis and characterization of complex 8	28
2.1.4	Polymerization experiments	31
2.1.4.1	General	31
2.1.4.2	Polymerization experiments with the complexes 4a-g, 5a-g, and 6a-g	33
2.1.4.2.1	Polymerization results of the complexes 4a-g	33
2.1.4.2.2	Polymerization results of the complexes 5a-g	35
2.1.4.2.3	Polymerization results of the complexes 6a-g	37
2.1.4.2.4	Comparison between the polymerization results of 4a-g, 5a-g, and 6a-g	38
2.1.4.3	Polymerization experiments with the complex 8	40
2.2.	Dinuclear complexes of $\alpha$ -diimines coupled with an ansa zirconocene unit	45
2.2.1	General	45
2.2.1.1	Preview of dinuclear complexes	45
2.2.1.2	Preview of hydrosilylation reaction	46
2.2.2	Synthesis and characterization of complex 9C	48
2.2.3	Synthesis and characterization of complexes 10-14	51
2.2.4	Polymerization experiments with the dinuclear complexes 10-14 and complex 9C	55

2.3.	Dinuclear complexes of $\alpha$ -diimines coupled with half sandwich complexes	61
2.3.1	General	61
2.3.2	Synthesis and characterization of the "free ligands"	62
2.3.2.1	Synthesis and characterization of compounds 15-17	62
2.3.2.2	Synthesis and characterization of compounds 18-20	66
2.3.3	Synthesis and characterization of dinuclear complexes	70
2.3.4	Polymerization experiments with the dinuclear precursors 18a,b; 19a,b; and 20a,b	73
<b>3</b>	<b>Experimental Part</b>	<b>79</b>
3.1	General	79
3.2	Measurement methods	79
3.2.1	NMR spectroscopy	79
3.2.2	Mass spectrometry	79
3.2.3	GC/MS	80
3.2.4	Gel permeation chromatography (GPC)	80
3.2.5	Elemental analysis	80
3.2.6	Crystal structure analysis	80
3.3	Synthesis procedures	81
3.3.1	General synthesis of the $\alpha$ -diimine compounds 1-3 and 7	81
3.3.2	General synthesis of the $\alpha$ -diimine compounds bearing allyl groups (4-6)	81
3.3.3	General synthesis of the complexes of $\alpha$ -diimines bearing allyl groups (4a-g, 5a-g, 6a-g and 8)	82
3.3.4	Synthesis of bis(cyclopentadienyl)methyl silane (9L)	82
3.3.5	Synthesis of the complex (C <sub>5</sub> H <sub>4</sub> -SiHMe-C <sub>5</sub> H <sub>4</sub> )ZrCl <sub>2</sub> (9C)	83
3.3.6	General synthesis procedure for the dinuclear precursors 10-14 via hydrosilylation reactions	83
3.3.7	General synthesis procedure for the $\alpha$ -diimine compounds bearing chloropropyl groups (15-17)	83
3.3.8	General synthesis of the $\alpha$ -diimine compounds bearing cyclopentadienyl groups (18-20)	84
3.3.9	General synthesis of the dinuclear precursors (18 <sub>a,b</sub> , 19 <sub>a,b</sub> , and 20 <sub>a,b</sub> )	84
3.4	Polymerization of ethylene in the 1 l Büchi autoclave	84

<b>4</b>	<b>Summary</b>	<b>86</b>
<b>5</b>	<b>Zusammenfassung</b>	<b>90</b>
<b>6</b>	<b>References</b>	<b>94</b>
<b>7</b>	<b>Appendices</b>	<b>101</b>
	Appendix A Mass spectra	101
	Appendix B: NMR spectra	113
	Appendix C: Elemental analysis	118
	Appendix D: Crystal structure analysis	125

# 1. Introduction

## *1.1 General*

The field of synthetic polymers or plastics is currently one of the fastest growing material's industries. The interest in plastics is driven by their manufacturability, recyclability, mechanical properties, and lower costs as compared to many alloys and ceramics. Also the macromolecular structure of plastics provides good biocompatibility and allows them to perform many biomimetic tasks that cannot be performed by other synthetic materials.

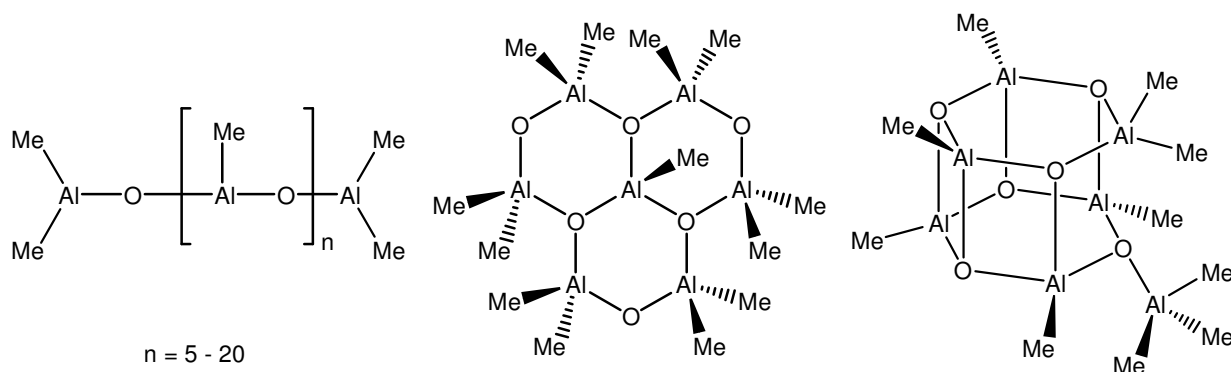
Prior to the early 1920's, chemists doubted the existence of molecules having molecular weights greater than a few thousand. This limiting view was challenged by Hermann Staudinger,<sup>[1-4]</sup> a German chemist who proposed that polymers consisted of long chains of atoms held together by covalent bonds. He formulated a polymeric structure for rubber, based on a repeating isoprene unit. For his contributions to chemistry, Staudinger received the Nobel Prize in 1953.<sup>[5]</sup>

Nowadays, the world's most widely used polymers are polyolefins (POs). Polyolefins are a group of plastics that are polymers of various alkenes or olefins. They include large-volume materials such as polyethylene (PE), polypropylene (PP), and specialty materials. Polyethylene is probably the polymer you see most in daily life and the most popular plastic in the world. It was first synthesized by the German chemist Pechmann<sup>[6]</sup> and characterized by his colleagues Bamberger and Tschirner<sup>[7]</sup> while the first industrially practical polyethylene synthesis was described in 1933 at the British company Imperial Chemical Industrial (ICI). The first commercial process to produce polyethylene (low density polyethylene, LDPE) was via radical polymerization using high pressure.<sup>[8]</sup> The next attempts in the synthesis of polyethylene were toward developing several types of catalysts that promote ethylene polymerization at milder temperature and pressure conditions. The first of these catalysts consisted of a chromium oxide catalyst supported on silica gel (the so-called "Phillips-catalyst"). By discovering that catalyst, Hogan and Banks<sup>[9]</sup> achieved the commercial production of polyethylene at low pressure. Even today, 40% of the worldwide polyethylene production uses this catalyst<sup>[10]</sup> because it is less expensive and easy to work with. Subsequent development was done in 1953 by Karl Ziegler and his workgroup who

discovered a catalytic system based on titanium halides and organoaluminum compounds that worked at even milder conditions than the Phillips catalyst to produce high density polyethylene (HDPE).<sup>[11,12]</sup> One year later, Giulio Natta used similar catalysts to polymerize propylene<sup>[13]</sup> since he thought polypropylene (PP) would be cheaper than polyethylene. In 1963, Ziegler and Natta was awarded the Nobel Prize in Chemistry<sup>[14,15]</sup> for the work on high molecular weight polymers and the development of the so-called “Ziegler-Natta catalyst”.

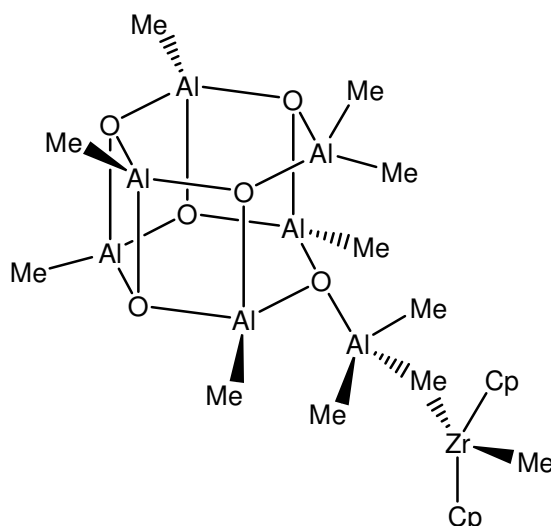
Up to now, the structure and function of polymerization active centers of Ziegler-Natta catalysts are not completely elucidated and understood. It is assumed that different catalyst species produce polymers with various molecular weight distributions. Polymers with defined structures became available with the discovery by Breslow and Newburg,<sup>[16]</sup> and Natta.<sup>[17]</sup> metallocene (titanocene) complexes in combination with aluminum alkyl halides can be used as homogeneous catalyst systems to polymerize ethylene. However, industrial application was not worthwhile due to low activity.

The discovery of methylaluminoxane (MAO) as cocatalyst by Sinn and Kaminsky<sup>[18,19]</sup> in 1980 marked the most significant breakthrough in the field of metallocene catalysis. The activity of the metallocene dichloride complexes of titanium, zirconium and hafnium could be increased by orders of magnitude through the use of this new cocatalyst. MAO is mainly obtained by controlled hydrolysis of trimethylaluminum (TMA). Despite the difficulty of assigning the structure of MAO due to the presence of multiple equilibria between different  $(AlOMe)_n$  oligomers coupled with the interaction between MAO and TMA, there were various structures that have been proposed to match the behaviour of MAO as a Lewis acid.<sup>[20-25]</sup> The structure of MAO could be linear (chains), cyclic, or cage like (with six or twelve monomeric MAO units).



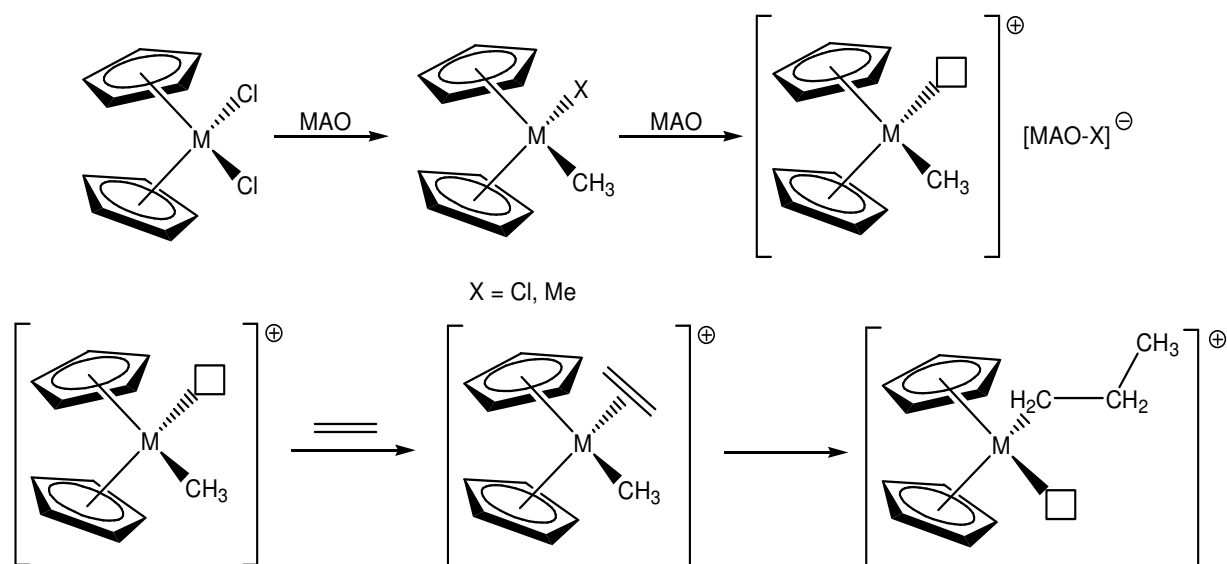
**Scheme 1. Proposed structures of MAO: linear (left), cyclic (middle), and cage (right).**

Experimental<sup>[26]</sup> and theoretical<sup>[27,28]</sup> studies have been performed to determine the structure of the dormant and active species in MAO-activated polymerization. The proposed structure by these studies is shown in Scheme 2.



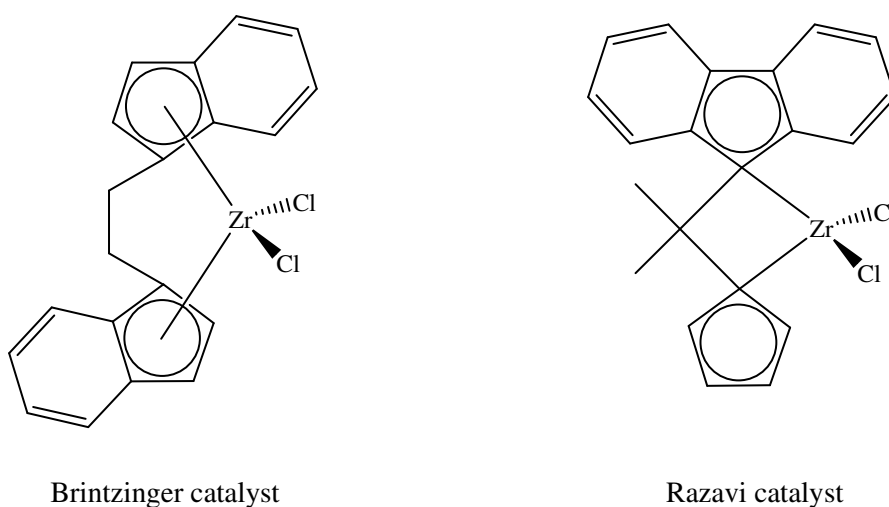
**Scheme 2. The structure predicted to form from the interaction of MAO with the metallocene complex  $\text{Cp}_2\text{ZrMe}_2$ .**

The most widely accepted mechanism for olefin polymerization on Ziegler-Natta and metallocene catalysts is the Cossee-Arlman<sup>[29-31]</sup> mechanism (see scheme 3). It is assumed that when MAO is used to activate a metallocene complex, the first step is to replace the chloride atoms on the metallocene dichloride with two methyl groups from the TMA molecules which locate into the cage of MAO, and the next step is the abstraction of one methyl group from the metallocene to form the metallocene cation and the counterion  $[\text{MAO-X}]^-$ . The metallocene cation has a vacant site on the metal atom (M). An olefin can coordinate to that vacant site followed by the insertion of the olefin into the metal methyl bond (M- $\text{CH}_3$ ) and the reformation of the vacant site on the metal atom. This mechanism shows that metallocene catalyst has only one active site where the starting monomers are linked to produce largely identical polymer chains in orderly fashion with narrow molecular weight distribution (MWD), therefore metallocene catalysts are called single-site catalysts (SSC).



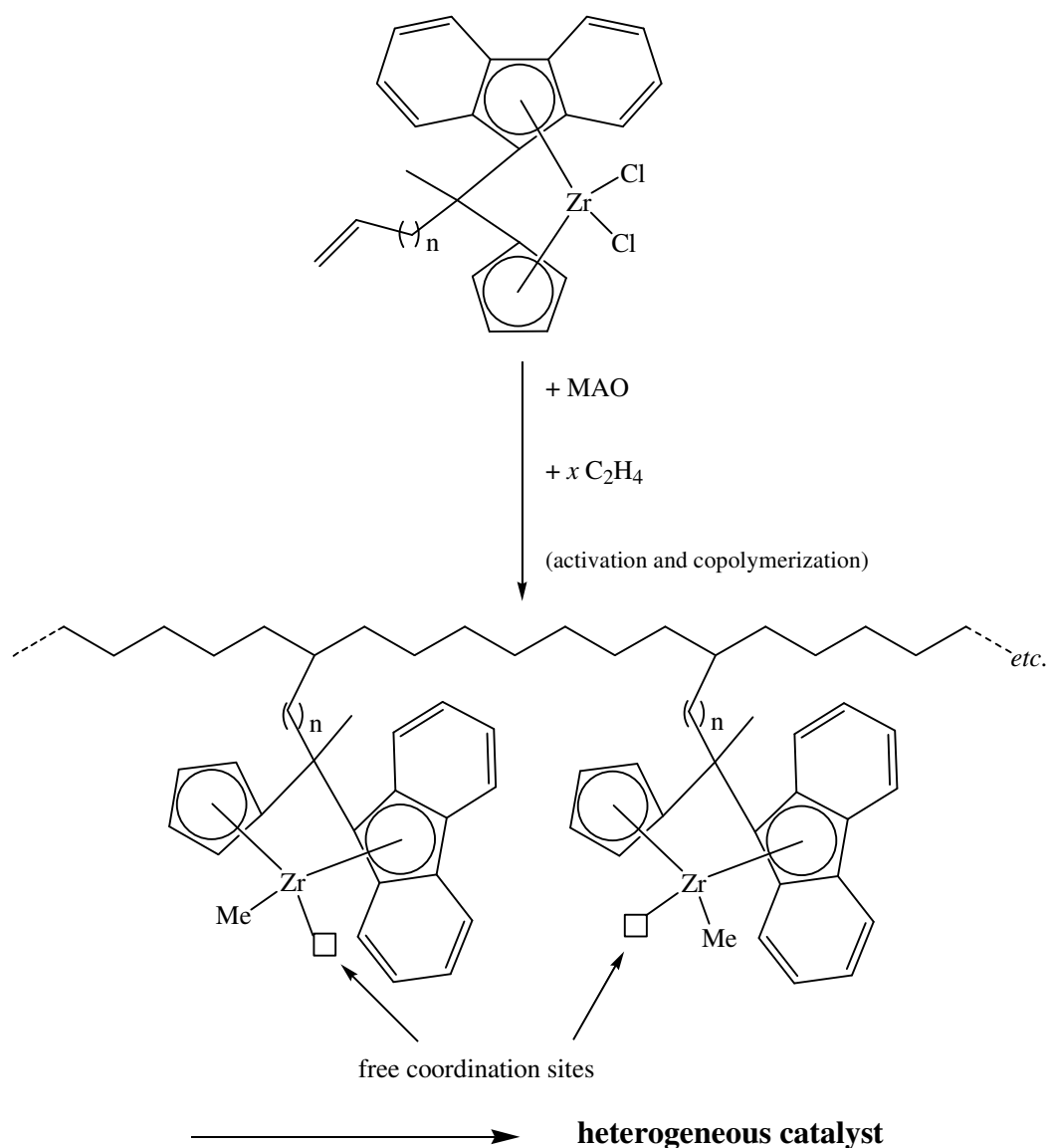
**Scheme 3. Cossee-Arlman mechanism: activation of a metallocene complex by MAO (top) and insertion of ethylene (bottom).**

In 1985, Brintzinger demonstrated that metallocenes are eminently suited as catalysts for stereospecific polypropylene synthesis. He synthesized isotactic polypropylenes using a chiral ethylene-bridged zirconocene derivative containing tetrahydroindenyl ligands.<sup>[32,33]</sup> Three years later, Razavi synthesized syndiotactic polypropylenes using isopropylidene-bridged zirconocene derivatives containing cyclopentadienyl-1-fluorenyl ligands.<sup>[34]</sup>



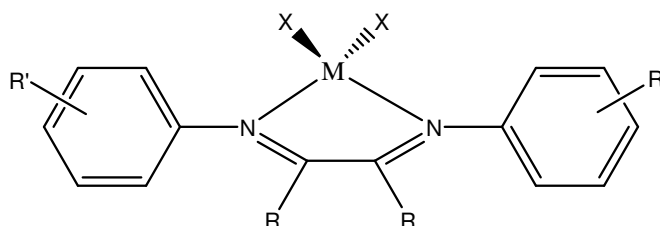
**Scheme 4. Catalysts for stereospecific polypropylene synthesis.**

One reason for the high activity of metallocene complexes is their homogeneous nature where every single molecule has the potential to act as catalyst.<sup>[35]</sup> Nevertheless, the homogeneous nature of these complexes causes reactor fouling: the formed polyolefin is deposited at the reactor walls, the stirring device, and the thermocouple and inhibits the reaction control. That makes a continuous polymerization process not possible. The solution to prevent reactor fouling is the heterogenization of metallocene catalysts. In 1998, Peifer and Alt<sup>[36]</sup> developed a heterogenization method called “self-immobilization”. It means to synthesize metallocene catalysts with an olefin or alkyne function that can be used as a comonomer in the polymerization process. The following complexes are typical examples for this approach.



**Scheme 5. Proposed mechanism for the “self-immobilization” of a homogeneous ansa-metallocene complex.**<sup>[36]</sup>

The drawback of metallocene catalysts is that they are unable to polymerize polar molecules, such as common acrylics or vinyl chloride. This is due to the high oxophilicity of the early transition metals, their propensity for binding to oxygen. Introduction of a polar monomer into a reaction system will bring the catalyst activity to almost zero. As a consequence, polymer chemists have started searching for new types of single site catalysts. A lot of research is now being directed at other types of catalysts that can produce polyolefins with the desired properties. Currently, work has progressed using metals from all over the Periodic Table but one area in particular is proving advantageous: late transition metal compounds. These compounds have good polymerization activities, although slightly less than metallocenes. However, crucially they can polymerize reactions with polar monomers. In 1995, Brookhart<sup>[37,38]</sup> developed the first class of post-metallocene catalysts. They were based upon palladium or nickel complexes bearing bulky, neutral,  $\alpha$ -diimine ligands. These complexes can be tuned to produce a variety of structures that range from high density polyethylene through hydrocarbon plastomers and elastomers by reducing the bulk of the  $\alpha$ -diimine used.



R = Alkyl, Aryl

R' = Alkyl, Halogen

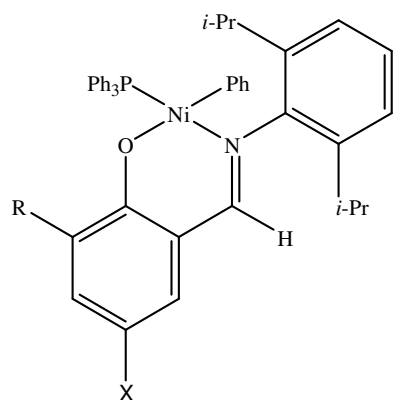
M = Ni, Pd

X = Cl, Br

### Scheme 6. General structure of $\alpha$ -diimine complexes discovered by Brookhart.

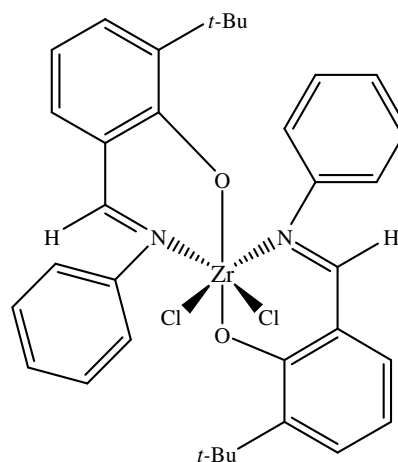
The second class of post-metallocene catalysts was discovered by Grubbs.<sup>[39]</sup> Several neutral nickel complexes with phenoxy-imine ligands were synthesized. They are active catalysts for the polymerization of ethylene under mild conditions in the presence of a phosphine scavenger. These catalysts can be tuned by varying the substituents on the phenoxy-imine ligands to enhance the polymerization activity.<sup>[40]</sup> Fujita et al.<sup>[41-43]</sup> used a similar ligand system to prepare a new family of zirconium complexes with two phenoxy-imine ligands.

These complexes showed a very high activity for ethylene polymerization and the catalysts are named FI catalysts.



R = H, *t*-Bu, Ph, 9-phenanthrenyl, 9-anthracenyl  
X = H, OMe, NO<sub>2</sub>

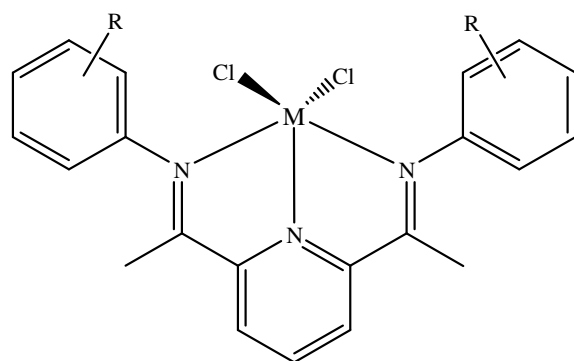
"Grubbs catalyst"



"Fujita catalyst"

### Scheme 7. Structures of some phenoxy-imine complexes.

In 1998, Gibson<sup>[44-47]</sup> and Brookhart<sup>[48-50]</sup> independently reported a new family of olefin polymerization and oligomerization catalysts, derived from iron and cobalt complexes bearing 2,6-bis(imino)pyridyl ligands.



R = Alkyl, Halogen

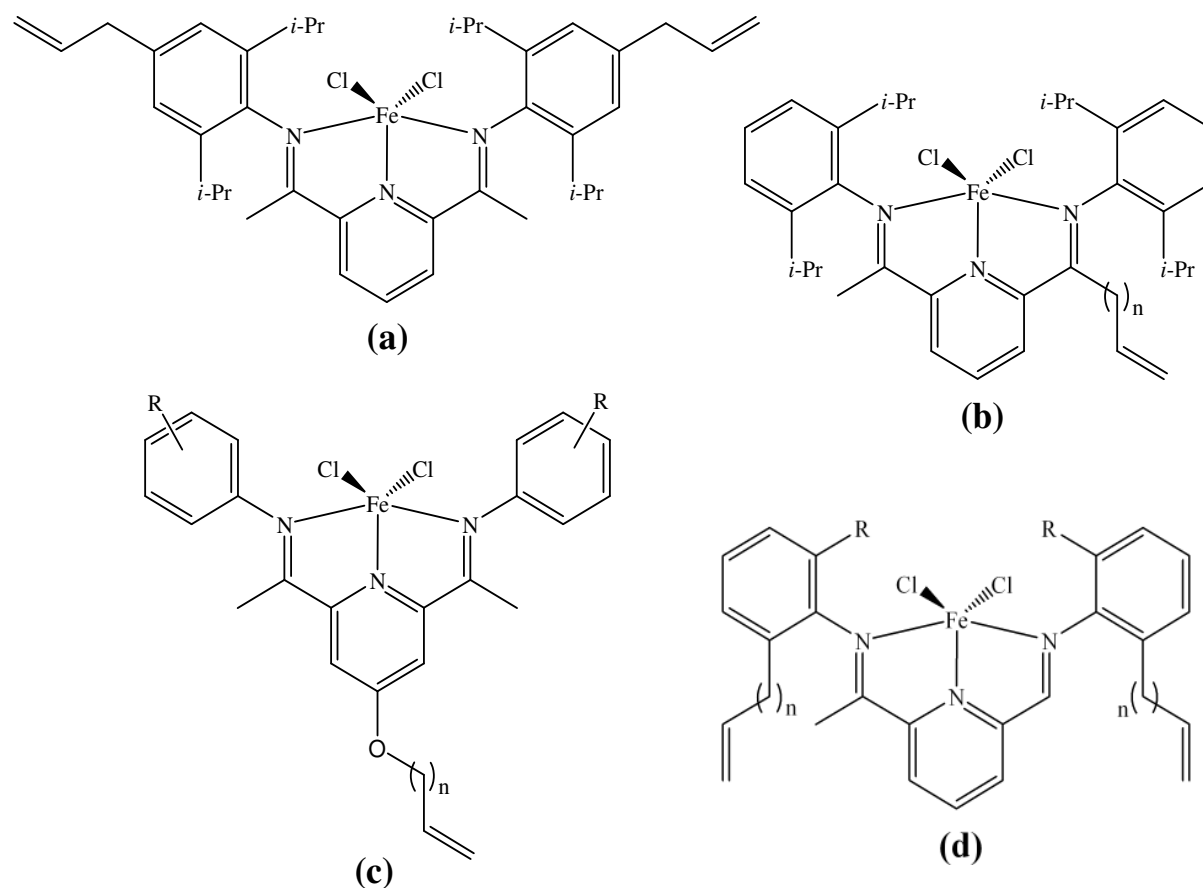
M = Fe, Co

X = Cl, Br

### Scheme 8. General structures of bis(imino)pyridine complexes for the polymerization and oligomerization of olefins.

The polyethylene produced by these catalysts is highly linear HDPE. Later studies found that substituents on the aniline part of the ligand backbone show the strongest influence on the catalytic behaviour.<sup>[51]</sup> For instance, by changing the pattern of substitution from 2-alkyl to 2,6-dialkyl, the catalysts no longer produce oligomers with 2–40 carbon atoms but high molecular weight polyethylenes.<sup>[52,53]</sup>

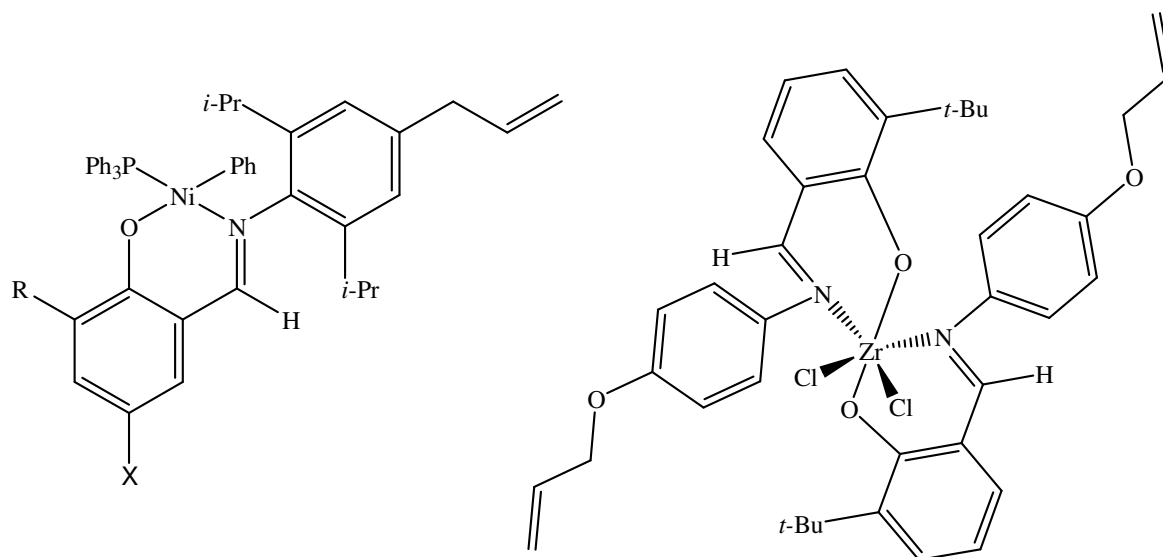
Similar to metallocene catalysts, the good activities of all late and early transition metal catalysts that were synthesized using  $\alpha$ -diimine, phenoxy-imine, or bis(imino)pyridine ligands arise from their homogeneous nature. Thus, the polymerization process cannot be continuous due to reactor fouling. The solution to avoid the reactor fouling is to heterogenize these catalysts. Self-immobilization is a very elegant method to heterogenize these catalysts and prevent reactor fouling. A first work to transfer this method to bis(imino)pyridine complexes was reported by Herrmann and co-workers<sup>[54]</sup> in 2002, who used  $\omega$ -alkenyl substituents at the imino carbon atom.



**Scheme 9.** Iron complexes of bis(imino)pyridine bearing  $\omega$ -alkenyl functions were reported by (a) Jin et al., (b) Herrmann, (c) Seitz and Alt, (d) Görl and Alt.

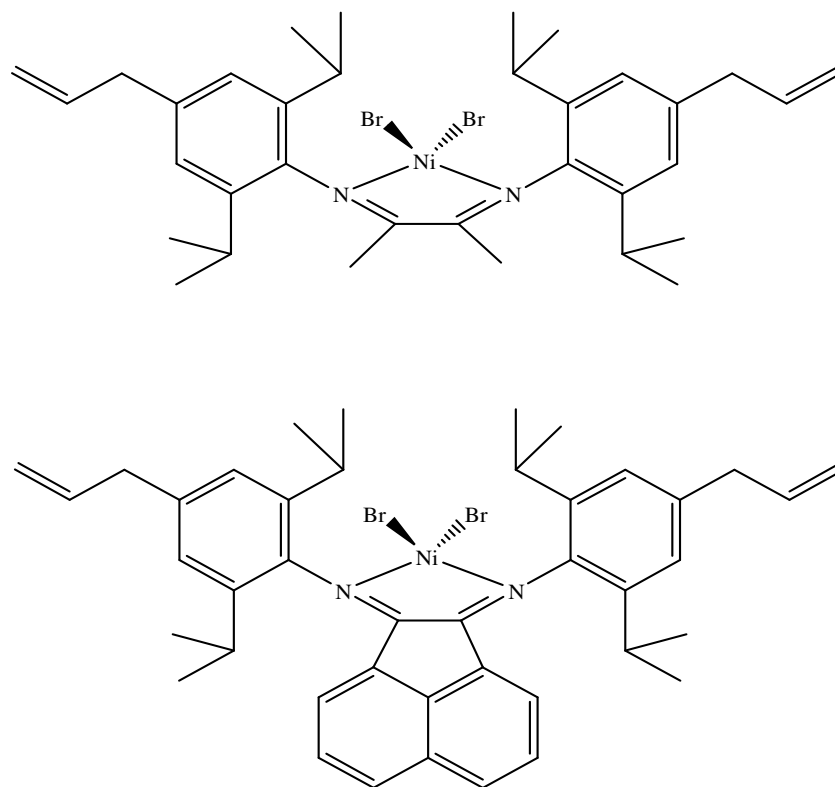
In the same year, Jin et al.<sup>[55]</sup> reported similar complexes bearing allyl functions at the para positions of anilines. Seitz and Alt<sup>[56]</sup> in 2006 reported some iron (II) complexes of bis(imino)pyridine ligands bearing alkenyloxy substituents in position 4 of the pyridine rings. One year later, Görl and Alt<sup>[57]</sup> reported a series of self-immobilized iron catalysts of bis(imino)pyridine ligands bearing  $\omega$ -alkenyl functions in position 2 of the aniline rings.

Jin et al.<sup>[58-60]</sup> heterogenized some catalysts with phenoxy-imine ligands via the self-immobilization method. The ligand frameworks of these phenoxy-imine catalysts possess allyl or allyloxy functions at the arene moieties of the ligands structures (see the examples in Scheme 10).



**Scheme 10. Complexes containing phenoxy-imine ligands bearing allyl or allyloxy functions reported by Jin et al.<sup>[58-60]</sup>**

Only few complexes with  $\alpha$ -diimine ligands bearing  $\omega$ -alkenyl functions were reported comparing to bis(imino)pyridine or phenoxy-imine complexes. Jin et al.<sup>[61,62]</sup> reported self-immobilized nickel catalysts of  $\alpha$ -diimine ligands bearing one or two allyl groups. These self-immobilized nickel catalysts not only kept the good activities of their analogous homogeneous catalysts but also improved the particle morphology of the produced polyethylene.<sup>[61]</sup>



**Scheme 11. Some nickel complexes with  $\alpha$ -diimine ligands bearing allyl groups.**

The use of single site catalysts for olefin polymerization has the disadvantage of producing narrow molecular weight distributions (MWD). It is due to identical active sites of the catalyst. This can cause problems for industrial processings like extrusion or injection moulding. The solution is to develop a new class of catalysts which are able to produce polyolefins with broader MWDs.

## *1.2 Aim of the work*

Polyolefins having a bi- or multi-modal or at least a broad MWD can be obtained from a variety of methods including mechanical blending, multi-stage reactors, mixed catalysts, and asymmetric dinuclear catalysts. The last method is the most desirable one in terms of capital expense and product properties. The dinuclear catalysts have the ability to produce the broad or multi-modal resin in a single reactor. This process will help to avoid the need for an additional reactor and controls.

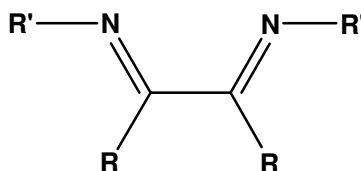
The goals of my work are to synthesize dinuclear catalysts that provide two different active sites for the oligomerization and polymerization of  $\alpha$ -olefins, especially ethylene. The precursors will contain a diimine moiety coordinated to late or early transition metals and a metallocene or half sandwich moiety. In order to achieve these goals, the plan is to functionalize an  $\alpha$ -diimine with allyl or alkyl halide groups and then couple this modified  $\alpha$ -diimine compound with a metallocene or a half sandwich complex.

## 2. General Part

### 2.1. $\alpha$ -Diimine compounds bearing allyl groups and their complexes

#### 2.1.1 General

Diimines or diketimines can be prepared by condensation reactions of two equivalents of amines or anilines with one equivalent of a diketone. 1,2-Diimines ( $\alpha$ -diimines) are important candidates in coordination chemistry and catalysis because they are well-known to stabilize organometallic complexes.<sup>[63-65]</sup>



**R , R' = alkyl or aryl**

#### Scheme 12. General structure of $\alpha$ -diimine compounds.

The use of  $\alpha$ -diimines as ligands in transition metal complexes has received a great deal of attention since 1995 when Brookhart and co-workers<sup>[37,38]</sup> discovered  $\alpha$ -diimine complexes of nickel(II) and palladium(II) as catalysts for the polymerization and oligomerization of olefins.<sup>[66-73]</sup> Several complexes were prepared later using various metal salts with  $\alpha$ -diimine ligands.<sup>[74-82]</sup> Among them, nickel catalysts attained special interest because of their tunable olefin polymerization activity and polymer microstructure by simple modification of the ligand architecture and the ability of producing polyethylene with branched structures without the use of  $\alpha$ -olefin comonomers.<sup>[72]</sup> Substituents on the arene moiety and/or the backbone of the ligand influence the active site of the catalyst during the polymerization reaction.<sup>[83-97]</sup> For instance, when the catalyst has bulky substituents at the ortho-positions of the arene moieties, the catalyst will produce high molecular weight polymer because the axial bulk provided by the ortho-substituents hinders the chain transfer and causes slow chain transfer relative to chain propagation.<sup>[87-97]</sup> When the steric bulk is eliminated, the rate of

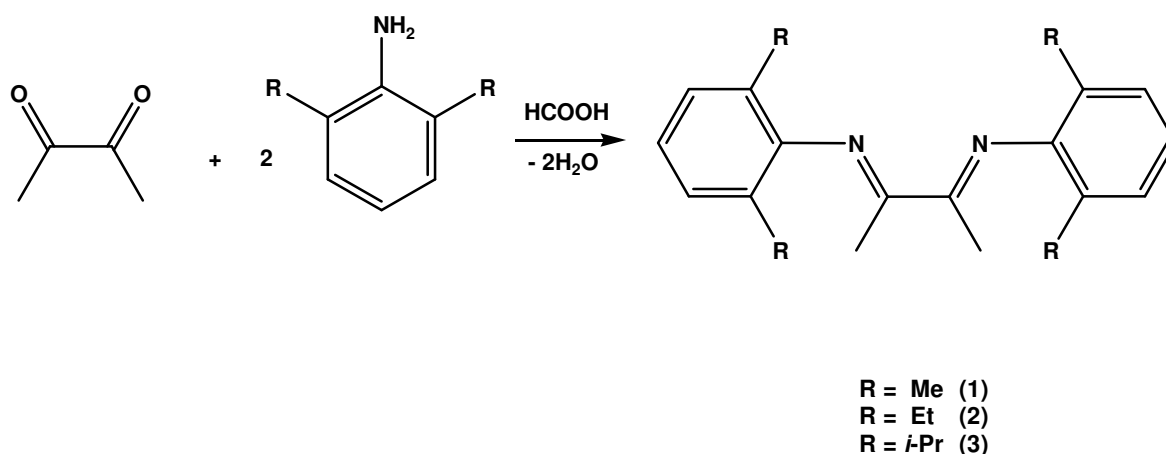
chain transfer will be increased and the catalyst will produce oligomer rather than polymer.<sup>[83-86]</sup> The productivities and the type of the produced polymers of the same nickel catalysts bearing bulky  $\alpha$ -diimine ligands depend not only on the ligand environment at the nickel centre but also on the type of co-catalyst,<sup>[98-99]</sup> the monomer pressure,<sup>[100-102]</sup> and the polymerization temperature.<sup>[101,102]</sup>

Despite the many advantages of  $\alpha$ -diimine nickel catalysts, the homogeneous nature of these catalysts can cause difficulties in controlling the polymer particle morphology and severe reactor fouling when they are used in slurry or gas-phase polymerization processes. To overcome these drawbacks, several works were carried out to heterogenize these catalysts via fixing them on different types of inorganic supports, such as silica,<sup>[103-107]</sup> or polymeric supports.<sup>[62,107]</sup> Although, self-immobilization is a very elegant method to heterogenize such catalysts, only few  $\alpha$ -diimine nickel complexes bearing  $\omega$ -alkenyl functions were prepared and heterogenized via the self-immobilization method.<sup>[61,62,107]</sup>

## 2.1.2 Synthesis and characterization of ligands

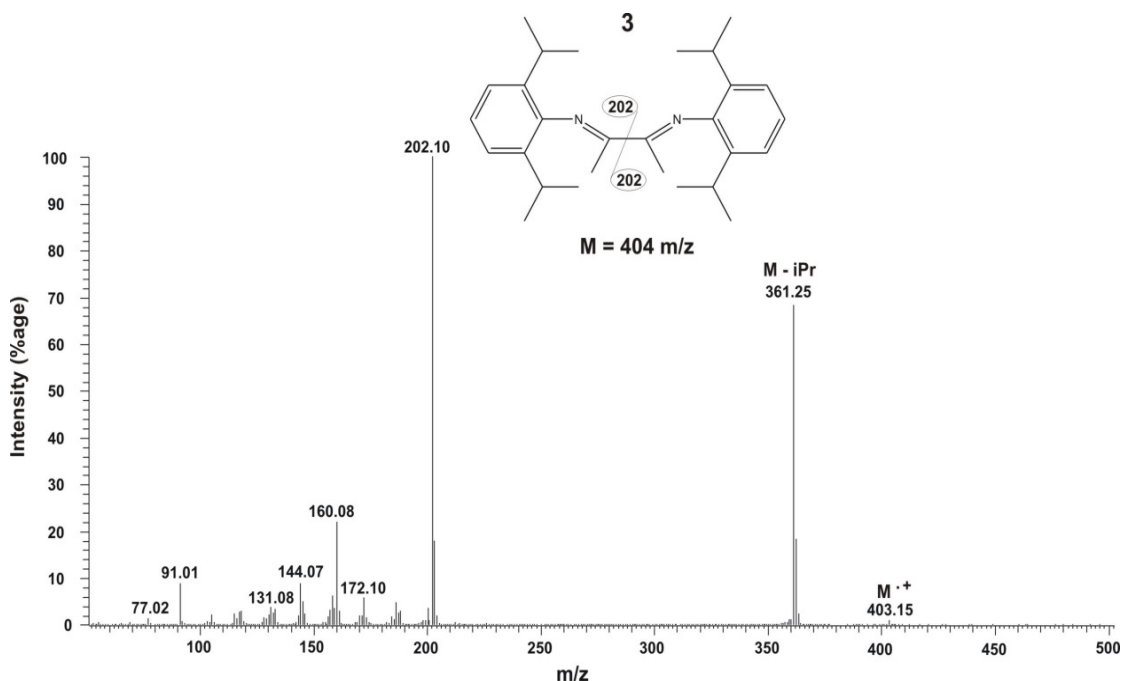
### 2.1.2.1 Synthesis and characterization of compounds 1-3

The  $\alpha$ -diimine compounds,  $\text{ArN}=\text{C}(\text{Me})-\text{C}(\text{Me})=\text{NAr}$  {where Ar = 2,6-dimethylphenyl (**1**); 2,6-diethylphenyl (**2**); or 2,6-diisopropylphenyl (**3**)} were synthesized by condensation reactions of two equivalents of substituted aniline derivatives with one equivalent of diacetyl (2,3-butadione) in the presence of formic acid (HCOOH) as catalyst.



**Scheme 13. The synthesis of  $\alpha$ -diimine compounds.**

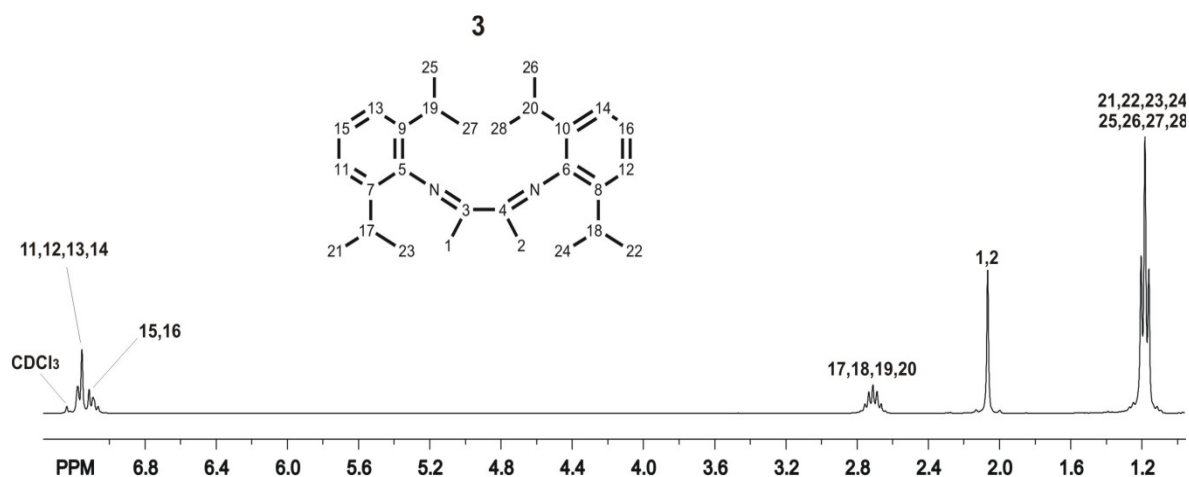
The compounds **1** - **3** were characterized via GC-MS,  $^1\text{H}$  NMR, and  $^{13}\text{C}$  NMR spectroscopy (see the appendices for the full analysis data). The mass and NMR spectra of compound **3** will be discussed as an example.



#### Scheme 14. Mass spectrum of the $\alpha$ -diimine compound **3**.

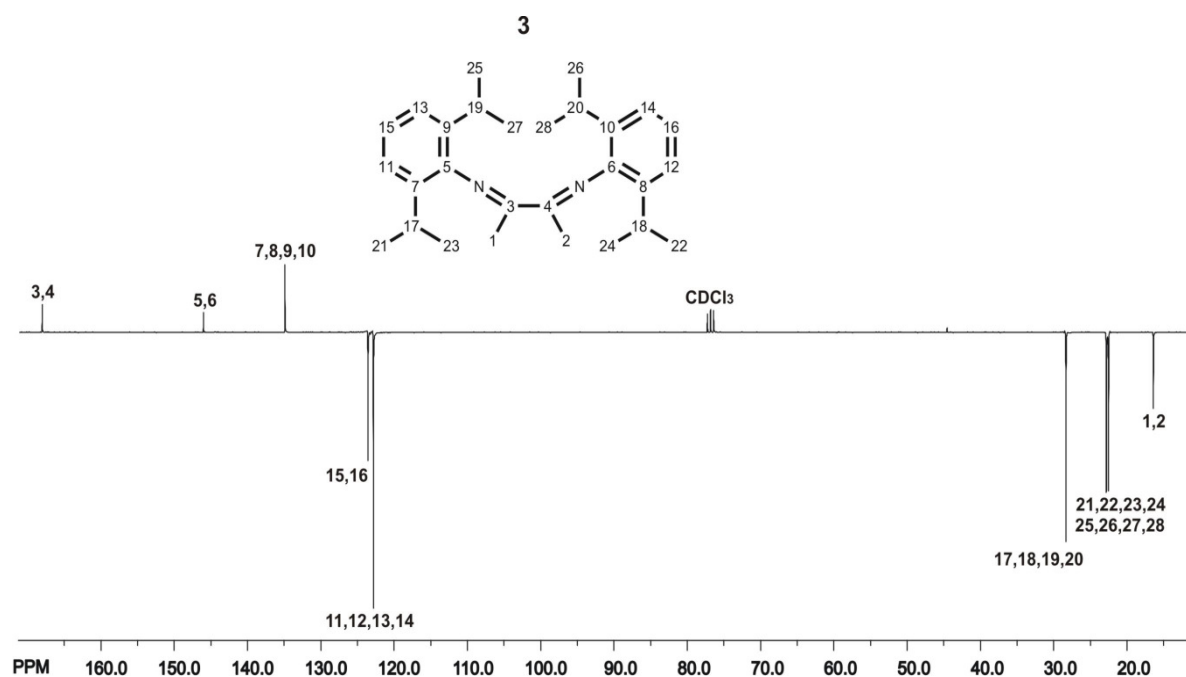
The mass spectrum of compound **3** (see Scheme 14) was obtained at the retention time of 804s. The molecular ion appears at  $m/z = 403$  with very weak intensity of 0.8% relative to the base peak. The loss of an isopropyl fragment leads to the peak at  $m/z = 361$ , while the base peak at  $m/z = 202$  can be explained with the fragmentation of the diimine compound to two identical imine molecules.

The  $^1\text{H}$  NMR spectrum of compound **3** (see Scheme 15) shows a signal at  $\delta = 7.20$  ppm which is assigned to the protons of the aromatic CH groups (11,12,13,14) while the signal at  $\delta = 7.13$  ppm arises from the protons of the aromatic CH groups (15,16). The protons belonging to the CH groups of the isopropyl functions give the septet signal at  $\delta = 2.75$  ppm. The singlet appearing at  $\delta = 2.10$  ppm is assigned to the protons of the methyl groups at the backbone of the compound structure while the protons of the methyl groups belonging to the isopropyl functions produce two doublet signals at  $\delta = 1.22$  and 1.18 ppm which overlapped to form a pseudo triplet signal.



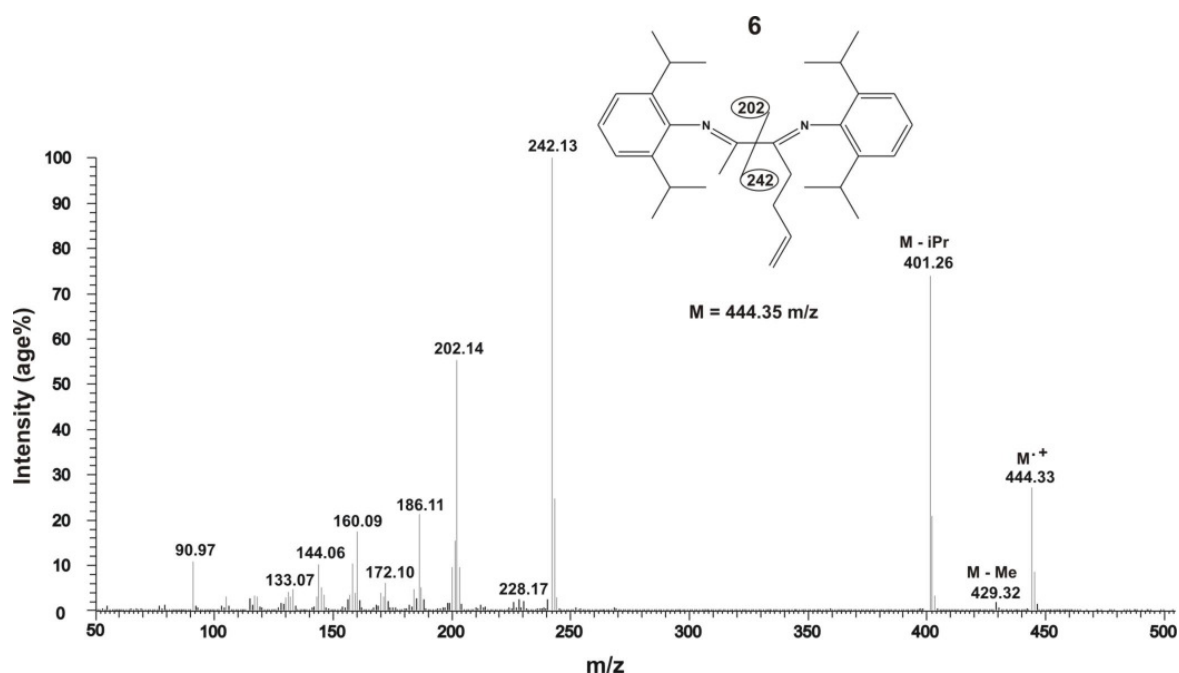
Scheme 15.  $^1\text{H}$  NMR spectrum of the  $\alpha$ -diimine compound **3**.

The  $^{13}\text{C}$  NMR spectrum of compound **3** (see Scheme 16) shows the signal of the imine carbon atoms at  $\delta = 168.0$  ppm. The signals belonging to the quaternary carbon atoms of the aromatic ring systems appear at  $\delta = 146.0$  and  $135.0$  ppm, while the signals at  $\delta = 123.8$  and  $123.0$  ppm can be assigned to the aromatic CH groups. The carbon atoms of the CH groups of the isopropyl functions give the signal at  $\delta = 28.5$  ppm while the signal at  $\delta = 22.8$  ppm is generated by the methyl groups of the isopropyl functions. The signal of the methyl groups at the backbone of the compound structure appears at  $\delta = 16.8$  ppm.



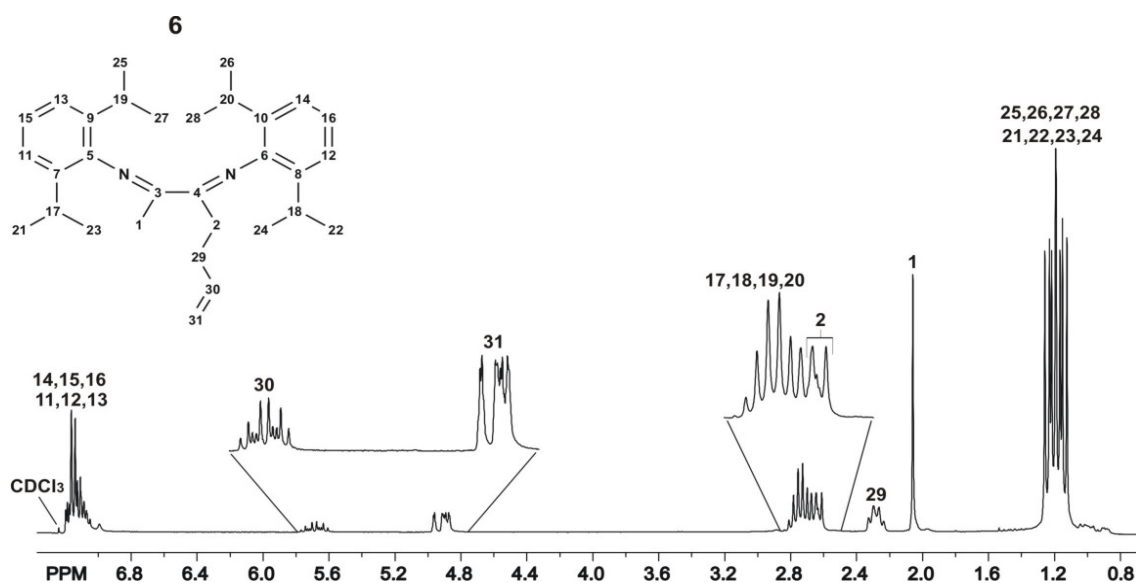
Scheme 16.  $^{13}\text{C}$  NMR spectrum of the  $\alpha$ -diimine compound **3**.





Scheme 18. Mass spectrum of the  $\alpha$ -diimine compound **6**.

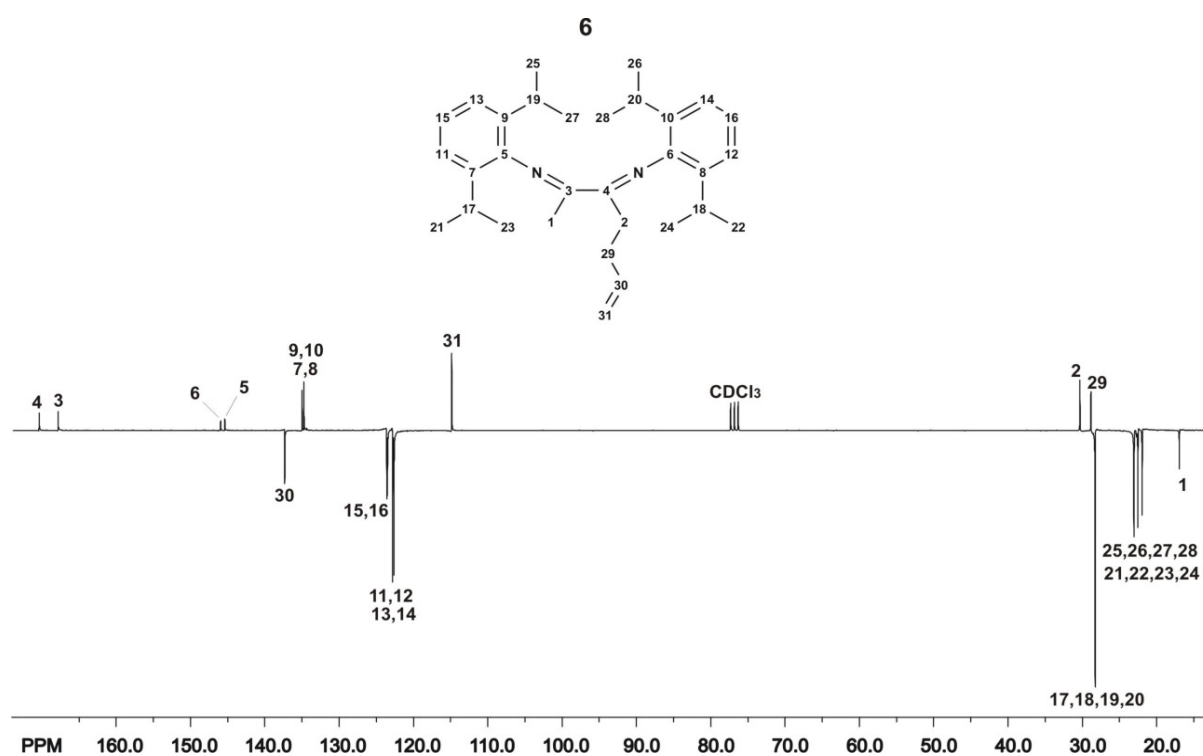
The  $^1\text{H}$  NMR spectrum of compound **6** (see Scheme 19) shows the overlapped signals at  $\delta = 7.16$  ppm which are assigned to the protons of the aromatic CH groups while the CH group of the allyl function produces the multiplet signal at  $\delta = 5.70$  ppm. The terminal methylene group of the allyl function give the proton NMR signal at  $\delta = 4.95$  ppm. The signal at  $\delta = 2.75$  ppm is assigned to the CH groups of the isopropyl functions which overlap with the signal of the methylene group (2) at  $\delta = 2.65$  ppm.



Scheme 19.  $^1\text{H}$  NMR spectrum of the  $\alpha$ -diimine compound **6**.

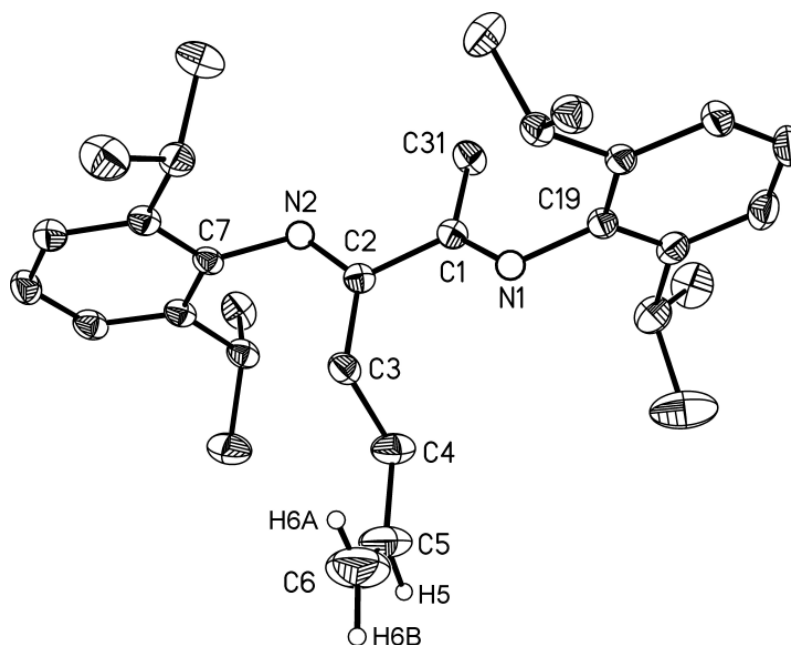
The quartet signal appearing at  $\delta = 2.27$  ppm is produced by the protons of the methylene group (29). The methyl groups at the backbone of the compound structure yield the resonance signal at  $\delta = 2.05$  ppm while the methyl groups belonging to the isopropyl functions produce the multiplet signal at  $\delta = 1.20$  ppm.

The  $^{13}\text{C}$  NMR spectrum of compound **6** (see Scheme 20) shows the signal of the imine carbon atom connected to the allyl group at  $\delta = 170.5$  ppm which is at higher field by 2.5 ppm than the other imine carbon atom at  $\delta = 168.0$  ppm. The signals belonging to the quaternary carbon atoms of the aromatic ring systems appear at  $\delta = 146.5$ , 145.5, 135.2, and 134.8 ppm, while the signal at  $\delta = 137.5$  ppm is produced by the CH group of the allyl function. The signals at  $\delta = 123.7$ , 123.0, and 122.7 ppm can be assigned to the aromatic CH groups. The terminal methylene group of the allyl function gives the signal at  $\delta = 115.0$  ppm while the methylene groups (2) and (29) can be assigned to the signals at  $\delta = 30.5$  and 29.0 ppm, respectively. The carbon atoms of the CH groups of the isopropyl functions generate the intensive signal at  $\delta = 28.5$  ppm. The signals at  $\delta = 23.3$ , 23.2, 22.7, and 22.1 ppm are assigned to the methyl groups of the isopropyl functions while the carbon atom of methyl group at the backbone of the compound structure appears at  $\delta = 17.1$  ppm.



Scheme 20.  $^{13}\text{C}$  NMR spectrum of the  $\alpha$ -diimine compound **6**.

Single crystals of **6** were obtained by slow solvent evaporation from a concentrated methanol solution. The molecular structure of compound **6** was unambiguously established by X-ray analysis. The numbering system is given in Scheme 21. The crystal data and structure refinement are listed in table D1 at the appendices.



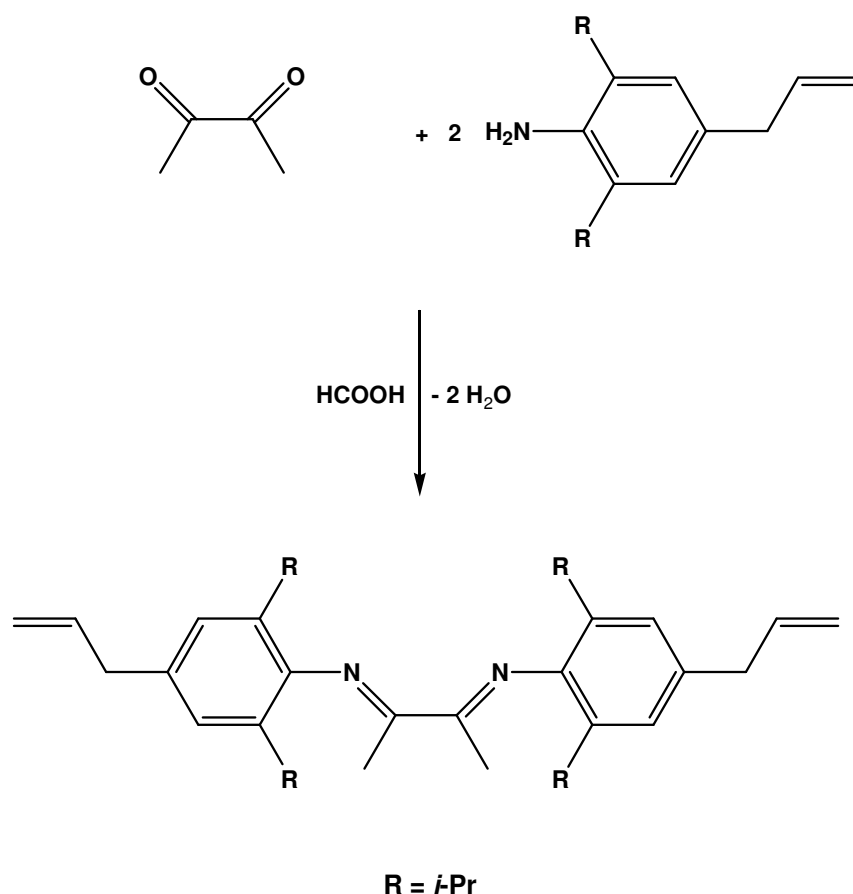
**Scheme. 21** Molecular structure of compound **6** (ORTEP plot at 40 % probability level, hydrogens except H5, H6A and H6B are omitted for clarity).

The selected bond lengths (Å): C1-N1 1.274(2), C1-C2 1.496(3), C1-C31 1.500(3), C2-N2 1.280(2), C2-C3 1.493(3), C3-C4 1.531(3), C4-C5 1.477(3), C5-C6 1.213(5), C7-N2 1.418(2). Selected bond angles (°): N1 C1 C2 115.78(15), N1 C1 C31 125.84(17), C2 C1 C31 118.29(16), N2 C2 C3 126.27(17), N2 C2 C1 115.64(16), C3 C2 C1 118.06(16), C2 C3 C4 112.51(16), C5 C4 C3 113.9(2), C6 C5 C4 131.0(3), C8 C7 N2 120.32(17), C12 C7 N2 117.79(17), C20 C19 N1 121.02(17), C24 C19 N1 116.99(16), C1 N1 C19 121.31(15), C2 N2 C7 122.42(15).

The principle plane contains N1C1C2N2 and they are not in the same plane. The mean deviation is 0.0752 Å due to different groups attached to the carbon atoms C1 and C2. The carbon atoms C7-C12 of the aromatic ring are in the same plane which has the angle 85.3° with the principle plane while the carbon atoms C19-C24 of the other aromatic ring are in the same plane which has the angle 84.9° with the principle plane. These two planes formed by the aromatic rings are not parallel to each other and slightly twisted by an angle of 6.8°.

### 2.1.2.3 Synthesis and characterization of compound 7

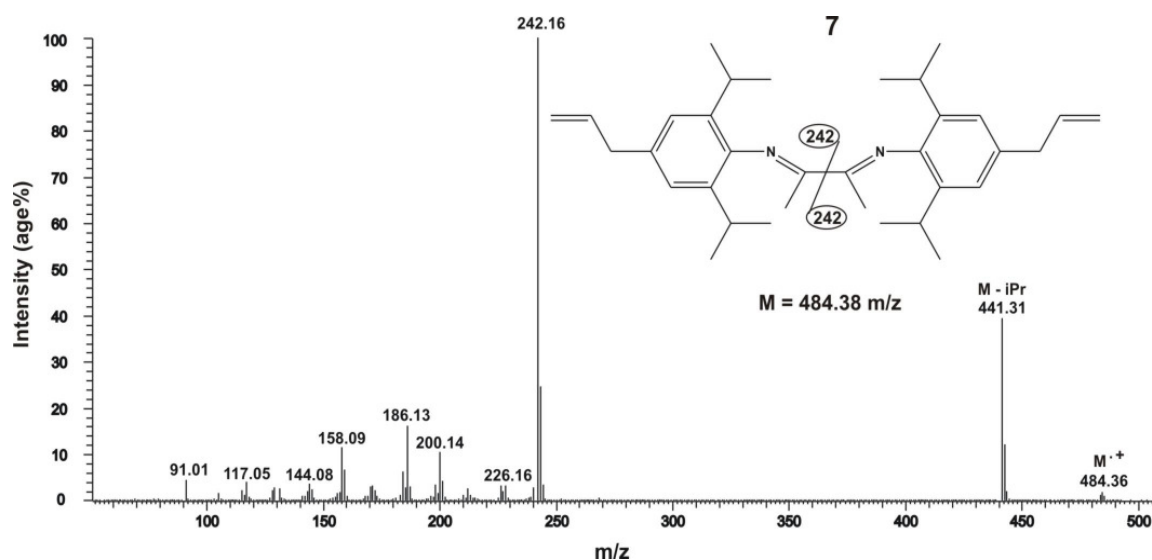
4-Allyl-2,6-diisopropylaniline was prepared according to the literature.<sup>[108]</sup> Compound 7 was synthesized via condensation reaction of one equivalent of 2,3-butanedione with two equivalents of 4-allyl-2,6-diisopropylaniline in the presence of formic acid as catalyst. The synthesis and the structure of compound 7 are shown in Scheme 22.



**Scheme 22. Synthesis of the  $\alpha$ -diimine compound 7.**

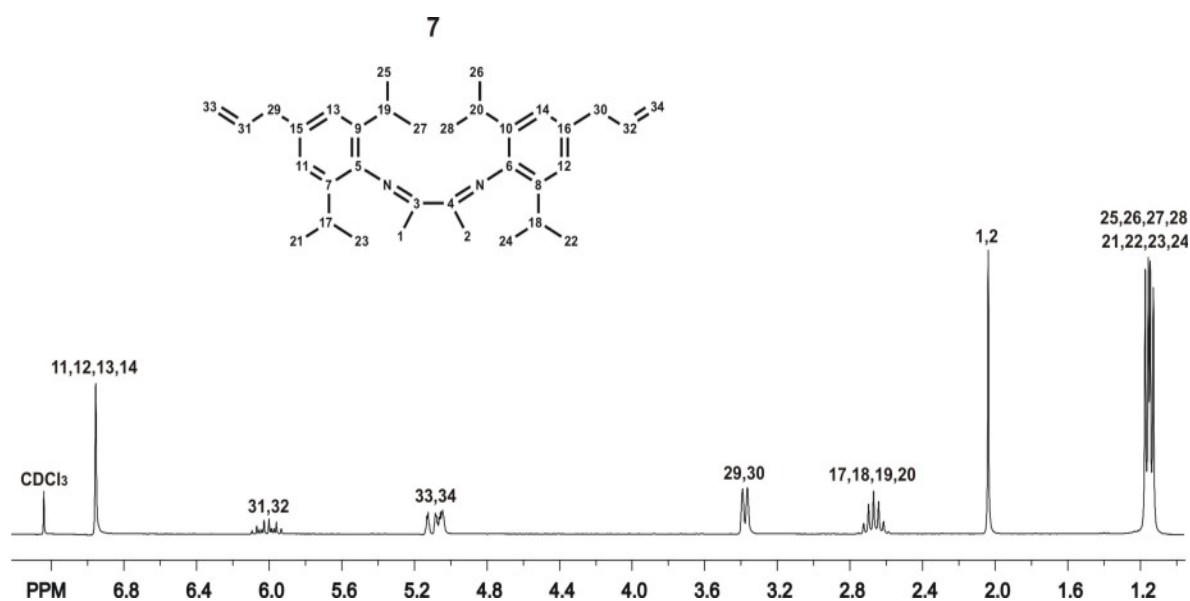
Compound 7 was characterized by GC-MS,  $^1\text{H}$  NMR, and  $^{13}\text{C}$  NMR spectroscopy (see the appendices for the full analysis data).

The mass spectrum of compound 7 (see Scheme 23) shows the molecular ion at  $m/z = 484$  with a weak intensity of 1% relative to the base peak, while the peak at  $m/z = 441$  with an intensity of 38% results from the loss of an isopropyl group. The base peak at  $m/z = 242$  is produced by the cleavage of the compound into two imine moieties having the same mass.



**Scheme 23.** Mass spectrum of the  $\alpha$ -diimine compound **7**.

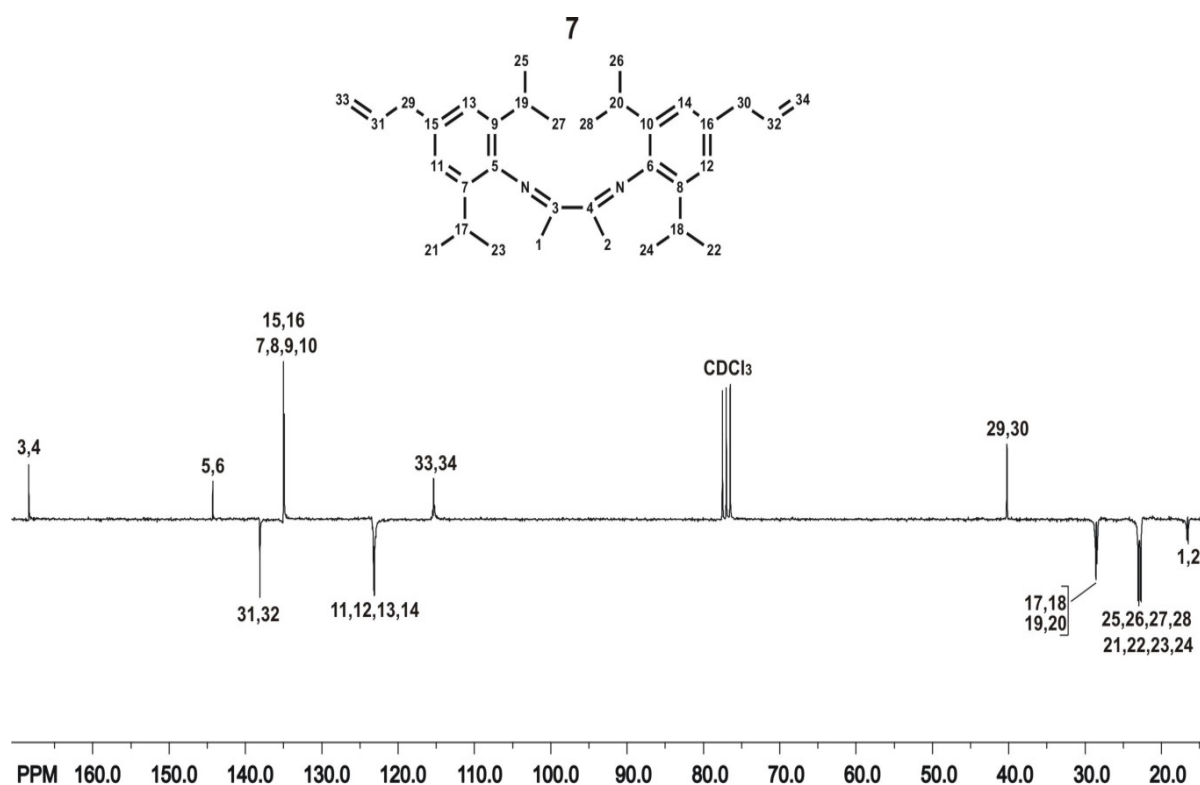
The  $^1\text{H}$  NMR spectrum of compound **7** (see Scheme 24) shows a singlet at  $\delta = 6.95$  ppm which is assigned to the protons of the aromatic CH groups while the CH groups of the allyl functions produce the multiplet signal at  $\delta = 6.01$  ppm. The terminal methylene groups of the allyl functions give a doublet of doublet proton NMR signal at  $\delta = 5.10$  ppm. The signal at  $\delta = 3.38$  ppm is assigned to the methylene groups 29 and 30 while the CH groups of the isopropyl functions produce the septet signal at  $\delta = 2.67$  ppm.



**Scheme 24.**  $^1\text{H}$  NMR spectrum of the  $\alpha$ -diimine compound **7**.

The singlet signal at  $\delta = 2.04$  ppm is assigned to the protons of the methyl groups at the backbone of the compound while the protons of the methyl groups of the isopropyl functions produce the two doublet signals at  $\delta = 1.17$  and  $1.14$  ppm.

The  $^{13}\text{C}$  NMR spectrum of compound **7** (see Scheme 25) shows the signal of the imine carbon atoms at  $\delta = 168.4$  ppm. The signals of the quaternary carbon atoms of the aromatic rings which are bonded to the imine moieties appear at  $\delta = 144.3$  ppm while the other quaternary carbon atoms of the aromatic rings produce the signal at  $\delta = 135.0$  ppm. The signal at  $\delta = 138.0$  ppm is assigned to the CH groups of the allyl function while the aromatic CH groups appear at  $\delta = 123.2$  ppm. The terminal methylene groups of the allyl functions give the signal at  $\delta = 115.3$  ppm while the signal at  $\delta = 40.2$  ppm is produced by the methylene groups 29 and 30. The carbon atoms of the CH groups of the isopropyl functions generate the signal at  $\delta = 28.5$  ppm. The signal at  $\delta = 22.8$  ppm is assigned to the methyl groups of the isopropyl functions while the signal of the methyl groups at the backbone of the compound appears at  $\delta = 16.5$  ppm.

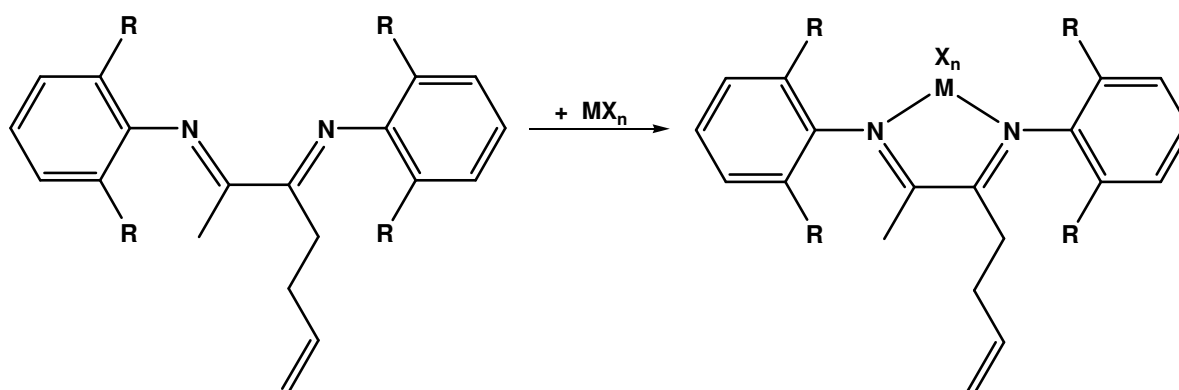


Scheme 25.  $^{13}\text{C}$  NMR spectrum of the  $\alpha$ -diimine compound **7**.

## 2.1.3 Synthesis and characterization of the complexes

### 2.1.3.1 Synthesis and characterization of the complexes *4a-g*, *5a-g*, and *6a-g*

The complexes **4a-g**, **5a-g**, and **6a-g** were synthesized via reacting the desired metal salt with the respective  $\alpha$ -diimine compound **4**, **5**, or **6**. The metal salts titanium tetrachloride ( $\text{TiCl}_4$ ), zirconium tetrachloride ( $\text{ZrCl}_4$ ), vanadium trichloride ( $\text{VCl}_3$ ), chromium trichloride ( $\text{CrCl}_3$ ), iron trichloride ( $\text{FeCl}_3$ ), dibromo(1,2-dimethoxyethane)nickel(II) ( $\text{NiBr}_2 \cdot \text{DME}$ ), or dichloro(1,5-cyclooctadiene)palladium(II) ( $\text{PdCl}_2 \cdot \text{COD}$ ) were used. The complexes **4a-g**, **5a-g**, and **6a-g** are bearing allyl groups on the backbones of the complex structures. The synthesis and the structure of the complexes are depicted in Scheme 26.

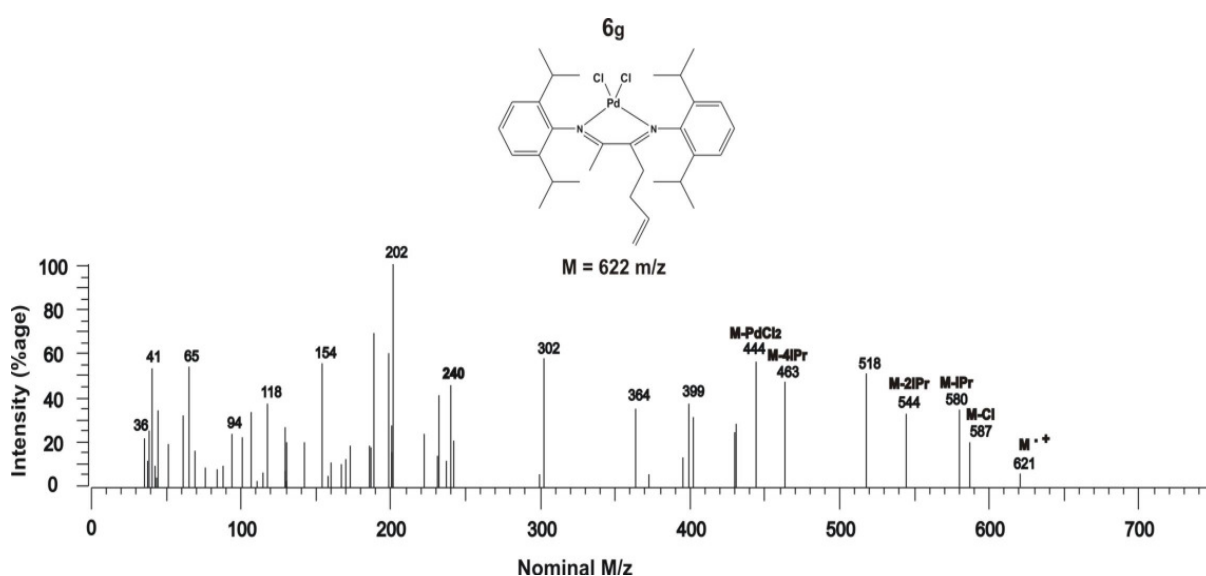


$\text{MX}_n =$	$\text{TiCl}_4$	$\text{ZrCl}_4$	$\text{VCl}_3$	$\text{CrCl}_3$	$\text{FeCl}_3$	$\text{NiBr}_2$	$\text{PdCl}_2$
$\text{R} = \text{Me}$	<b>4a</b>	<b>4b</b>	<b>4c</b>	<b>4d</b>	<b>4e</b>	<b>4f</b>	<b>4g</b>
$\text{R} = \text{Et}$	<b>5a</b>	<b>5b</b>	<b>5c</b>	<b>5d</b>	<b>5e</b>	<b>5f</b>	<b>5g</b>
$\text{R} = i\text{-Pr}$	<b>6a</b>	<b>6b</b>	<b>6c</b>	<b>6d</b>	<b>6e</b>	<b>6f</b>	<b>6g</b>

**Scheme 26.** Synthesis of the  $\alpha$ -diimine complexes *4a-g*, *5a-g*, and *6a-g*.

The complexes **4a-g**, **5a-g**, and **6a-g** were characterized via mass spectroscopy and elemental analysis. The complex **6g** was characterized by  $^1\text{H}$  NMR, and  $^{13}\text{C}$  NMR spectroscopy, (see the appendices for the full analysis data). The mass and NMR spectra of complex **6g** will be discussed as example.

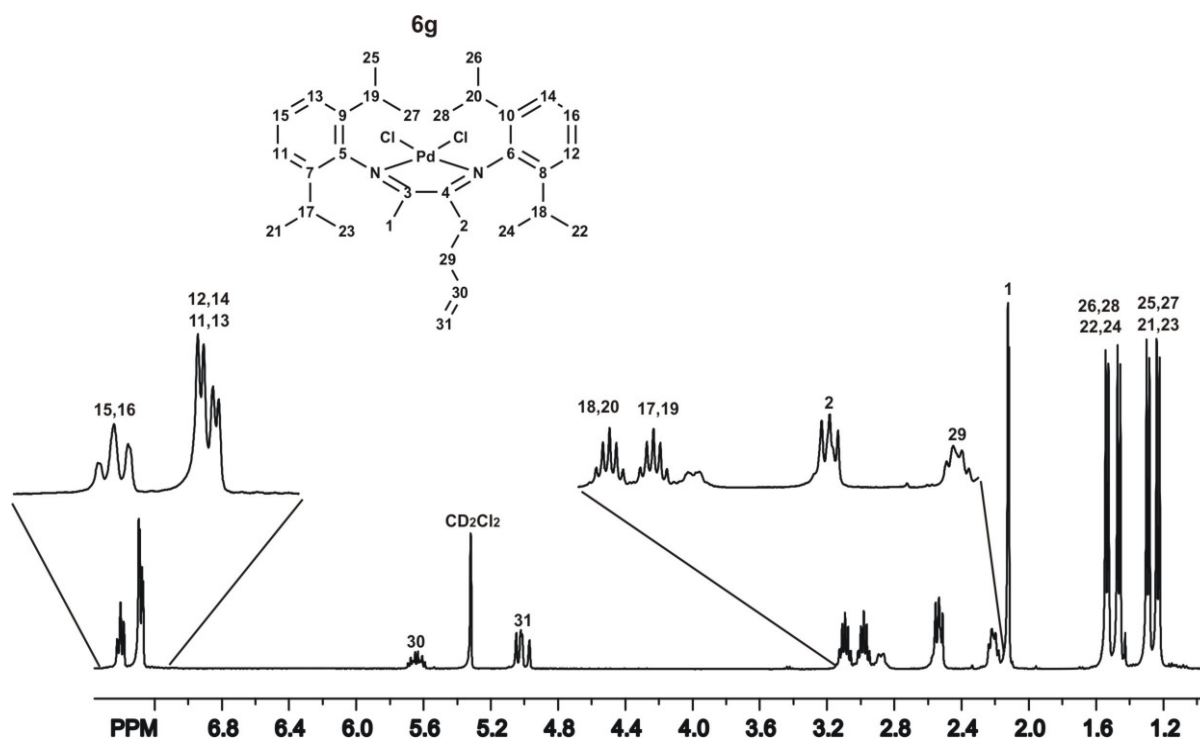
The mass spectrum of complex **6g** (see Scheme 27) shows the peak of the molecular ion at  $m/z = 621$  with an intensity of 7% relative to the base peak. The loss of a chloro group results in a peak at  $m/z = 587$  (intensity 20%) while the peak at  $m/z = 580$  with an intensity of 35% is assigned to the loss of an isopropyl group. The peaks appearing at  $m/z = 544$  and 463 with the intensities 32% and 48% are produced by the loss of two and four isopropyl groups. The loss of both chloro groups and the palladium center results in the molecular ion of the  $\alpha$ -diimine ligand at  $m/z = 444$  with an intensity of 58%. Further cleavage of the  $\alpha$ -diimine ligand framework gives two imine moieties where the one bearing the allyl group appears at  $m/z = 240$  with an intensity of 45% and the other produces the base peak at  $m/z = 202$ .



**Scheme 27.** Mass spectrum of the  $\alpha$ -diimine complex **6g**.

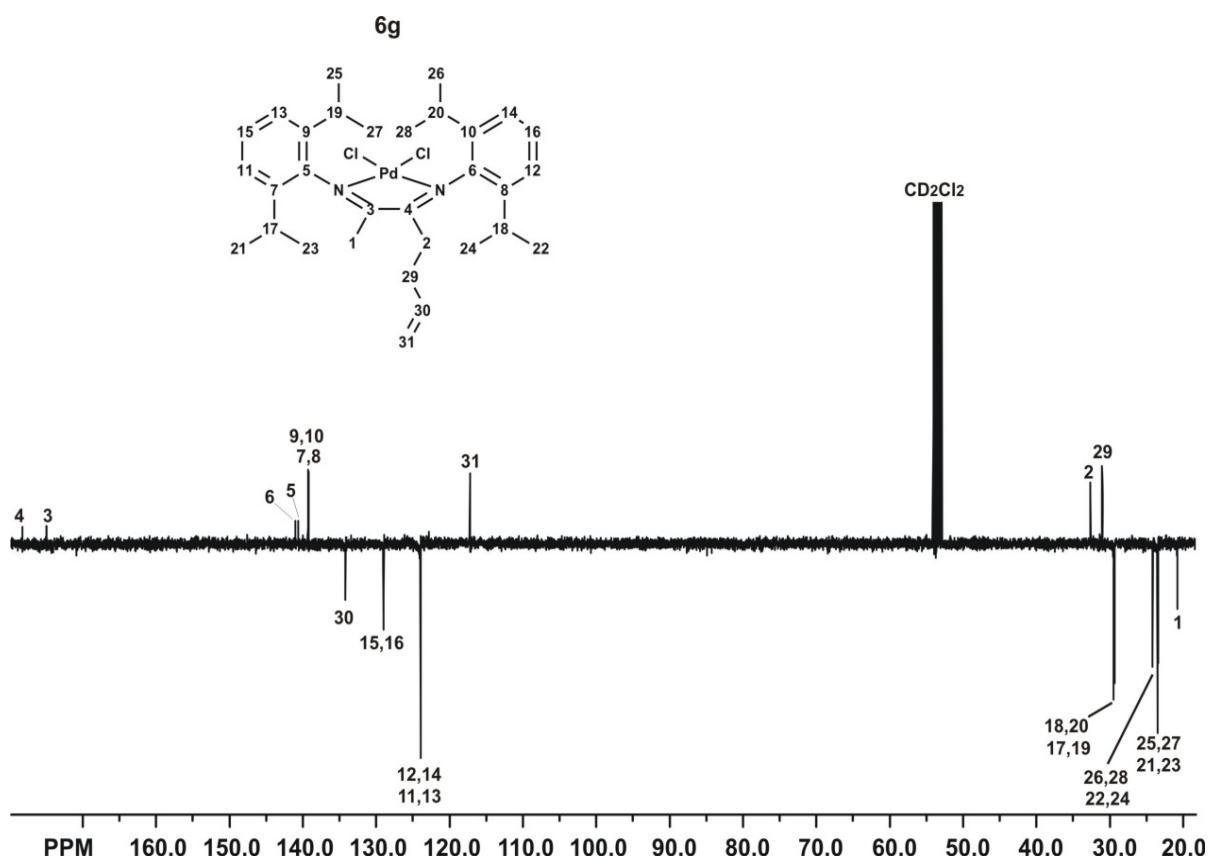
The  $^1\text{H}$  NMR spectrum of complex **6g** (see Scheme 28) shows a triplet signal at  $\delta = 7.40$  ppm which is assigned to the protons of the aromatic CH groups 15 and 16. The signal of the other aromatic CH groups is splitted into two doublet signals at  $\delta = 7.29$  and 7.27 ppm. The CH group of the allyl function produces the multiplet signal at  $\delta = 5.64$  ppm while the terminal methylene group of the allyl function gives a doublet of doublets at  $\delta = 5.01$  ppm. The signal of the CH groups of the isopropyl functions is split into two septet signals at  $\delta = 3.10$  and 2.98 ppm. The methylene group 2 produces the triplet signal at  $\delta = 2.54$  ppm while the pseudo quartet signal at  $\delta = 2.21$  ppm is assigned to the methylene group 29. The methyl group at the backbone of the complex structure yields the intensive singlet signal at  $\delta = 2.13$

ppm while the methyl groups belonging to the isopropyl functions produce four doublet signals at  $\delta = 1.54, 1.47, 1.29$  and  $1.23$  ppm.



**Scheme 28.**  $^1\text{H}$  NMR spectrum of the  $\alpha$ -diimine complex **6g**.

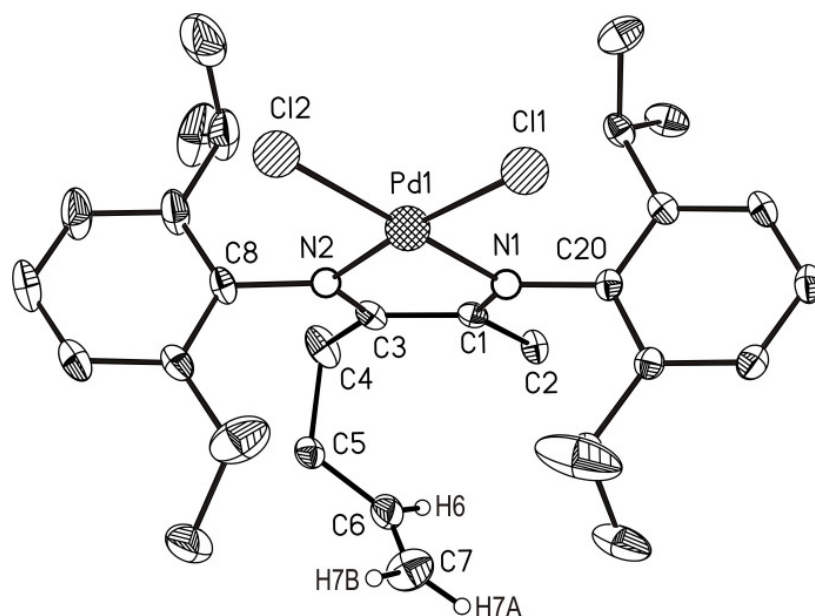
The  $^{13}\text{C}$  NMR spectrum of complex **6g** (see Scheme 29) shows the signal of the imine carbon atom connected to the allyl group at  $\delta = 178.6$  ppm which is higher by 8 ppm than the signal of the analogous atom of the free ligand. The signal of the other imine carbon atom appears at  $\delta = 174.0$  ppm while the analogous atom of the free ligand appears at  $\delta = 168.0$  ppm. The signals of the quaternary carbon atoms of the aromatic ring systems appear at convergent values:  $\delta = 141.3, 140.9,$  and  $139.3$  ppm. The CH group of the allyl function produces the signal at  $\delta = 134.2$  ppm while the signals at  $\delta = 129.0$  and  $124.0$  ppm can be assigned to the aromatic CH groups. The terminal methylene group of the allyl function is assigned to the signal at  $\delta = 117.3$  ppm while the methylene groups 2 and 29 give the signals at  $\delta = 32.6$  and  $31.0$  ppm. The carbon atoms of the CH groups of the isopropyl functions generate the signals at  $\delta = 29.5$  and  $29.3$  ppm while the signals at  $\delta = 24.2$  and  $23.5$  ppm are assigned to the methyl groups of the isopropyl functions. The methyl group at the backbone of the complex appears at  $\delta = 20.8$  ppm which is higher by 3.7 ppm than the signal for the analogous group of the free ligand.



**Scheme 29.**  $^{13}\text{C}$  NMR spectrum of the  $\alpha$ -diimine complex **6g**.

Single crystals of complex **6g** were obtained by slow solvent evaporation from a concentrated methylene chloride solution. The molecular structure of complex **6g** was unambiguously established by X-ray analysis. The numbering system is given in Scheme 30. The crystal data and structure refinement are listed in table D2 at the appendices.

The selected bond lengths ( $\text{\AA}$ ): C1-N1 1.294(4), C1-C3 1.484(4), C1-C2 1.505(11), C3-N2 1.297(4), C3-C4 1.523(17), C4-C5 1.621(19), C5-C6 1.478(8), C6-C7 1.278(18), C8-N2 1.445(4), C20-N1 1.447(4), N1-Pd1 2.009(2), N2-Pd1 2.010(3), Cl1-Pd1 2.2803(8), Cl2-Pd1 2.2752(8). Selected bond angles ( $^\circ$ ): N1 C1 C3 114.3(3), N1 C1 C2 120.5(5), C3 C1 C2 125.2(5), N2 C3 C1 114.2(3), N2 C3 C4 121.3(7), C1 C3 C4 124.5(7), C3 C4 C5 110.8(11), C6 C5 C4 120.5(7), C7 C6 C5 125.3(10), C1 N1 C20 121.4(2), C1 N1 Pd1 116.1(2), C20 N1 Pd1 122.48(18), C3 N2 C8 121.5(3), C3 N2 Pd1 116.1(2), C8 N2 Pd1 122.4(2), N1 Pd1 N2 78.74(10), N1 Pd1 Cl2 173.75(8), N2 Pd1 Cl2 96.33(8), N1 Pd1 Cl1 95.35(7), N2 Pd1 Cl1 173.84(8), Cl2 Pd1 Cl1 89.68(3).



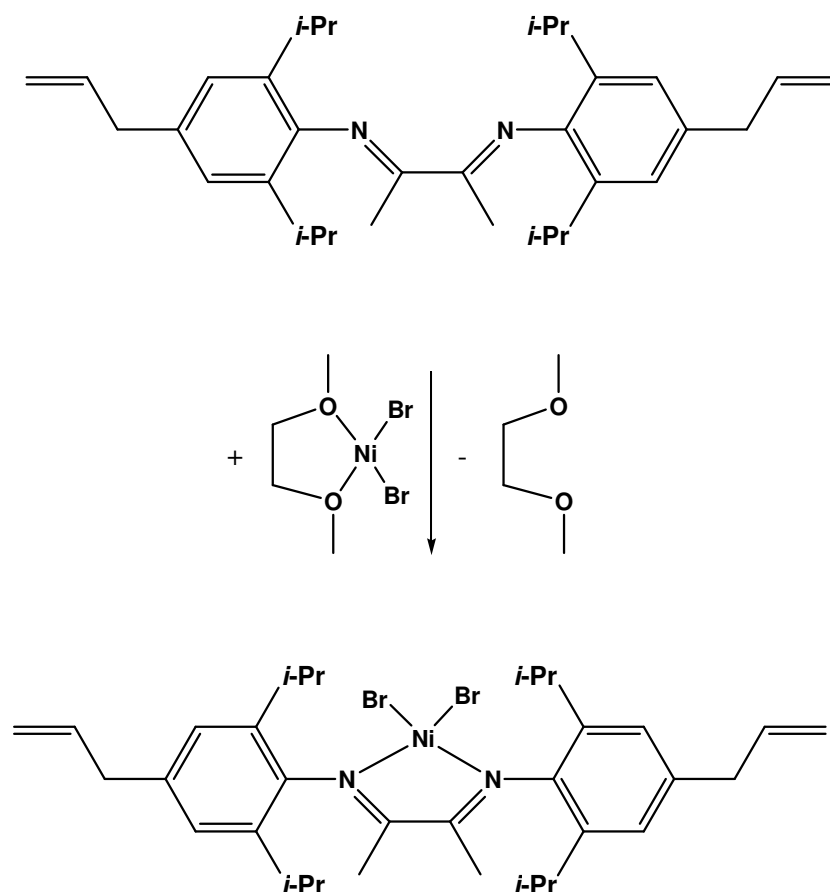
**Scheme 30.** Molecular structure of complex **6g** (ORTEP plot at 30 % probability level, hydrogens except H6, H7A and H7B are omitted for clarity).

The coordination number of the palladium(II) center of complex **6g** is four and the geometry around the palladium is square planar. The unit cell includes a methylene chloride molecule. The principle plane contains N1N2Pd1Cl1Cl2 which are slightly deviated from this principle plane; the mean deviation is 0.0423 Å. The deviation is caused by the different groups attached to the backbone structure of the complex. The carbon atoms C8-C13 of the aromatic ring are in the same plane and their plane is slightly twisted from being perpendicular to the principle plane by an angle of 91.6° while the analogous plane of the free ligand is twisted by an angle of 85.3°. The carbon atoms C20-C25 of the other aromatic ring are in the same plane, too, and their plane is twisted against the principle plane by an angle of 89.6° while the analogous angle of the free ligand is 84.9°. Therefore, the planes are formed by the aromatic rings are closer to be perpendicular to the principle plane in the complex than in the ligand. These two planes formed by the aromatic rings are twisted by an angle of 20.7° from each other where the analogous angle of the free ligand is 6.8° which means that these planes are closer to be parallel to each other in the free ligand than in the complex. The bond lengths of C1-N1 (1.294(4) Å) and C3-N2 (1.297(4) Å) in complex **6g** are longer compared with those (1.274(2) Å) and (1.280(2) Å) in compound **6**. The bond lengths between the two carbon atoms of the diimine moiety in complex **6g** (1.484(4) Å) are shorter than the analogous bonds in compound **6** (1.496(3) Å). The bond angles N1C1C3 (114.3(3)°) and N2C3C1 (114.2(3)°)

in complex **6g** are smaller compared with the analogous angles ( $115.78(15)^\circ$ ) and ( $115.64(16)^\circ$ ) in the ligand precursor **6**.

### 2.1.3.2 Synthesis and characterization of complex **8**

Complex **8** was synthesized via reacting the  $\alpha$ -diimine compound **7** with dibromo(1,2-dimethoxyethane)nickel(II) ( $\text{NiBr}_2\cdot\text{DME}$ ). The prepared  $\alpha$ -diimine nickel complex **8** is bearing two allyl groups on the arene moieties. The synthesis of the complex is shown in Scheme 31.

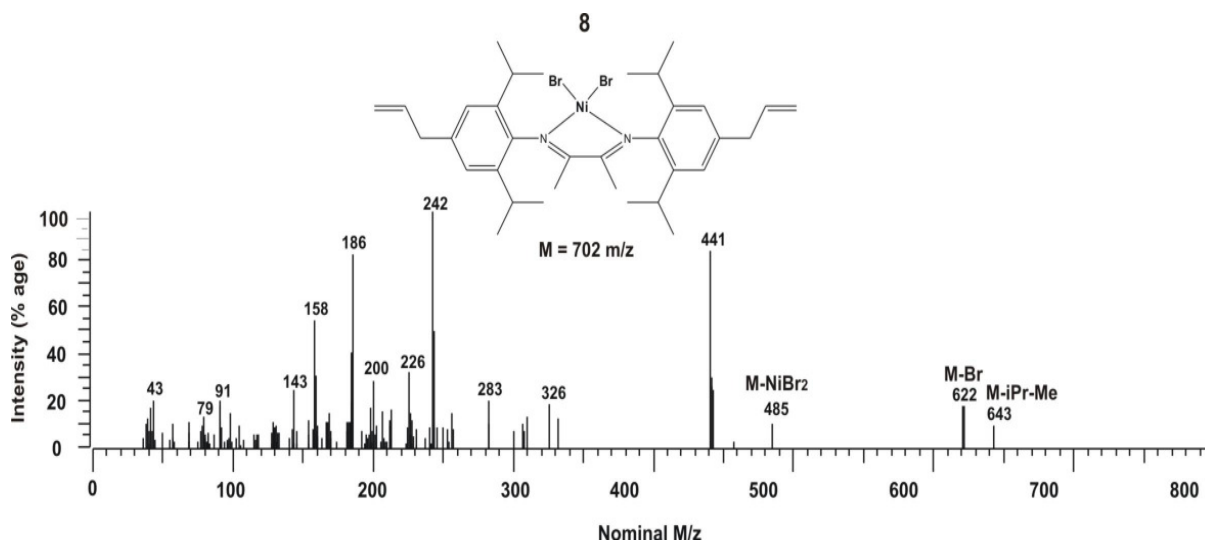


**Scheme 31.** Synthesis of the  $\alpha$ -diimine nickel complex **8**.

Complex **8** could not be characterized by NMR spectroscopy due to the paramagnetic nature of the nickel center. Therefore, mass spectroscopy and elemental analysis were used for

characterization (see the appendices for the full analysis data). A single crystal of the complex was isolated and analyzed via X-ray diffraction.

The mass spectrum of complex **8** (see Scheme 32) shows a peak from the molecule losing a methyl and an isopropyl group at  $m/z = 643$  with an intensity of 10% relative to the base peak. The loss of a bromo substituent produces the peak at  $m/z = 622$  with the intensity of 18% while the peak appearing at  $m/z = 485$  with an intensity of 9% is assigned to the loss of both bromo groups and the nickel center. Further cleavage of the  $\alpha$ -diimine ligand framework gives two imine moieties having the same mass which yields the base peak at  $m/z = 242$ .

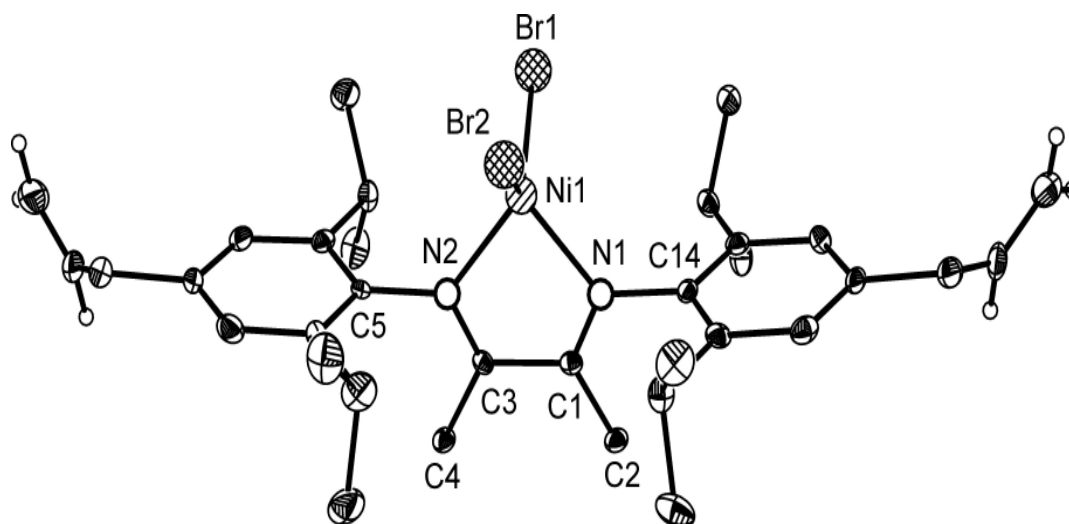


**Scheme 32. Mass spectrum of the  $\alpha$ -diimine nickel complex **8**.**

Single crystals of complex **8** were obtained by slow solvent evaporation from a concentrated methylene chloride solution. The molecular structure of complex **8** was unambiguously established by X-ray analysis. The numbering system is given in Scheme 33. The crystal data and structure refinement are listed in table D3 at the appendices.

Selected bond lengths ( $\text{\AA}$ ): C1-N1 1.276(7), C1-C2 1.497(8), C1-C3 1.498(8), C3-N2 1.284(7), C3-C4 1.495(7), C5-N2 1.441(7), C14-N1 1.462(7), N1-Ni1 1.979(4), N2-Ni1 1.993(4), Ni1-Br2 2.3045(10), Ni1-Br1 2.3443(9). Selected bond angles ( $^\circ$ ): N1 C1 C2 126.1(5), N1 C1 C3 114.4(5), C2 C1 C3 119.4(5), N2 C3 C4 125.5(5), N2 C3 C1 114.9(5),

C4 C3 C1 119.5(5), C1 N1 C14 120.4(5), C1 N1 Ni1 115.4(4), C14 N1 Ni1 124.2(3), C3 N2 C5 120.4(5), C3 N2 Ni1 114.2(4), C5 N2 Ni1 125.4(3), N1 Ni1 N2 80.52(17), N1 Ni1 Br2 118.31(13), N2 Ni1 Br2 114.90(13), N1 Ni1 Br1 105.53(12), N2 Ni1 Br1 108.11(13), Br2 Ni1 Br1 121.81(4).



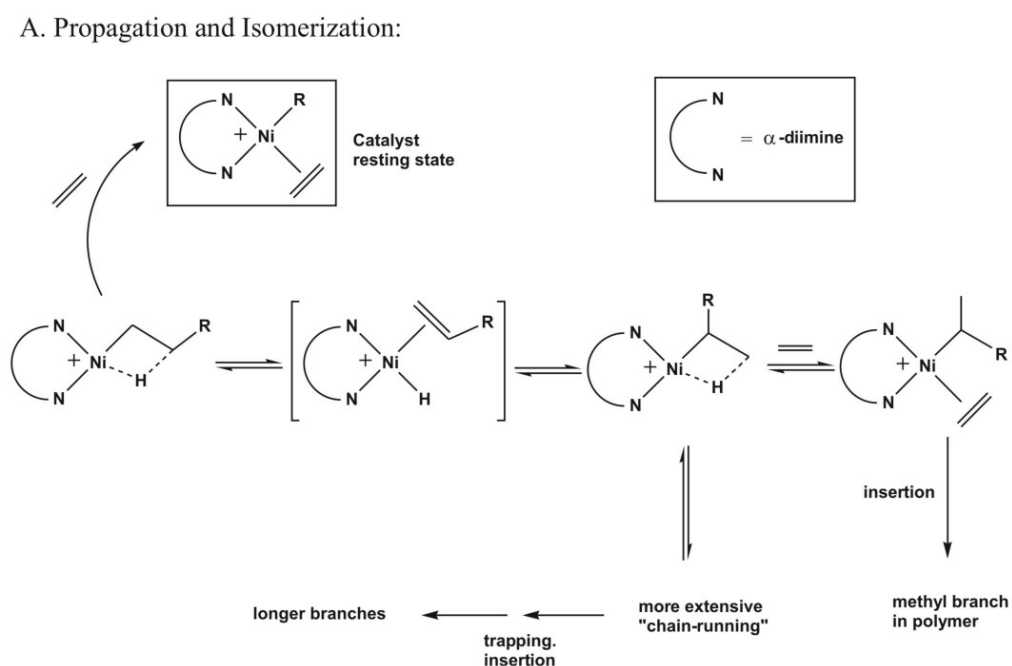
**Scheme 33. Molecular structure of complex 8 (ORTEP plot at 30 % probability level, hydrogens are omitted for clarity).**

The geometry around the nickel(II) center of complex **8** is tetrahedral. The nickel center has the coordination number four where it is coordinated to two bromo groups and the two nitrogen atoms of the diimine moiety. The unit cell contains two independent molecules of the nickel complex which are not twins based on the high value, 98.6 %, of the parameter (Completeness to  $\theta = 25.7^\circ$ ). The principle plane contains C1N1Ni1N2C3 which are slightly deviated from this principle plane, the mean deviation is 0.0345 Å. The deviation is caused by the allyl groups attached to the arene moieties. The carbon atoms C5-C10 of the aromatic ring are in the same plane and their plane is slightly twisted from being perpendicular to the principle plane by an angle of  $89.7^\circ$ . The carbon atoms C20-C25 of the other aromatic ring are in the same plane, too, and their plane is twisted against the principle plane by an angle of  $90.8^\circ$ . These two planes formed by the aromatic rings are twisted from each other by an angle of  $13.8^\circ$ .

## 2.1.4 Polymerization experiments

### 2.1.4.1 General

The olefin polymerization or oligomerization using ( $\alpha$ -diimine)nickel(II) complexes activated with methylalumoxane (MAO) is explained with the so-called "chain running" or "chain walking" mechanism and depends on the structure of the catalyst precursor<sup>[66-73 , 83-97]</sup> (Scheme 34).



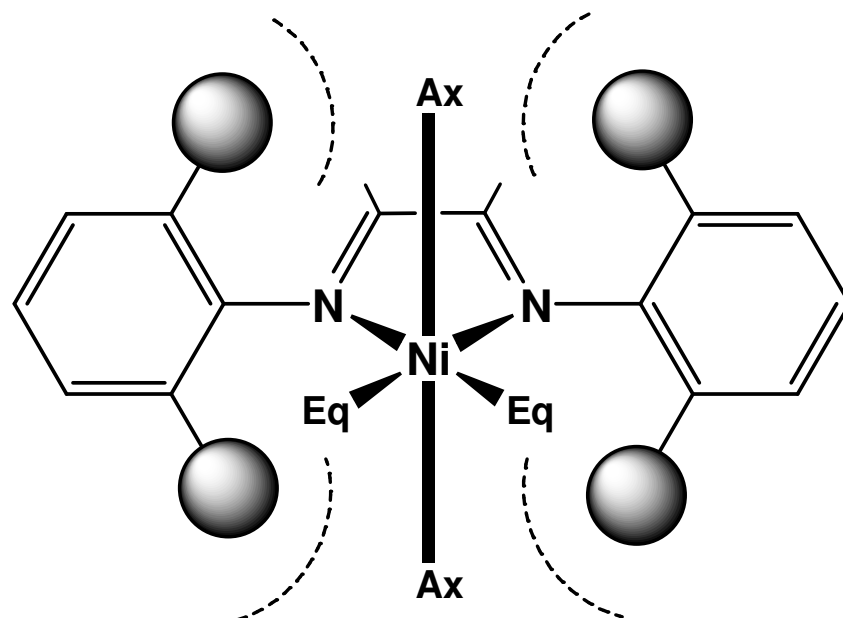
### B. Chain Transfer:

#### (1) Associative displacement:

#### (2) Concerted $\beta$ -H transfer to bound monomer:

**Scheme 34. Chain running mechanism.**<sup>[66-73 , 83-97]</sup>

It is found that when bulky substituents are introduced at the *ortho*-positions of the arene moieties of ( $\alpha$ -diimine)nickel(II) catalysts, the catalysts will produce high molecular weight polymers because the axial bulk provided by the *ortho*-substituents hinders the chain transfer and causes slow chain transfer relative to chain propagation.<sup>[87-97]</sup> When the steric bulk is eliminated, the rate of chain transfer will be increased and the catalyst will produce oligomers rather than polymer.<sup>[83-86]</sup> Deng et al.<sup>[109,110]</sup> proved this with calculations for the transition states of the chain propagation and the chain transfer reaction. The *ortho*-substituents have a considerable influence on the monomer addition to the catalytic center and the dissociation of the formed polymer from the metal due to their interaction with the axial coordination sites of the metal center.



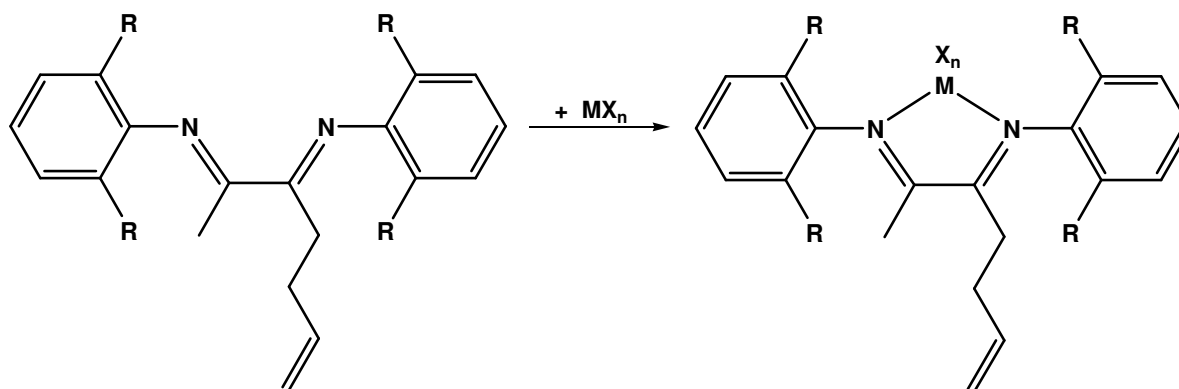
**Scheme 35. Axial (Ax) and equatorial (Eq) coordination sites of the metal center and their steric interactions with the bulky *ortho*-substituents.**<sup>[109,110]</sup>

The effect of introducing bulky substituents at the backbone of ( $\alpha$ -diimine)nickel(II) catalysts is an increase of the molecular weight of the produced polymers and a decrease of the catalyst activity.<sup>[83-86,91]</sup> The bulky substituents reduce the free rotation of the aryl rings. Therefore, the axial coordination sites of the metal center are sterically more hindered and the coordination of the olefin monomer via these axial coordination sites is hindered, too.<sup>[84-86]</sup>

### 2.1.4.2 Polymerization experiments with the complexes *4a-g*, *5a-g*, and *6a-g*

#### 2.1.4.2.1 Polymerization results of the complexes **4a-g**

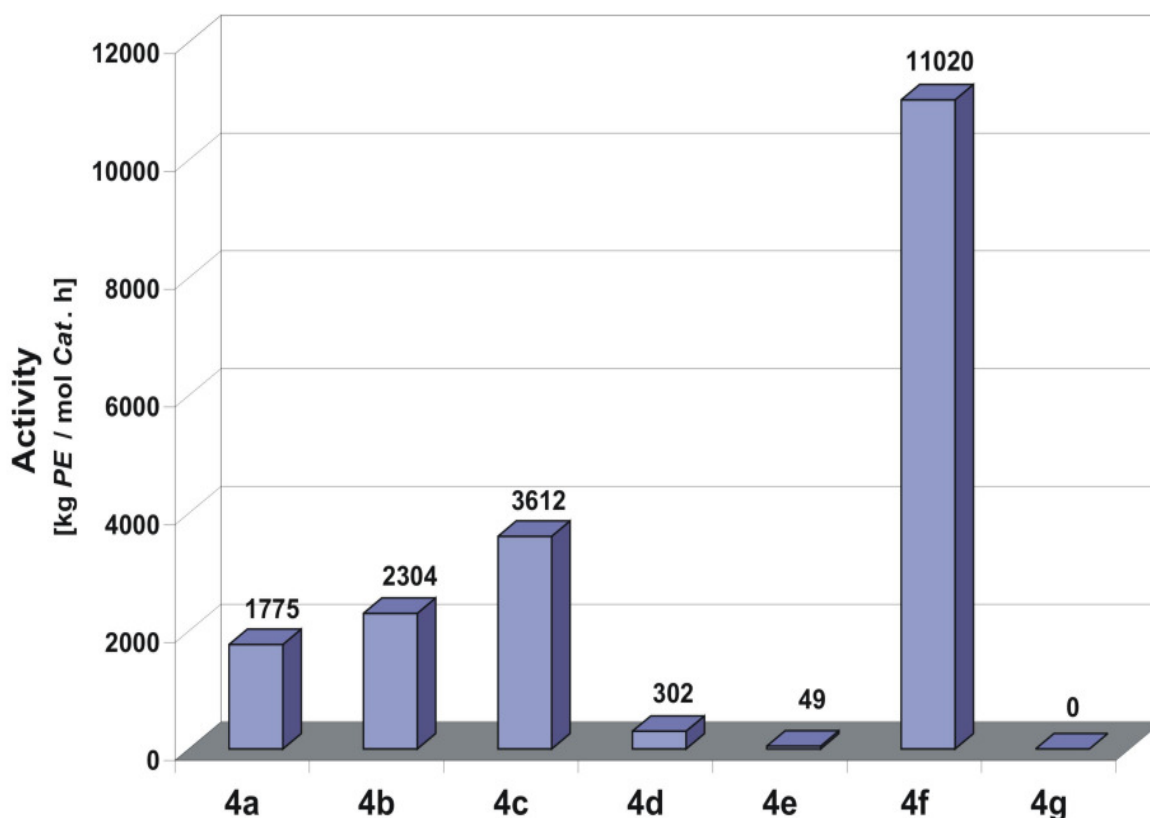
The complexes **4a-g** are a series of  $\alpha$ -diimine complexes bearing allyl groups at the backbone of their structures and methyl substituents at the ortho positions of their arene moieties. These bulky substituents suppose to provoke the catalyst to produce polymer rather than oligomers according to the suggested mechanism. The structures of these complexes are shown in Scheme 36.



$MX_n =$	$TiCl_4$	$ZrCl_4$	$VCl_3$	$CrCl_3$	$FeCl_3$	$NiBr_2$	$PdCl_2$
$R = Me$	<b>4a</b>	<b>4b</b>	<b>4c</b>	<b>4d</b>	<b>4e</b>	<b>4f</b>	<b>4g</b>

**Scheme 36.** The structures of  $\alpha$ -diimine complexes *4a-g*.

Suspensions of a few milligrams of these complexes in around 5 ml toluene were activated with methylaluminoxane (MAO), the M:Al ratio was 1:1500. The catalysts were transferred to a 1 l Büchi laboratory autoclave under inert atmosphere and tested for the polymerization of ethylene (in 250 ml of *n*-pentane, 10 bar ethylene, and polymerization temperature of 65° C). The results of the ethylene polymerizations are illustrated in Scheme 37.



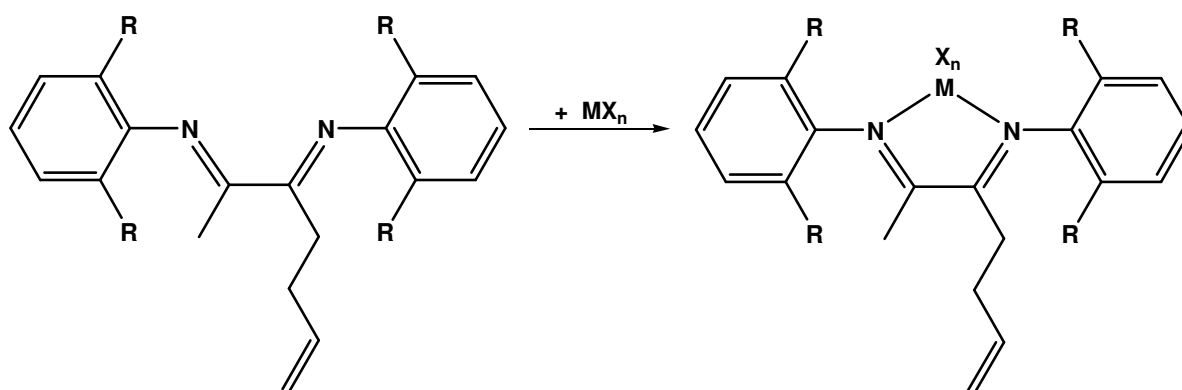
**Scheme 37. The polymerization activities of the  $\alpha$ -diimine complexes 4a-g.**

The most active catalyst among the series is the nickel catalyst **4f** and the second most active catalyst is the vanadium catalyst **4c**. The palladium catalyst **4g** showed no activity for ethylene polymerization. This may be attributed to internal interactions between the active sites of the palladium catalysts with the allyl functions attached to the backbone of the catalyst with the result of blocking the active sites. This unique behavior occurred only with the palladium catalyst. The iron catalyst **4e** showed the lowest activity (49 kg PE / mol cat. h). Also, a low activity (302 kg PE / mol cat. h) was observed using the chromium catalyst **4d**. The zirconium catalyst **4b** showed higher activity in comparison to the titanium catalyst **4a**. This can be assigned to the better separation between the cationic active species of the catalyst and the anionic MAO species in the zirconium catalyst. The better separation allows more monomers to reach the active sites of the catalyst raising the polymerization activity. The activity of the vanadium catalyst **4c** was higher than for the titanium catalyst **4a** and the zirconium **4b**. This may attribute to the different metal and the lower number of ligands

coordinated to the vanadium center than in case of the titanium or zirconium catalysts resulting in less interactions with the methyl substituents at the ortho positions of the arene moieties. These interactions can hinder the coordination sites of the metal center and lower the catalyst activity. The same explanation can be used to interpret the higher activity of the nickel catalyst **4f** compared with the vanadium catalyst **4c**.

#### 2.1.4.2.2 Polymerization results of the complexes **5a-g**

The complexes **5a-g** are  $\alpha$ -diimine complexes similar to the complexes **4a-g** bearing allyl groups at the backbone of their structures but different in having ethyl substituents at the ortho positions of their arene moieties. The structures of these complexes are shown in Scheme 38.

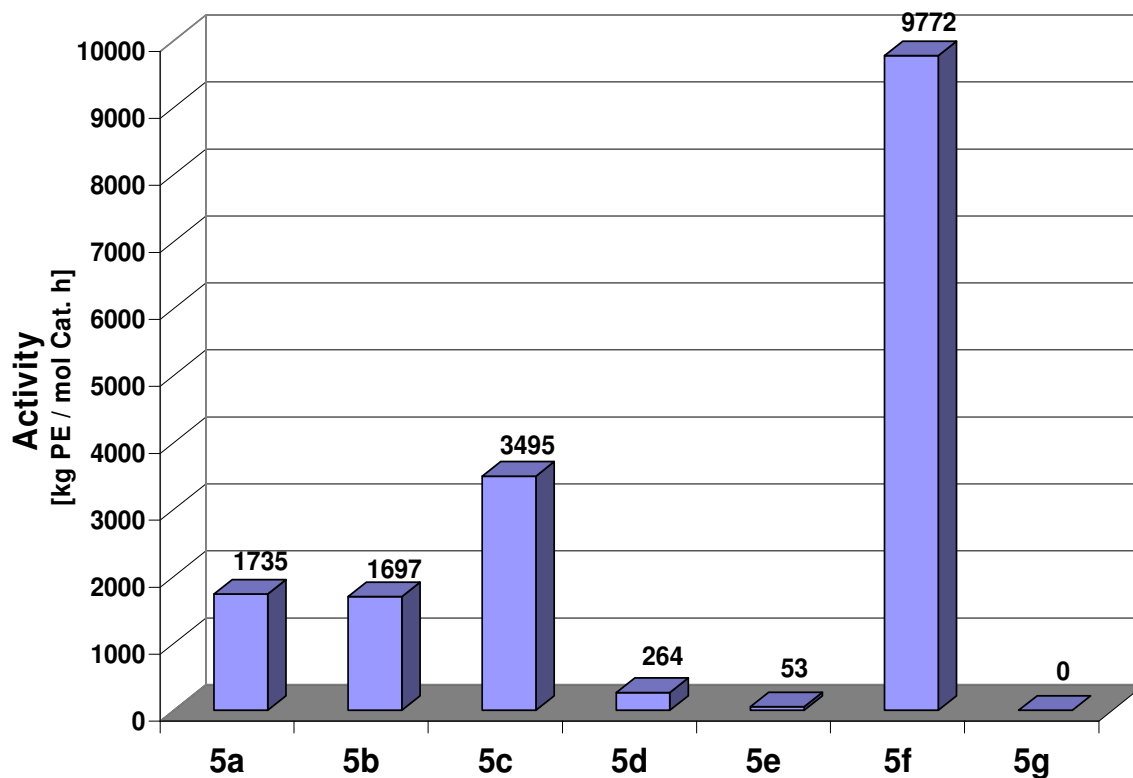


$MX_n =$	$TiCl_4$	$ZrCl_4$	$VCl_3$	$CrCl_3$	$FeCl_3$	$NiBr_2$	$PdCl_2$
$R = Et$	<b>5a</b>	<b>5b</b>	<b>5c</b>	<b>5d</b>	<b>5e</b>	<b>5f</b>	<b>5g</b>

**Scheme 38.** The structures of  $\alpha$ -diimine complexes **5a-g**.

The complexes **5a-g** were activated with MAO, the M:Al ratio was 1:1500. The catalysts were tested for the polymerization of ethylene by applying the same polymerization

conditions used for catalysts **4a-g**. The results of the ethylene polymerizations are illustrated in Scheme 39.

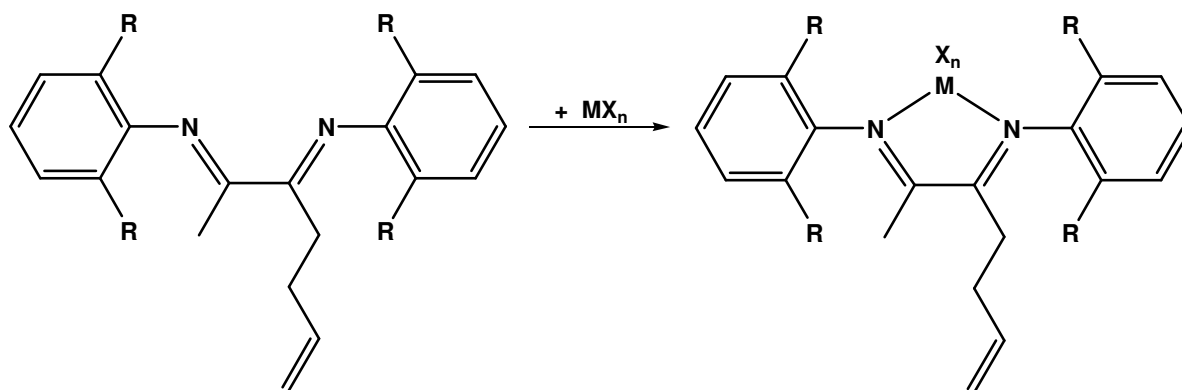


**Scheme 39.** The polymerization activities of the  $\alpha$ -diimine complexes **5a-g**.

The catalysts bearing ligand **5** showed a similar trend in the polymerization activities like catalysts **4a-g** with the exception of the titanium and zirconium catalysts. The titanium catalyst **5a** showed higher polymerization activity than the zirconium catalyst **5b** while it was the opposite for the titanium and zirconium catalysts **4a** and **4b**. Reduced catalyst activities were found for the catalysts of ligand **5** compared to the catalysts of **4** except for the iron catalyst **5e** which showed a slight increase in the activity compared to the iron catalyst **4e**. The lower activities are assigned to the ethyl substituents introduced into the ligand frameworks of the catalysts **5a-g**. They are bulkier than the methyl substituents of the catalysts bearing the ligand **4**. The palladium catalyst **5g** showed no activity for ethylene polymerization while the most active catalyst was the nickel compound **5f**.

2.1.4.2.3 Polymerization results of the complexes **6a-g**

The complexes **6a-g** are analogous to the complexes **4a-g** and **5a-g** with the difference of having isopropyl groups substituting the ortho positions of the arene moieties. The structures of these complexes are shown in Scheme 40.

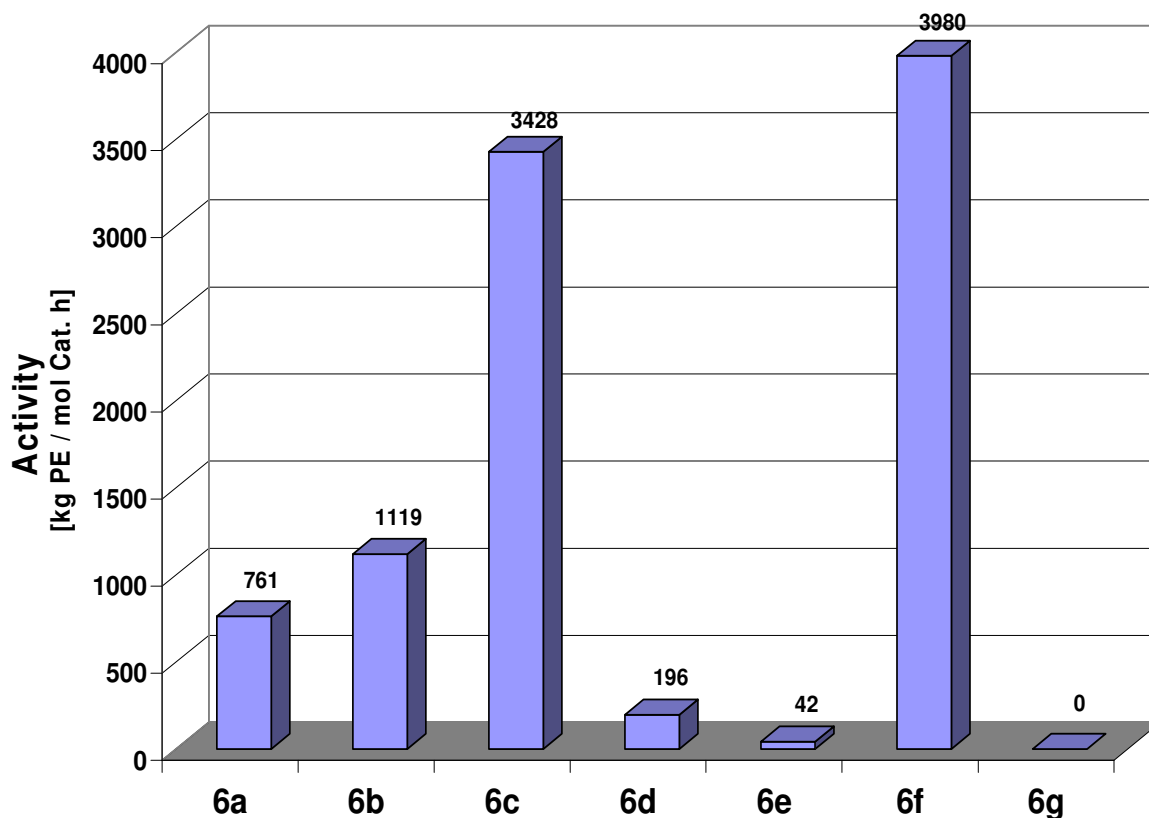


$MX_n =$	$TiCl_4$	$ZrCl_4$	$VCl_3$	$CrCl_3$	$FeCl_3$	$NiBr_2$	$PdCl_2$
$R = i\text{-Pr}$	<b>6a</b>	<b>6b</b>	<b>6c</b>	<b>6d</b>	<b>6e</b>	<b>6f</b>	<b>6g</b>

**Scheme 40.** The structures of the  $\alpha$ -diimine complexes **6a-g**.

The complexes **6a-g** were activated with MAO, the M:Al ratio was 1:1500. The catalysts were tested for the polymerization of ethylene by applying the same polymerization conditions used for catalysts **4a-g** and **5a-g**. The results of the ethylene polymerizations are illustrated in Scheme 41.

The catalysts **6a-g** showed the lowest polymerization activities in comparison with the analogous catalysts bearing the ligands **4** and **5**. The lower activity is assigned to the isopropyl substituents which are bulkier than the substituents of either the catalysts **4a-g** or the catalysts **5a-g**. The trend resulting from the change in polymerization activity by changing the metal center of the catalysts **6a-g** was the same as observed for catalysts **4a-g**.

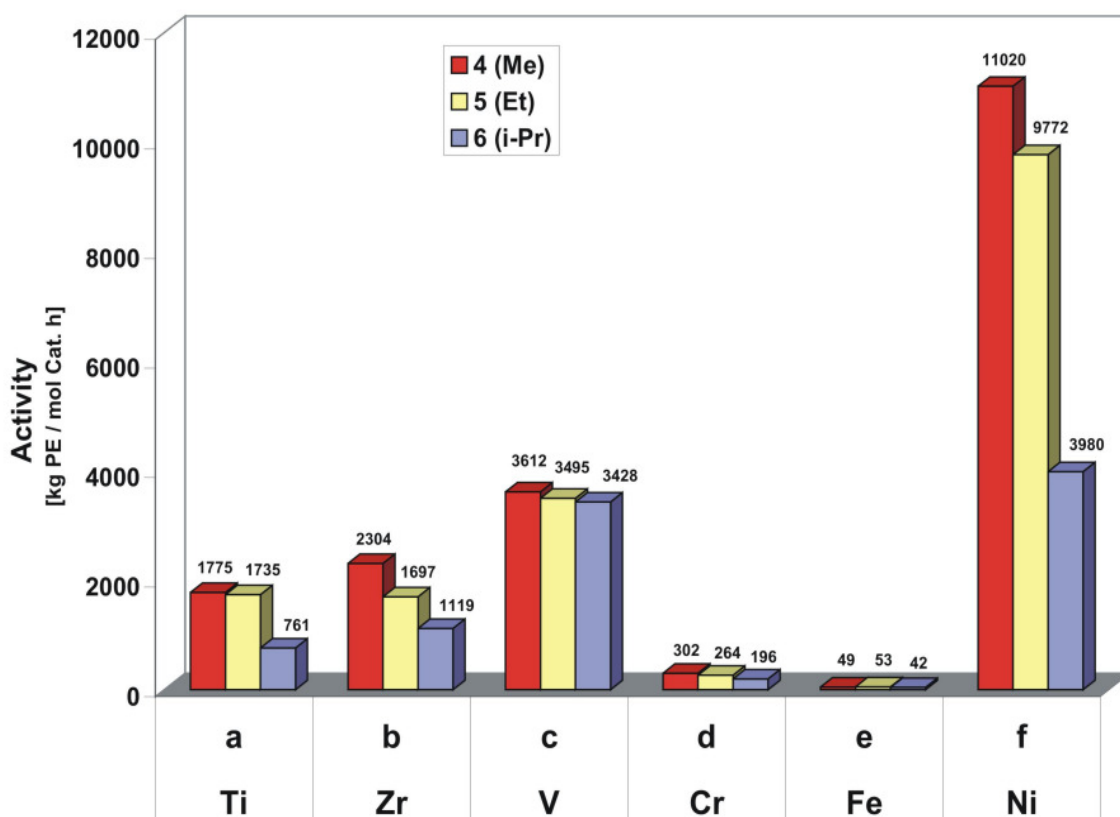


**Scheme 41.** The polymerization activities of the  $\alpha$ -diimine complexes *6a-g*.

#### 2.1.4.2.4 Comparison between the polymerization results of *4a-g*, *5a-g*, and *6a-g*

The palladium catalysts **4g**, **5g**, and **6g** showed no polymerization activities. That may attribute to the allyl functions attached to the backbone of the catalyst structures which can interact with the active sites of the palladium catalysts resulting in blocking the active sites and deactivating the catalyst. This behavior was not observed with the other metals and was a distinguished behavior by palladium. The chromium catalysts **4d**, **5d**, and **6d** showed higher activities than the analogous iron catalysts which showed very low activities. The vanadium catalysts **4c**, **5c**, and **6c** showed lower activities than the analogous nickel catalysts which showed the highest activities. The zirconium catalysts showed higher activity compared to the titanium catalysts with the exception of catalyst **5b**. Both of the titanium and zirconium catalysts had lower activities than the vanadium catalysts. The change in polymerization activity with the change of the ortho substituents at the arene moieties of the catalyst

structures showed that the bulkier the substituents, the lower the polymerization activity. This result is compatible with the chain running mechanism which suggests that the bulky substituents can hinder the monomers from reaching the active catalytic centers due to their interaction with the axial coordination sites of the metal centers resulting in lower activities. The influence of the substituent's size on the catalyst activity was higher in the case of nickel and zirconium catalysts.



**Scheme 42.** Change of polymerization activities when changing the structure of  $\alpha$ -diimine complexes and the metal centers.

Samples of the produced polyethylene by the nickel catalysts **4f**, **5f**, and **6f** were analyzed by gel permeation chromatography (GPC). The aim was to study the effect of varying the bulk of the ortho substituents at the arene moieties on the molecular weight (MW) of the produced polyethylene and the molecular weight distribution (MWD). The results of GPC are summarized in Table 1.

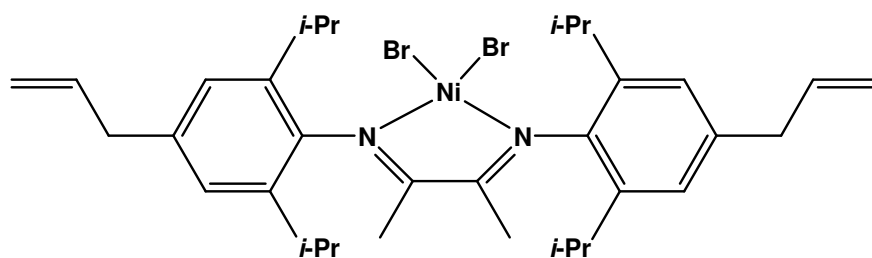
**Table 1. GPC results of the polyethylenes produced by the catalysts 4f, 5f, and 6f.**

Complex Number	ortho-substituents	Mw ( g/mol )	MWD
<b>4f</b>	<b>Me</b>	<b>362916</b>	<b>4.34</b>
<b>5f</b>	<b>Et</b>	<b>422106</b>	<b>3.96</b>
<b>6f</b>	<b><i>i</i>-Pr</b>	<b>1153553</b>	<b>3.93</b>

The GPC results showed an increase in the molecular weights and a decrease in the molecular weight distributions when increasing the bulk of the ortho substituents at the arene moieties. The results can be explained by referring to the chain running mechanism suggesting that the bulkier the ortho substituents the more hinderance at the axial plane of the nickel center. This causes a slow chain transfer relative to chain propagation and thus, a polyethylene with higher molecular weight will be produced.

#### 2.1.4.3 Polymerization experiments with the complex 8

Compound **8** is an  $\alpha$ -diimine nickel complex bearing two allyl groups at the para positions of the arene moieties. The complex was prepared via reacting the dibromo(1,2-dimethoxyethane)nickel(II) (NiBr<sub>2</sub>.DME) with compound **7**. The structure of complex **8** is shown in Scheme 43.

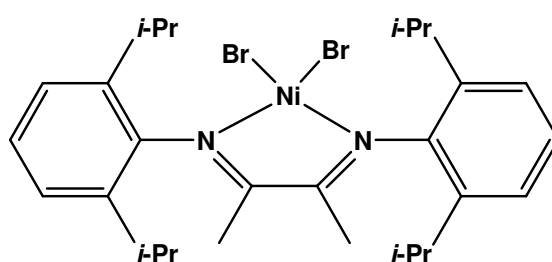
**Scheme 43. The structure of  $\alpha$ -diimine complex 8.**

Complex **8** was activated with MAO, the M:Al ratio was 1:1500. The catalyst was tested for the polymerization of ethylene using the same polymerization conditions as for the nickel catalyst **6f**. The catalyst **8** demonstrated higher polymerization activity than catalyst **6f** by a factor of one and a half. The ethylene polymerization results are listed in Table 2.

**Table 2. Polymerization results of the catalysts 6f and 8.**

Complex Number	Allyl group position	Activity (kg PE / mol cat. h)
<b>6f</b>	at the backbone	<b>3980</b>
<b>8</b>	at the arene moiety	<b>5912</b>

In order to have a better understanding for the effect of introducing allyl groups in the structure of the  $\alpha$ -diimine nickel(II) catalysts at either the backbone or the para positions of the arene moieties, the Brookhart nickel catalyst was prepared according to the literature.<sup>[37]</sup> The structure of the catalyst is shown in Scheme 44.



**Scheme 44. The structure of an  $\alpha$ -diimine nickel(II) catalyst described by Brookhart.**<sup>[37]</sup>

The complexes **6f**, **8**, and Brookhart's nickel complex were activated with MAO, the M:Al ratios were 1:1500. The catalysts were transferred to a 1 l Büchi laboratory autoclave under inert atmosphere and tested for the polymerization of ethylene (in 250 ml of *n*-pentane and 10



the backbone caused by the allyl group reducing the free rotation of the aryl rings. Therefore, the axial coordination sites of the metal center are sterically hindered and the coordination of the ethylene monomer via these axial coordination sites is hindered, too. Accordingly, reduction in the catalyst activity was observed. The reduced activity of catalyst **8** compared to the Brookhart nickel(II) catalyst by a factor of 2.3 is assigned to the allyl groups attached to the arene moieties. These allyl groups have a similar effect to the one attached to the backbone of the catalyst structure except they have less influence on reducing the free rotation of the aryl rings. The allyl groups in the structure of catalyst **8** are away from the coordination plane of the nickel center. Thus, catalyst **8** shows higher polymerization activity than catalyst **6f**.

Samples of the produced polyethylene by the nickel catalysts **6f**, **8**, and the Brookhart catalyst were analyzed by gel permeation chromatography (GPC) to study the effect of introducing allyl groups in the ligand framework of Brookhart nickel(II) catalyst on the molecular weight (MW) of the produced polyethylene. The GPC results are summarized in Table 3.

**Table 3. GPC results of the polyethylenes produced by the catalysts *6f*, *8* and the Brookhart catalyst.**

<b>Complex Number</b>	<b>Allyl group position</b>	<b>Mw ( g/mol )</b>	<b>MWD</b>
<b>6f</b>	at the backbone	<b>1203511</b>	<b>3.97</b>
<b>8</b>	at the arene moiety	<b>792580</b>	<b>4.90</b>
<b>Brookhart catalyst</b>	-	<b>674295</b>	<b>3.64</b>

The GPC results showed that the introduction of allyl groups in the ligand framework of the Brookhart catalyst caused an increase of the molecular weight of the produced polyethylene. The allyl groups at either the para positions of the arene moieties, such as in **8**, or at the

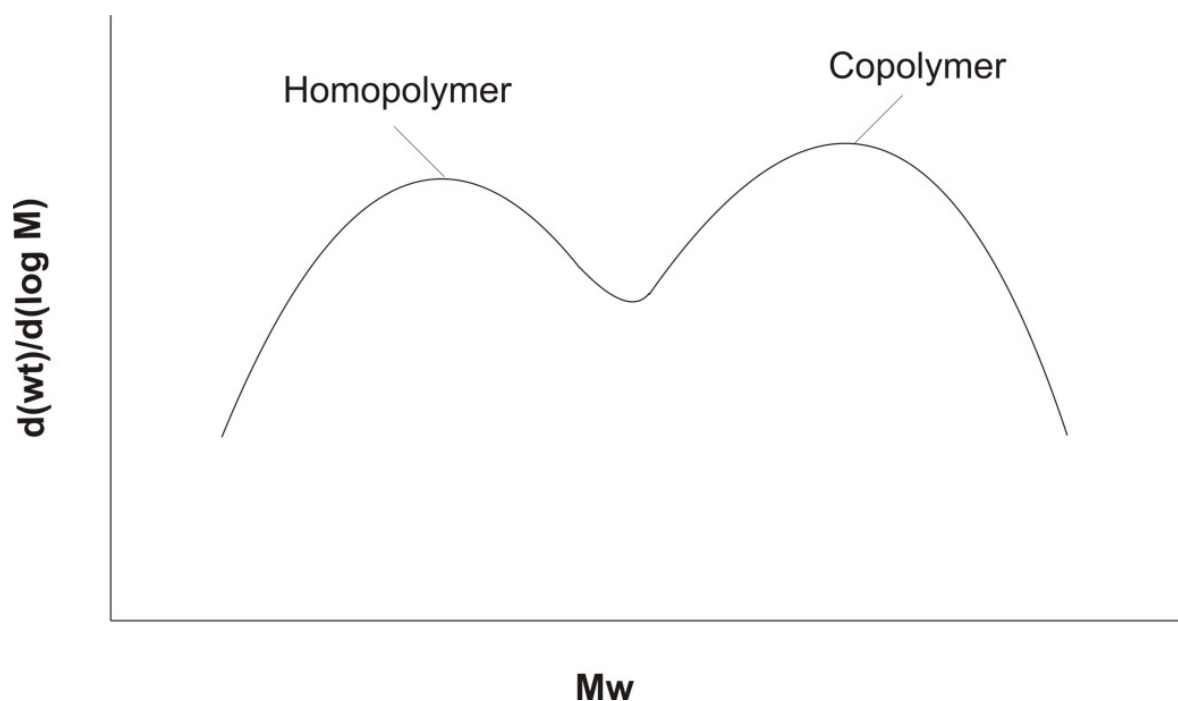
backbone of the catalyst structure, such as in **6f**, can fix the planes of the aryl rings closer to be perpendicular to the coordination plane of the nickel center. The positions of the aryl ring planes cause the ortho substituents at these rings to hinder the axial plane of the nickel center. As a result the chain transfer relative to the chain propagation slows down, and a polyethylene with a high molecular weight is produced. The molecular weight of the polyethylene produced with the nickel catalyst **6f** was higher than the one of **8**. This result can be attributed to the increased hindrance at the axial plane of the nickel center caused by the allyl group at the backbone than the hindrance caused by the allyl group at the para positions of the arene moieties.

## 2.2. Dinuclear complexes of $\alpha$ -diimines coupled with an ansa zirconocene unit

### 2.2.1 General

#### 2.2.1.1 Preview of dinuclear complexes

The use of single site catalysts for olefin polymerization reactions has the disadvantage of producing narrow molecular weight distributions (MWD) due to the identical active sites of the catalyst. This can cause problems for industrial processings like extrusion or injection moulding. The solution is to have polyolefins with bimodal or broader MWDs. Polyolefins having a bimodal MWD are desirable because they can combine the advantageous mechanical properties of the high molecular weight fraction, such as toughness, strength, and environmental stress cracking resistance, with the improved processing properties of the low molecular weight fraction. An ideal polyolefin would consist of a low molecular weight homopolymer and a high molecular weight copolymer.<sup>[111]</sup>

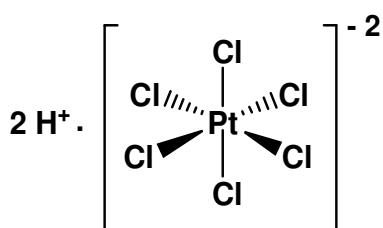


**Scheme 46.** The ideal molecular weight distribution of polyolefins for technical processing.<sup>[111]</sup>

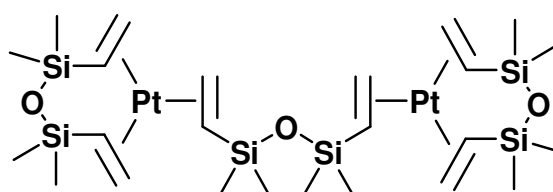
There are several methods for the production of polyolefin resins with bimodal or broad molecular weight distributions: melt blending, reactor in series configuration, or single reactor with dual site catalysts. Melt blending suffers from the disadvantages brought on by the requirement of complete homogenization and high cost. The method of having two reactors linked in series results in an expensive production due to the costly process required. The method of using dual site catalysts in a single reactor is widely employed.<sup>[111-133]</sup> In most cases, mixtures of two mononuclear catalysts often lead to resins with averaged molecular weights while the dinuclear catalysts containing combined ligand frameworks seemed to produce resins with bimodal or broad molecular weight distributions when the metal centers are kept separately from each other by the ligand frameworks.

### 2.2.1.2 Preview of hydrosilylation reaction

The hydrosilylation reaction involves the addition of a hydrosilane unit (Si-H) onto a carbon-carbon double or triple bond to generate an alkyl- or a vinylsilane. The significance of this reaction is assigned to the produced organosilicon compounds which are useful as intermediates in organic synthesis.<sup>[134-138]</sup> Several electron-rich complexes of late transition metals such as Co(I), Rh(I), Ni(0), Pd(0), or Pt(0) are used to activate the hydrosilylation reaction while the most used catalysts are Speier's catalyst<sup>[139-142]</sup> (chloroplatinic acid,  $\text{H}_2\text{PtCl}_6$ ) and Karstedt's catalyst<sup>[143-144]</sup> ( $\text{Pt}_2\{[(\text{CH}_2=\text{CH})\text{Me}_2\text{Si}]_2\text{O}\}_3$ ).



**Speier's catalyst**

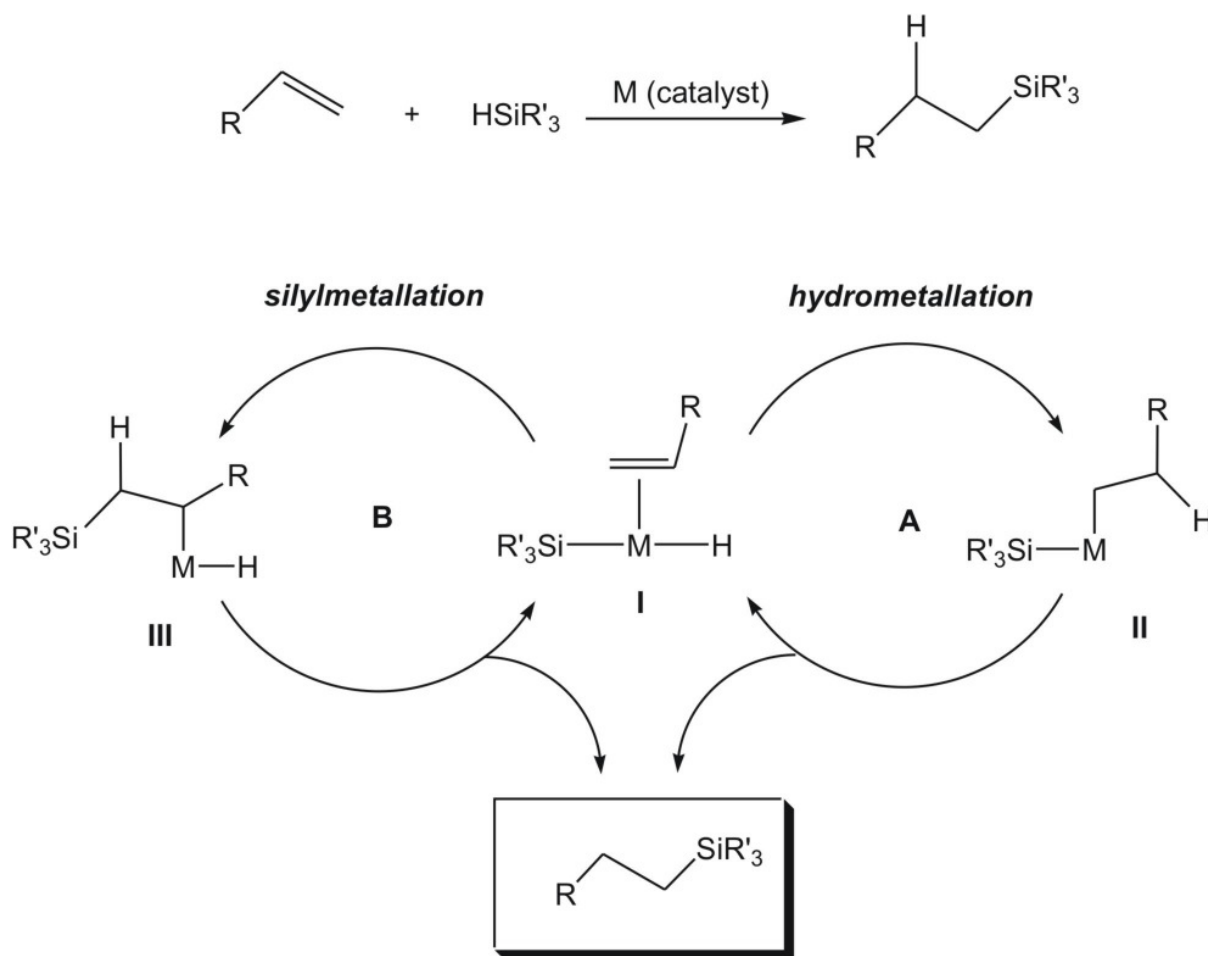


**Karstedt's catalyst**

**Scheme 47. The structure of Speier's and Karstedt's catalysts.**

The hydrosilylation reaction is generally assumed to proceed by the Chalk-Harrod mechanism<sup>[145-148]</sup> (cycle A, in Scheme 48) or the modified Chalk-Harrod mechanism<sup>[149-154]</sup> (cycle B) depending on the substituents on the silicon atom and the nature of the metal

catalyst.<sup>[148]</sup> The Chalk-Harrod mechanism suggests an oxidative addition of a hydrosilane giving a hydrido-silyl complex (I) which is coordinated with the substrate alkene. Complex I undergoes migratory insertion of the alkene into the M-H bond (*hydrometallation*) to give the alkyl-silyl species (II). Reductive elimination of the alkyl and silyl ligands from the alkyl-silyl species II forms the hydrosilylation product. The modified Chalk-Harrod mechanism has been proposed as an alternative mechanism which involves preferentially an alkene insertion into the M-Si bond (*silylmetallation*) to form the  $\beta$ -silylalkyl-hydrido intermediate (III), followed by reductive elimination to complete the hydrosilylation.



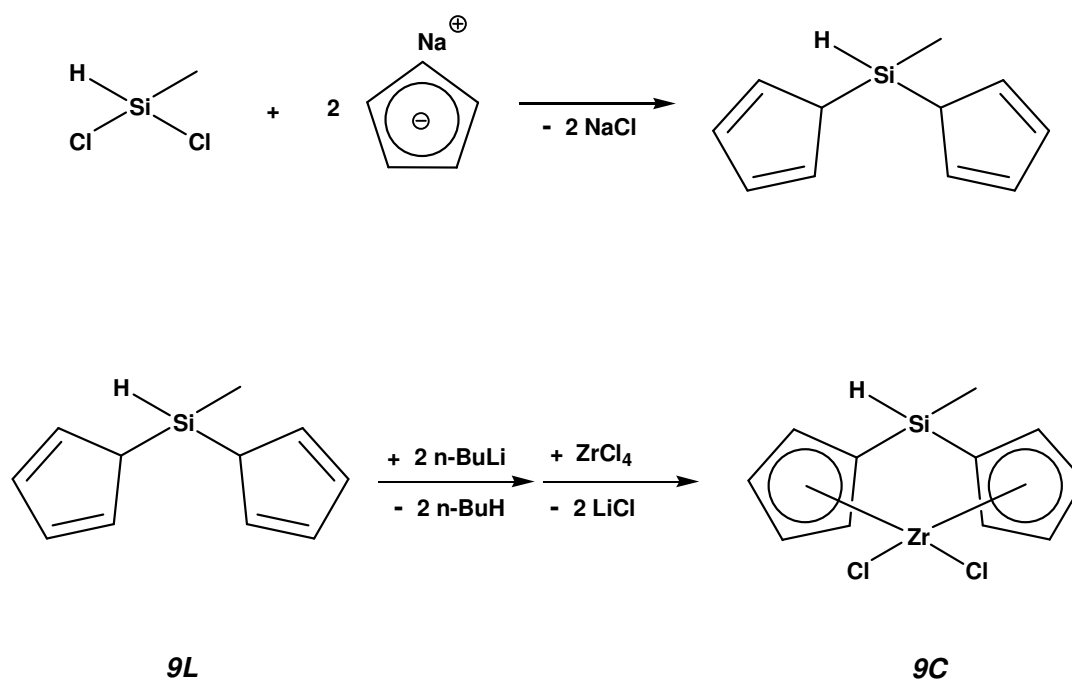
**Scheme 48. The proposed mechanisms of hydrosilylation reaction.**

The hydrosilylation reaction has been used to synthesize dinuclear or multinuclear complexes via coupling two or more moieties where at least one contains a hydride silane and the other possesses an alkenyl group.<sup>[155-159]</sup> The two moieties can be either two mononuclear complexes or two organic compounds which can coordinate metal centers.

Herein, the complexes **4a-g**, **5a-g**, and **6a-g** bear allyl groups which can be coupled with a complex possessing a hydride silane moiety via hydrosilylation reaction to afford a dinuclear complex.

### 2.2.2 Synthesis and characterization of complex **9C**

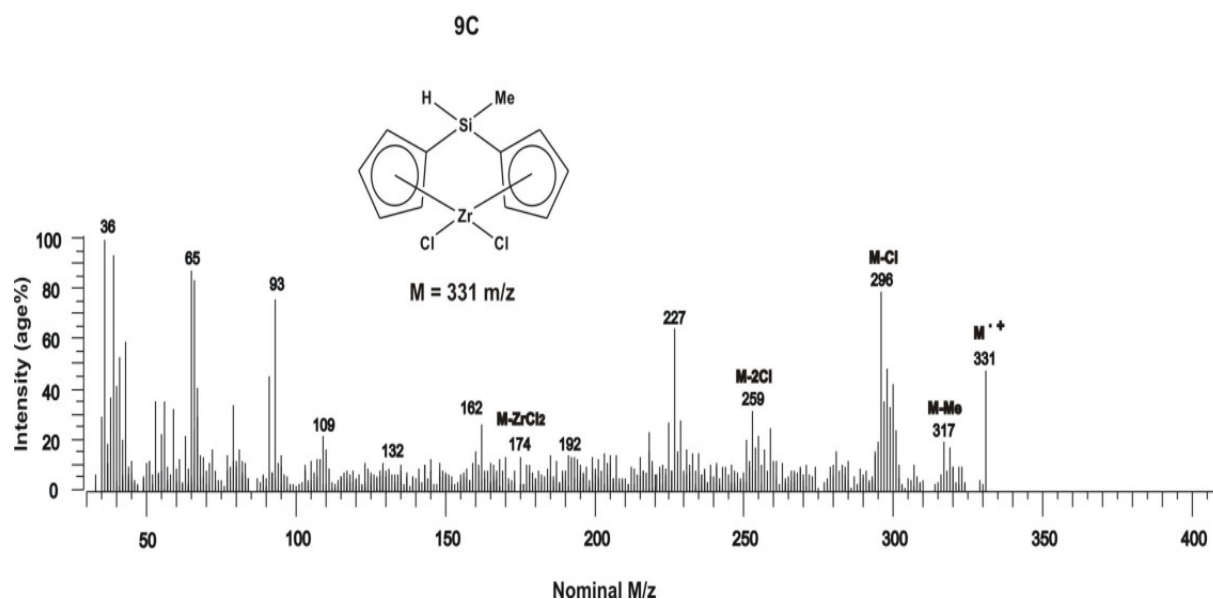
Bis(cyclopentadienyl)methyl silane **9L** was prepared first via reacting methylchlorosilane with two equivalents of sodium cyclopentadienide to produce the compound **9L** by salt elimination reaction. The next step was treating the **9L** with two equivalents of n-butyllithium (n-BuLi) followed by the addition of zirconium tetrachloride ( $\text{ZrCl}_4$ ) to yield the silyl bridged zirconocene complex **9C**. The synthesis equations for the compound **9L** and the complex **9C** are shown in Scheme 49.



**Scheme 49.** The synthesis of compound **9L** and the complex **9C**.

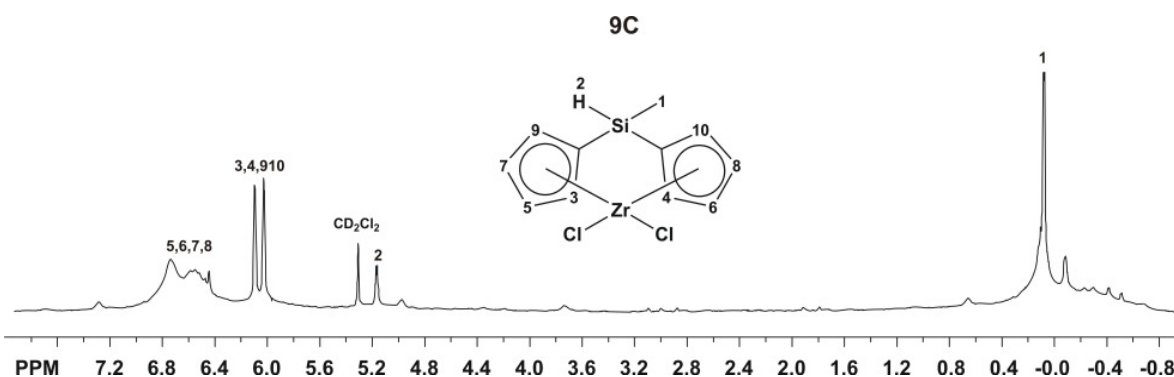
Compound **9L** was characterized by GC-MS while the complex **9C** was characterized via mass spectroscopy,  $^1\text{H}$  NMR and  $^{13}\text{C}$  NMR spectroscopy, and elemental analysis (see the appendices for full analysis data).

The mass spectrum of complex **9C** (see Scheme 50) shows the peak of the molecular ion at  $m/z = 331$  with an intensity of 48% relative to the base peak. The loss of a methyl group results in a peak with an intensity of 18% at  $m/z = 317$  while the peak at  $m/z = 296$  (intensity 78%) is assigned to the loss of a chloro substituent. The peak appearing at  $m/z = 259$  (intensity 23%) is produced by the loss of two chloro groups while further loss of the zirconium center yields the ligand fragment at  $m/z = 174$  with an intensity of 14%.



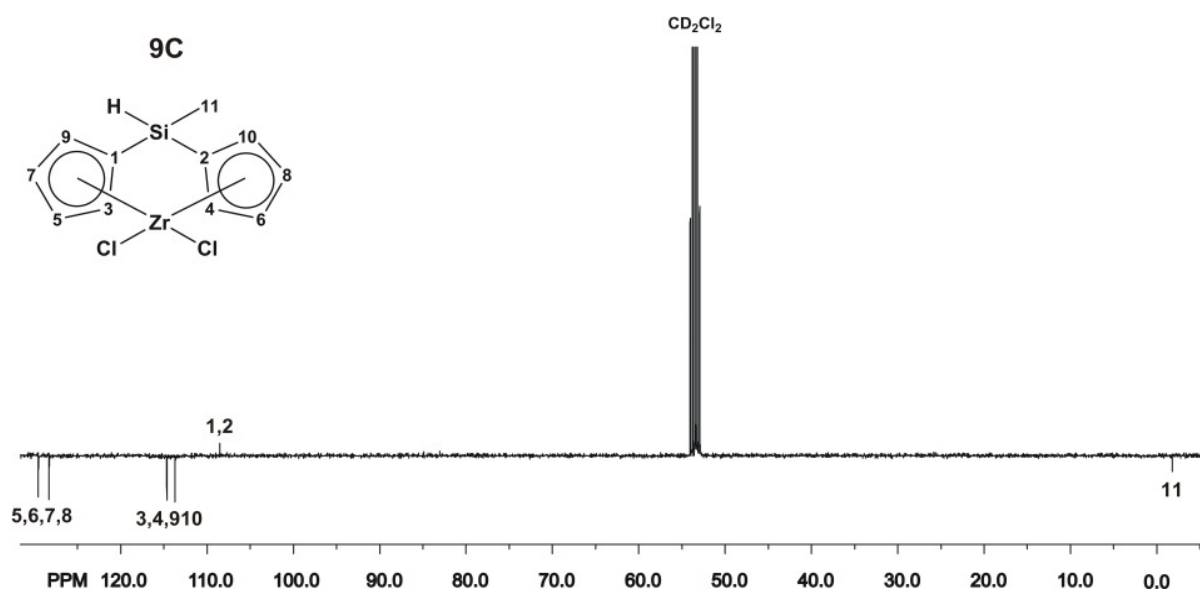
**Scheme 50. Mass spectrum of complex 9C.**

The  $^1\text{H}$  NMR spectrum of complex **9C** (see Scheme 51), shows a multiplet signal at  $\delta = 6.80\text{--}6.40$  ppm which is assigned to the protons of the cyclopentadienyl rings (5, 6, 7, 8) while the other protons (3, 4, 9, 10) produce the doublet signal at  $\delta = 6.10$  ppm. The signal of the proton attached to the silicon atom appears at  $\delta = 5.16$  ppm. The intensive singlet signal at  $\delta = 0.10$  ppm is produced by the methyl group bonded to the silicon atom.



**Scheme 51.**  $^1\text{H}$  NMR spectrum of the complex **9C**.

The  $^{13}\text{C}$  NMR spectrum of compound **9C** (see Scheme 52) shows the signals of the carbon atoms of the cyclopentadienyl rings (5, 6, 7, 8) at  $\delta = 130.0$  and  $128.0$  ppm while the other carbon atoms (3, 4, 9, 10) produce the signals at  $\delta = 115.0$  and  $114.0$  ppm. The quaternary carbon atoms of the cyclopentadienyl rings yield the signal at  $\delta = 108.0$  ppm while the signal at low chemical shift ( $\delta = -2.0$  ppm) is produced by the methyl group bonded to the silicon atom.



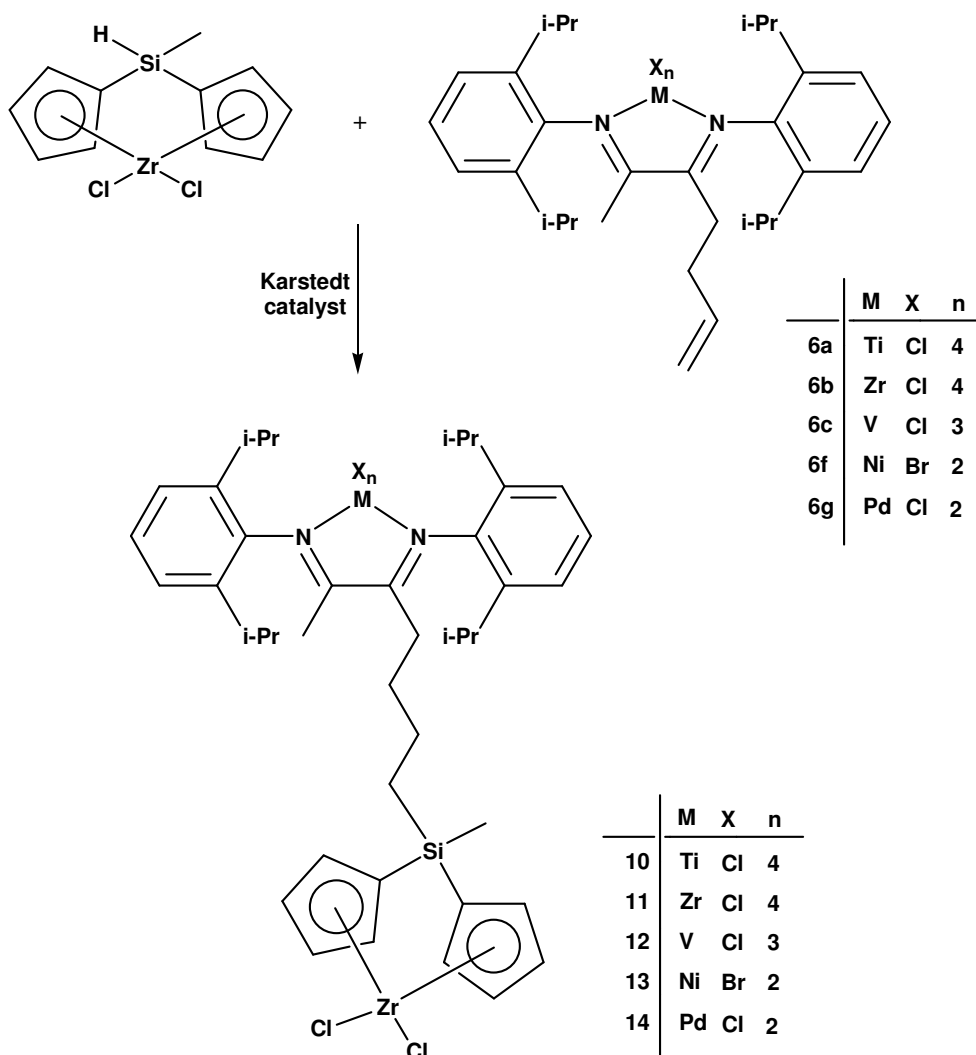
**Scheme 52.**  $^{13}\text{C}$  NMR spectrum of complex **9C**.

The synthesis of complex **9C** which possesses a hydride silane moiety affords one of the two required complexes for preparing a dinuclear precursor via hydrosilylation reaction. The other required complex can be one of the  $\alpha$ -diimine compounds **4a-g**, **5a-g**, and **6a-g** which

bear terminal alkenyl groups. Five new dinuclear precursors were synthesized by combining complex **9C** with some  $\alpha$ -diimine compounds as will be described hereafter.

### 2.2.3 Synthesis and characterization of complexes **10-14**

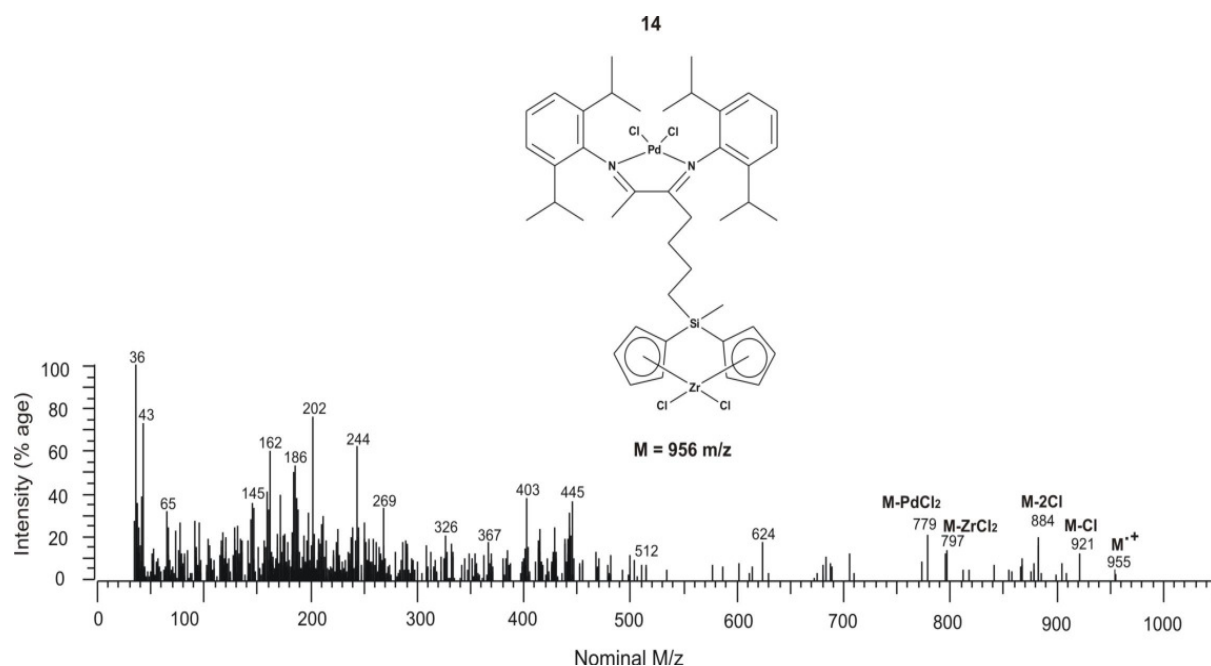
The silyl bridged zirconocene complex **9C** was coupled with the  $\alpha$ -diimine complexes **6a-c**, **6f**, and **6g** via hydrosilylation reaction using Karstedt's catalyst, platinum(0)-1,3-divinyl-1,1,3,3-tetramethyldisiloxane (0.1 M in xylene), to produce the corresponding dinuclear precursors **10-14**. The structures and the synthesis equation of these precursors are shown in Scheme 53.



Scheme 53. The synthesis of the dinuclear complexes **10-14**.

The dinuclear complexes **10-14** were characterized via mass spectroscopy and elemental analysis while complex **14** was characterized by  $^1\text{H}$  NMR spectroscopy too, (see the appendices for the full analysis data). The mass and NMR spectra of complex **14** will be discussed as example.

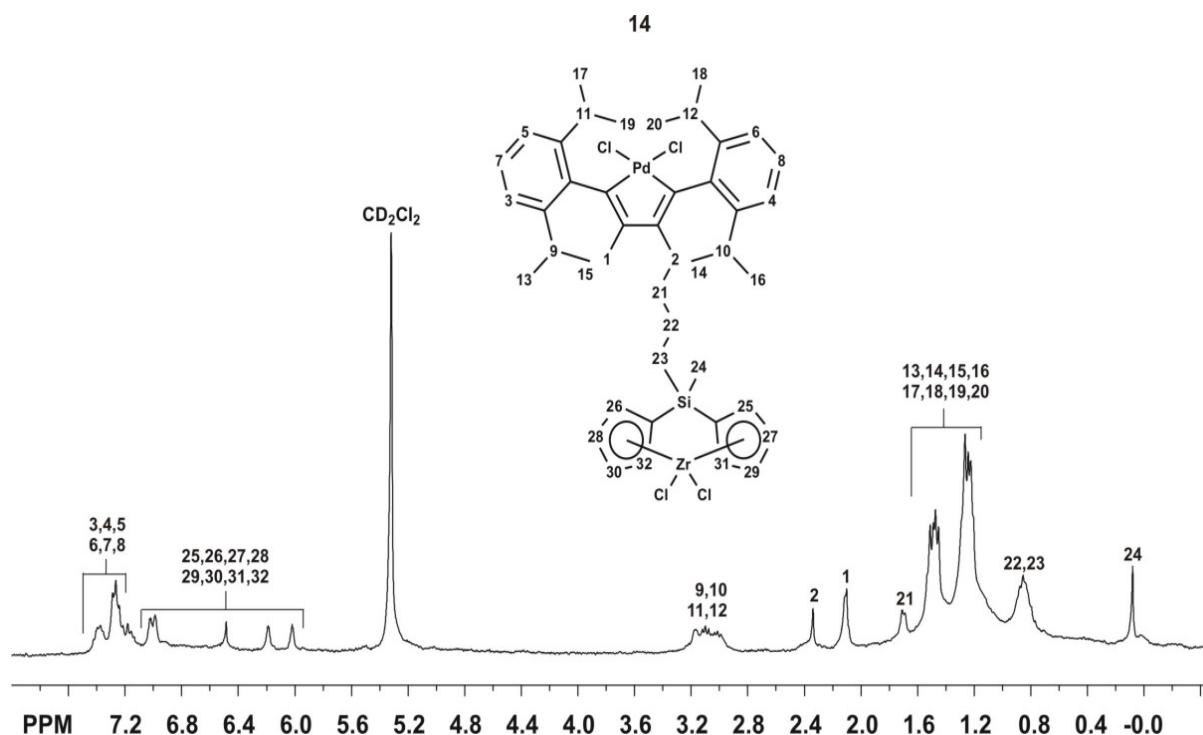
The mass spectrum of complex **14** (see Scheme 54), shows the peak of the molecular ion at  $m/z = 955$  with an intensity of 5% relative to the base peak. The dissociation of a chloro substituent results in a peak with an intensity of 13% at  $m/z = 921$  while the peak at  $m/z = 884$  with an intensity of 16% is assigned to further loss of another chloro group. The peak appearing at  $m/z = 797$  with an intensity of 15% is produced by the dissociation of the zirconium dichloride moiety while the loss of the palladium dichloride center yields the fragment at  $m/z = 779$  with an intensity of 20%.



**Scheme 54. Mass spectrum of the dinuclear complex 14.**

The  $^1\text{H}$  NMR spectrum of complex **14** (see Scheme 55) shows a multiplet signal at  $\delta = 7.40$ - $7.20$  ppm which is assigned to the protons of the aromatic rings while the signals at  $\delta = 7.00$ ,  $6.50$ ,  $6.20$ , and  $6.00$  ppm are attributed to the protons of the cyclopentadienyl rings. The CH groups of the isopropyl functions yield the multiplet signal at  $\delta = 3.10$  ppm while the

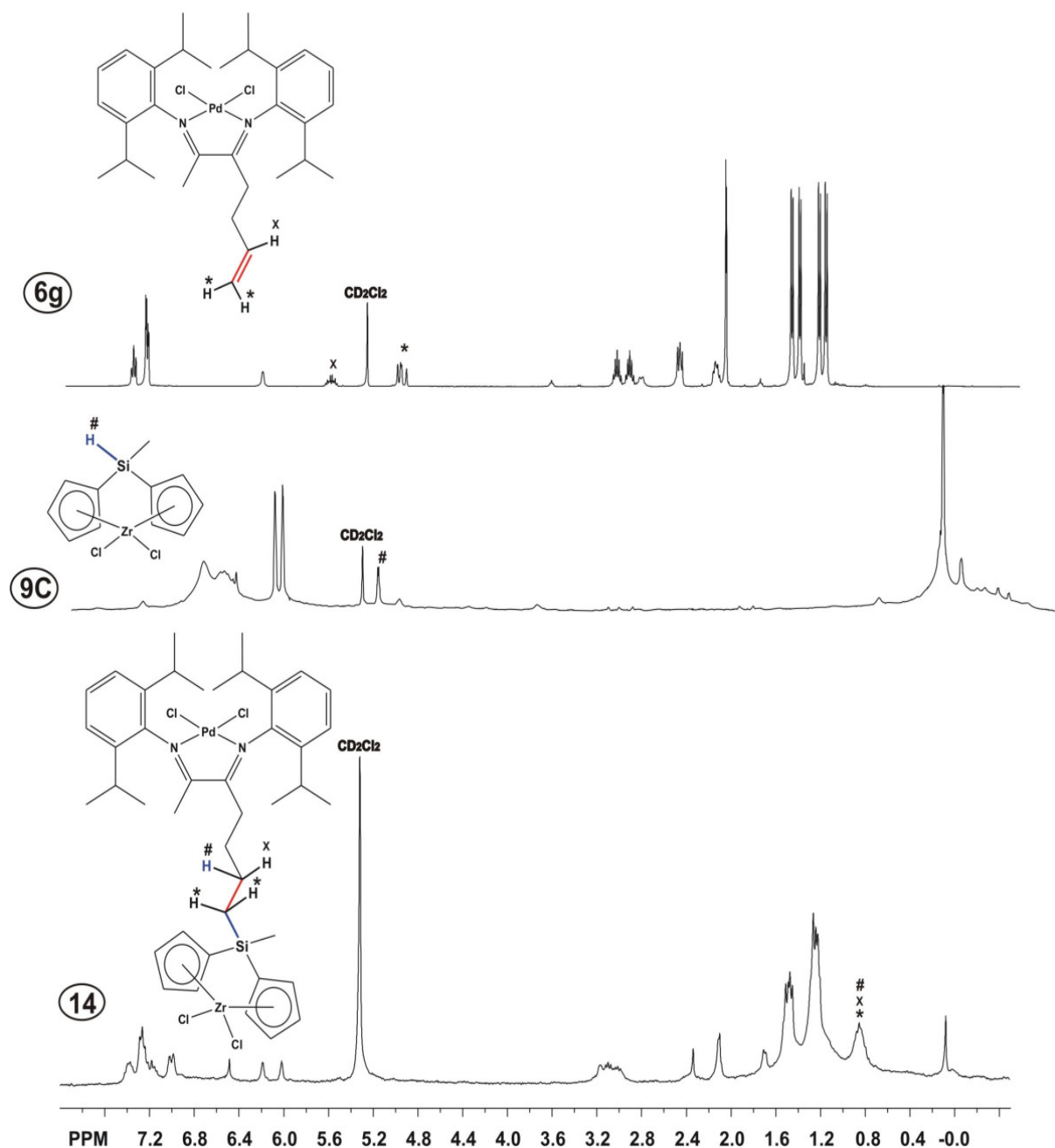
methylene group (2) produces the signal at  $\delta = 2.35$  ppm. The singlet signal at  $\delta = 2.10$  ppm is assigned to the methyl group bonded to the diimine moiety while the methylene group (21) affords the signal at  $\delta = 1.70$  ppm. The methylene groups of the isopropyl functions produce the multiplet signals at  $\delta = 1.50$  and 1.30 ppm. The methylene groups (22, 23) generate a broad signal at  $\delta = 0.90$  ppm while the singlet signal at  $\delta = 0.10$  ppm is attributed to the methyl group attached to the silicon atom.



**Scheme 55.**  $^1\text{H}$  NMR spectrum of the dinuclear complex **14**.

The  $^1\text{H}$  NMR spectrum of complex **14** proves the completion of the hydrosilylation reaction when it was compared with the  $^1\text{H}$  NMR spectra of the starting complexes **6g** and **9C** (see Scheme 56). The spectrum of complex **14** shows the disappearance of three proton signals:

- The two signals observed from the spectrum of complex **6g** at  $\delta = 5.64$  and 5.01 ppm which are assigned to the protons of the terminal double bond ( $-\text{CH}=\text{CH}_2$ ) of the allyl group.
- The signal produced by the proton of the silane group in the spectrum of complex **9C** which appears at  $\delta = 5.16$  ppm.



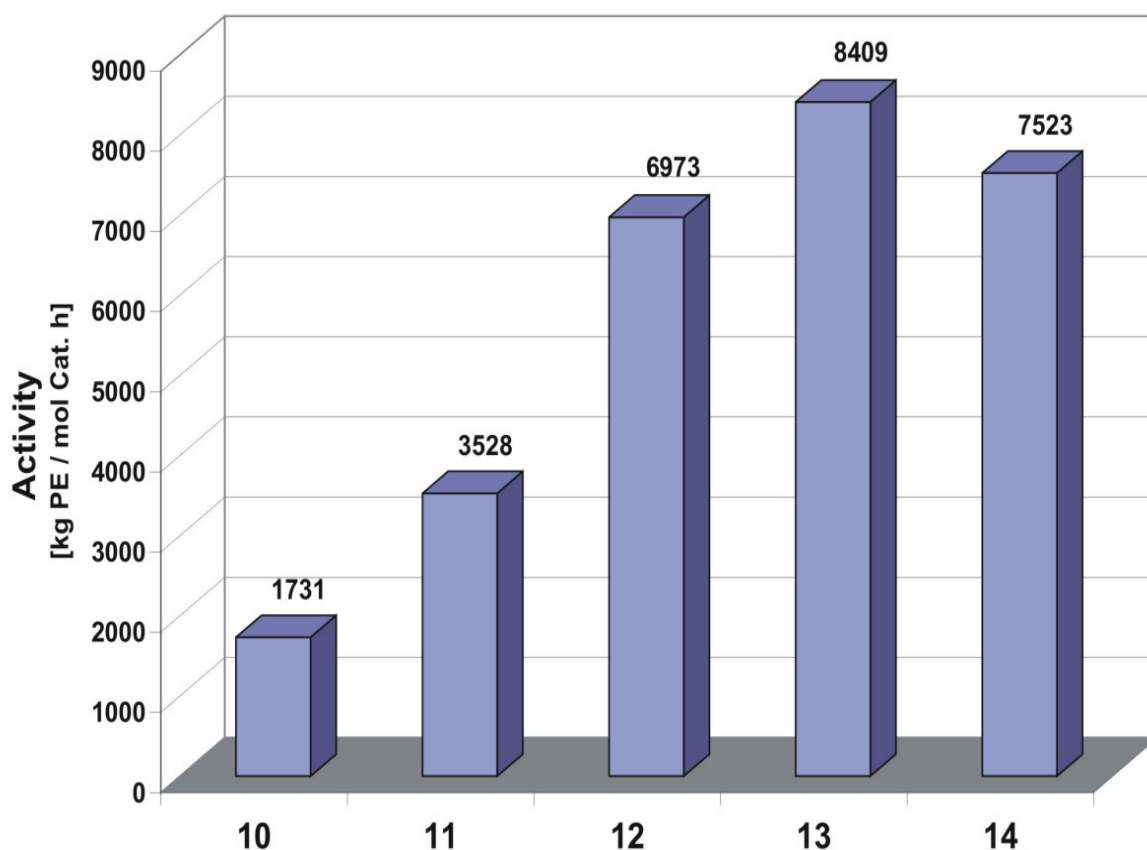
**Scheme 56.** Comparison of the  $^1\text{H}$  NMR spectrum of the dinuclear complex **14** with the spectra of complexes **6g** and **9C**.

The disappearance of these signals can be explained by the addition of the hydrosilane group (Si-H) into the double bond of the allyl function, the hydrosilylation reaction. The evidence of this addition is observed from the formation of a new signal at  $\delta = 0.90$  ppm which is attributed to the methylene groups of the linkage (-CH<sub>2</sub>-CH<sub>2</sub>-Si-) replacing the terminal double bond of the allyl group (-CH=CH<sub>2</sub>). Hence, the proton NMR spectroscopy assisted to evince and monitor the hydrosilylation reaction.

## 2.2.4 Polymerization experiments with the dinuclear complexes **10-14** and complex **9C**

The dinuclear complexes **10-14** were suspended in toluene and activated with methylaluminoxane (MAO), the M:Al ratio was 1:1500. The activated complexes were transferred to a 1 l Büchi laboratory autoclave under inert atmosphere and tested for the polymerization of ethylene (in 250 ml of *n*-pentane, 10 bar ethylene, and a polymerization temperature of 65°C).

The bridged silyl zirconocene moiety is the same for all dinuclear complexes **10-14**. Therefore, the polymerization activities of the catalysts **10-14** are expected to show dependence on the variant metal centers of the  $\alpha$ -diimine moiety. The results of ethylene polymerization using the dinuclear catalysts **10-14** were illustrated in Scheme 57.



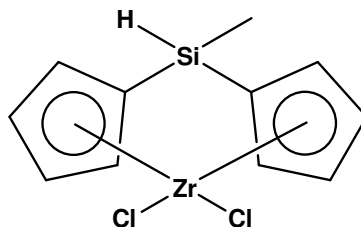
Scheme 57. The polymerization activities of the dinuclear complexes **10-14**.

The mononuclear complex **6g** which was used to prepare the dinuclear precursor **14** showed no polymerization activity while the dinuclear catalyst **14** produced polyethylene with the second highest activity among the dinuclear series **10-14**. This result can be explained hereinafter. The inactivity of the catalyst **6g** is assigned to the allyl functions attached to the backbone of the ligand frameworks which can interact with the active sites of the metal centers resulting in blocking the active sites and deactivating the catalyst. In the hydrosilylation reaction used to prepare the dinuclear precursor **14**, the allyl function of complex **6g** reacted with the silane group of complex **9C** and disappeared upon forming the silyl-alkyl link coupling the two dinuclear moieties. Consequently, both catalytic parts of the dinuclear catalyst **14** can polymerize ethylene. The ethylene polymerization activities of the dinuclear catalysts **10-13** were almost double of the activities of their analogous  $\alpha$ -diimine precursors **6a-c** and **6f** (see table 4). The trend resulting from the change in polymerization activity by changing the metal center of the dinuclear catalysts **10-13** was the same observed for the catalysts **6a-c** and **6f**.

**Table 4. Comparison of the polymerization activities of the dinuclear catalysts 10-14 versus the catalysts 6a-c, 6f, and 6g.**

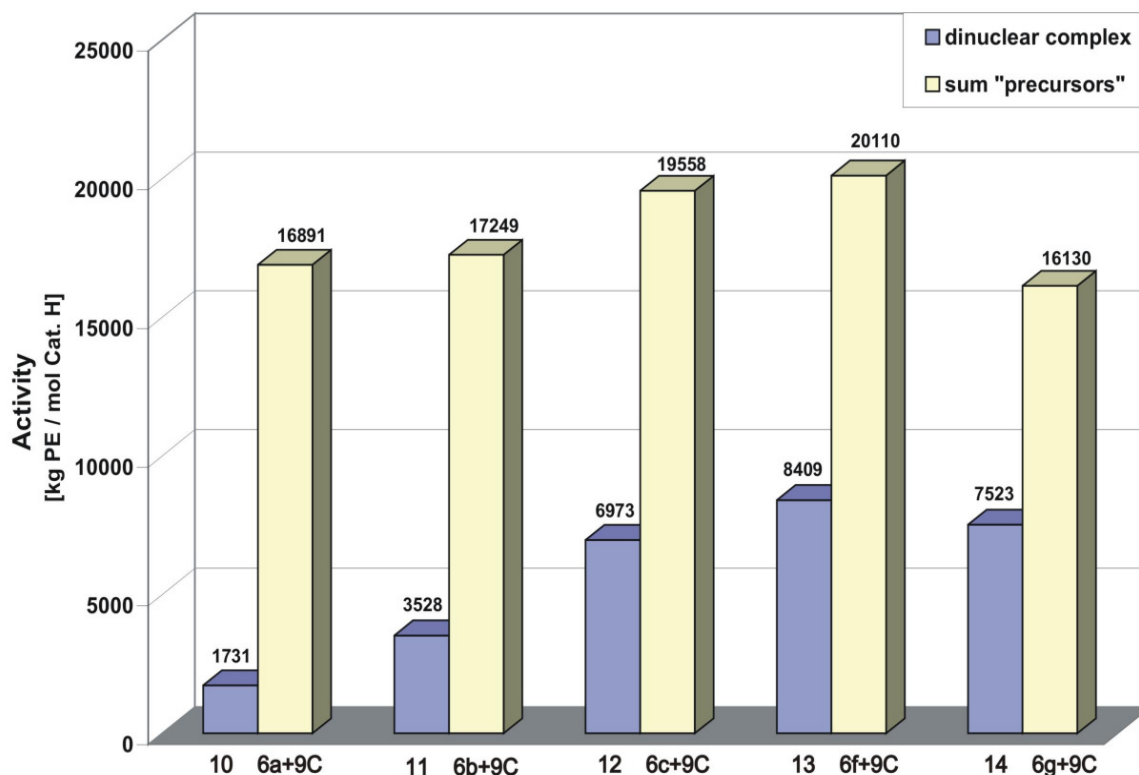
<b>Complex No.</b>	<b>Activity (kg PE / mol Cat. h)</b>	<b>Complex No.</b>	<b>Activity (kg PE / mol Cat. h)</b>
<b>6a</b>	761	<b>10</b>	1731
<b>6b</b>	1119	<b>11</b>	3528
<b>6c</b>	3428	<b>12</b>	6973
<b>6f</b>	3980	<b>13</b>	8409
<b>6g</b>	0	<b>14</b>	7523

For comparison, the silyl bridged zirconocene complex **9C** (see Scheme 58) was activated with MAO, the Zr:Al ratio was 1:1500. The catalyst was tested for the polymerization of ethylene using the same polymerization conditions of the dinuclear catalysts **10-14**.



**Scheme 58. Structure of the silyl bridged zirconocene complex 9C.**

The ethylene polymerization activity of the silyl bridged zirconocene catalyst **9C** was 16130 kg PE / mol Cat. h. The dinuclear catalysts **10-14** showed lower polymerization activities compared to the summarized activities of their mononuclear precursors (see Scheme 59).



**Scheme 59. Comparison of the ethylene polymerization activities of the dinuclear complexes 10-14 and their "precursor" complexes.**

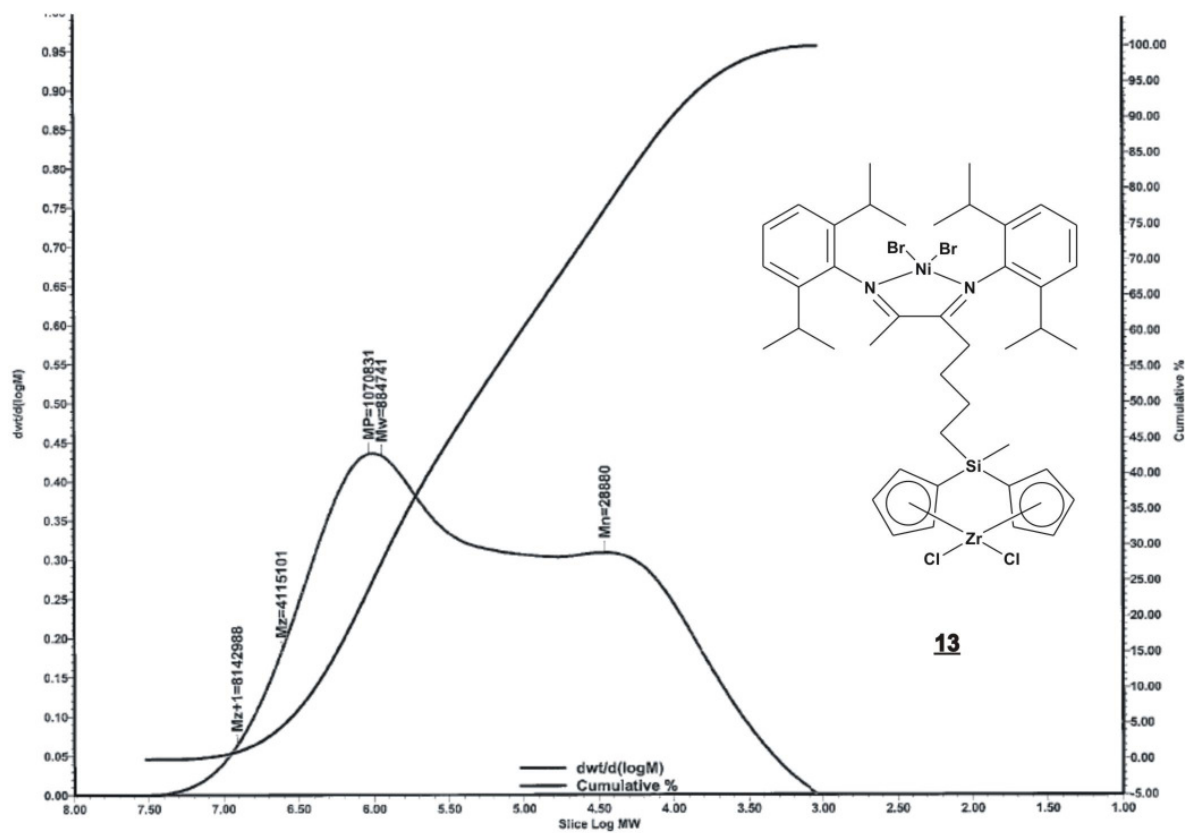
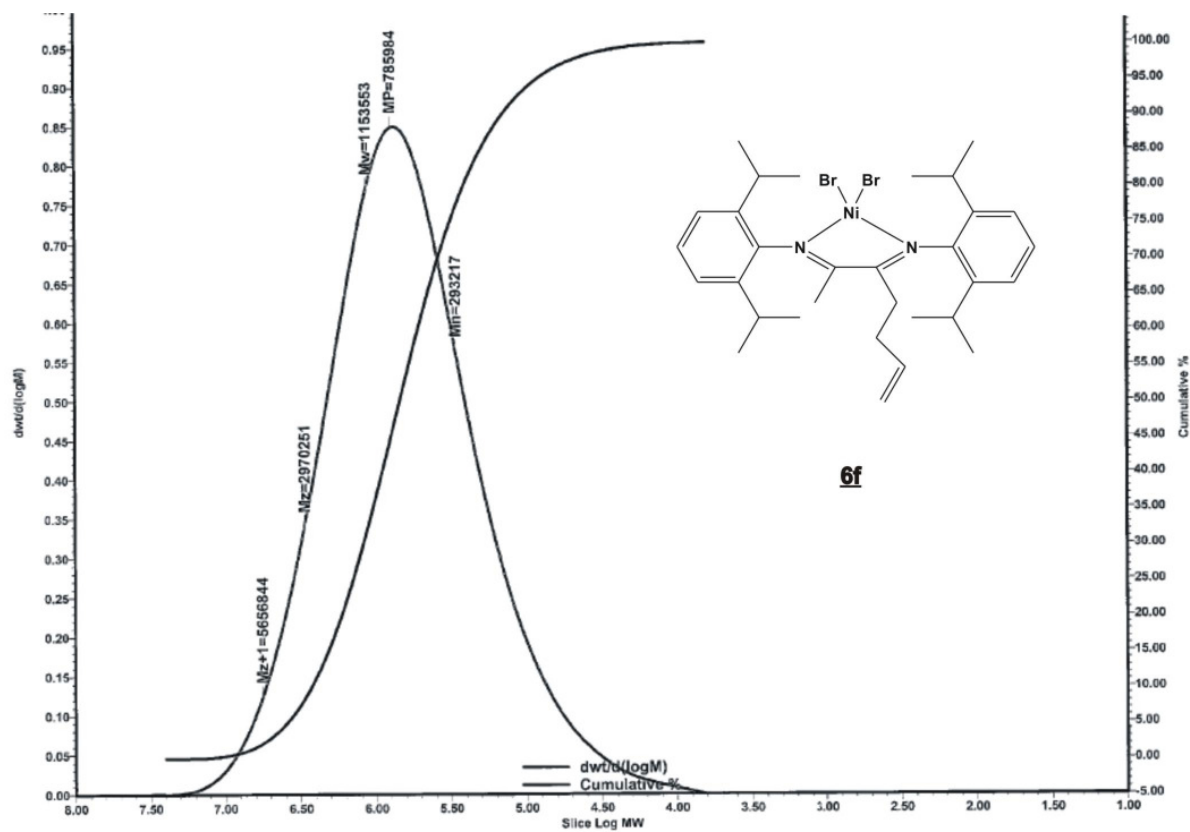
These low activities are attributed to the reduced activity of the silyl bridged zirconocene complex when coupled with the  $\alpha$ -diimine precursors **6a-c**, **6f**, and **6g**. The coupling increases the steric hindrance around the active zirconium sites and prevents the ethylene molecules from reaching these sites leading to a reduced activity.

Samples of the produced polyethylene by the dinuclear catalysts **11-13** and the single site catalyst **9C** were analyzed by gel permeation chromatography (GPC). The GPC results are summarized in Table 5.

**Table 5. GPC results of the polyethylenes produced by the dinuclear catalysts 11-13 and the catalyst 9C.**

<b>Complex Number</b>	<b>Mw (g/mol)</b>	<b>Mn (g/mol)</b>	<b>MWD</b>
<b>11</b>	<b>392266</b>	<b>8323</b>	<b>47.13</b>
<b>12</b>	<b>763410</b>	<b>10251</b>	<b>74.47</b>
<b>13</b>	<b>884741</b>	<b>28880</b>	<b>39.43</b>
<b>9C</b>	<b>200745</b>	<b>69556</b>	<b>2.89</b>

The GPC spectra of the polyethylenes produced with the dinuclear catalysts displayed the desired broad or bimodal molecular weight distributions due to the dual site catalysts. The molecular weight of the polyethylene resulting from the silyl bridged zirconocene catalyst **9C** is 200745 g/mol. Consequently, the ansa zirconocene unit of the dinuclear precursors is estimated to produce the lower molecular weight fraction. The GPC spectrum of polyethylene produced with the dinuclear catalyst **13** will be discussed as example and will be compared to the GPC spectrum of polyethylene produced with its mononuclear catalyst **6f** (see Scheme 60).



Scheme 60. GPC spectra of the polyethylenes produced with the mononuclear catalyst **6f** (top) and the dinuclear catalyst **13** (bottom).

The GPC spectrum of the polyethylene resulting from the nickel catalyst **6f** shows a narrow molecular weight distribution (MWD = 3.93) while a broad molecular weight distribution (MWD = 39.43) is afforded by the polyethylene of the dinuclear catalyst **13**. The nickel center of the dinuclear catalyst **13** yielded the higher molecular weight fraction.

## 2.3. *Dinuclear complexes of $\alpha$ -diimines coupled with half sandwich complexes*

### 2.3.1 General

Hydrosilylation reactions are convenient routes for connecting two mononuclear complexes to tailor dinuclear precursors for producing polyethylene resins having specific molecular weight distributions. Although these methods are simple approaches to afford dinuclear complexes in one step reactions, they may encounter purification difficulties when the coupling reactions do not produce the ultimate yield. These difficulties arise from the similarities in solubilities between the unreacted mononuclear complexes and the produced dinuclear precursors in addition to the need of performing the purification work under inert gas atmosphere due to the instability of these precursors when they are exposed to air. Consequently, the purification process will probably lower the yield of the produced dinuclear complexes.

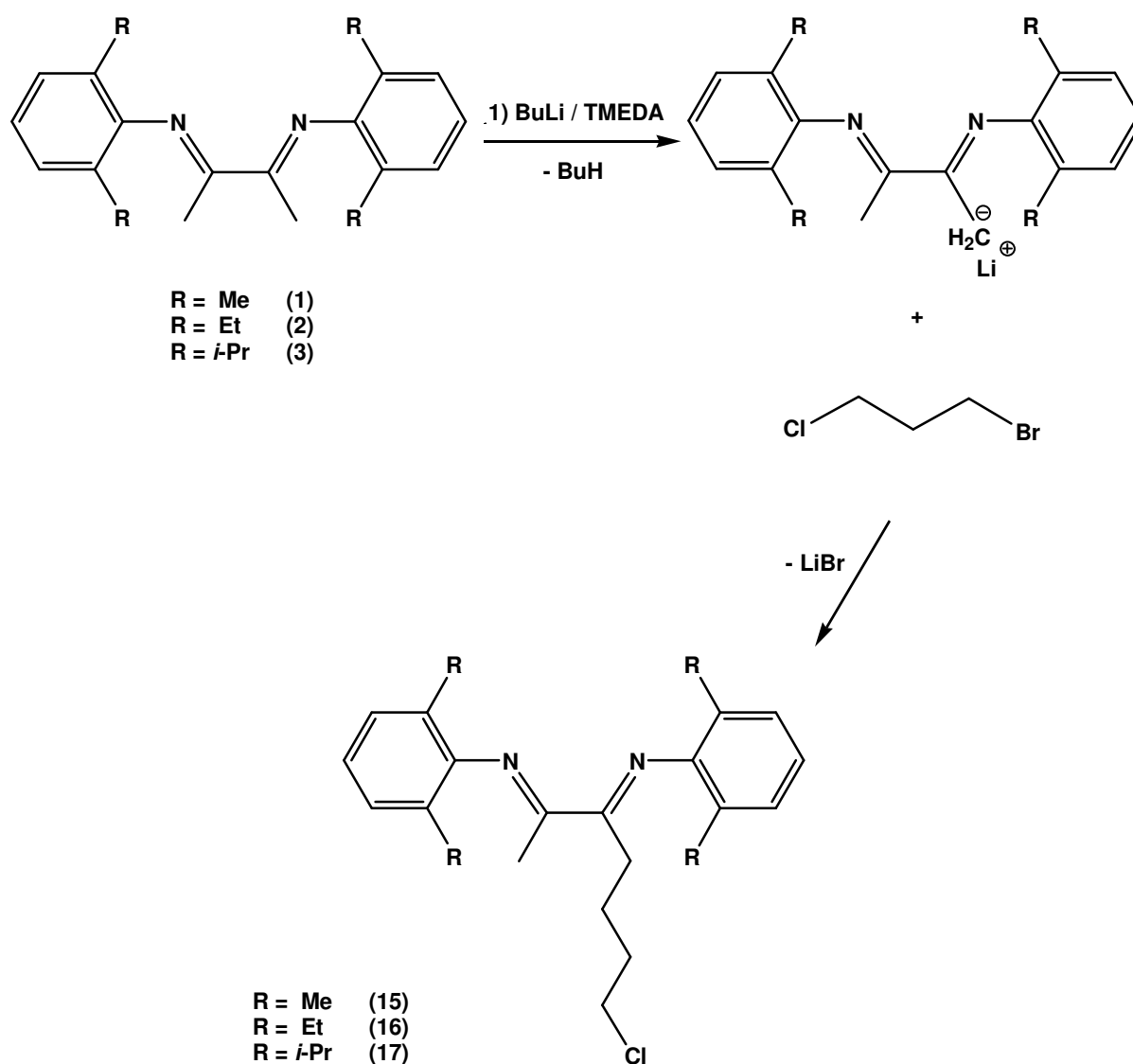
The method of preparing a potential organic ligand possessing two different moieties which are able to coordinate two different metal centers can be an alternative method to synthesize dinuclear complexes.<sup>[114,129,133,156-158]</sup> This method will help to avoid the purification difficulties facing the method of coupling two complexes because of the ease of separation and the higher stability of the organic ligand compared to the complex.

Herein, some  $\alpha$ -diimine compounds bearing different ortho substituents at their aryl rings were modified to have cyclopentadienyl groups. These modified compounds were easily synthesized and purified with good yields to be promising ligand systems for dinuclear complexes. The  $\alpha$ -diimine moiety can coordinate early or late transition metals while the cyclopentadienyl group can combine an early transition metal to afford a half sandwich complex. These modified  $\alpha$ -diimine compounds are able to generate dinuclear complexes with only one metal salt. The different molecular weights of the polyethylenes produced by the  $\alpha$ -diimine and the half sandwich catalysts make their combination to be an elegant system to produce bimodal or broad molecular weight distributions.

## 2.3.2 Synthesis and characterization of the "free ligands"

### 2.3.2.1 Synthesis and characterization of compounds 15-17

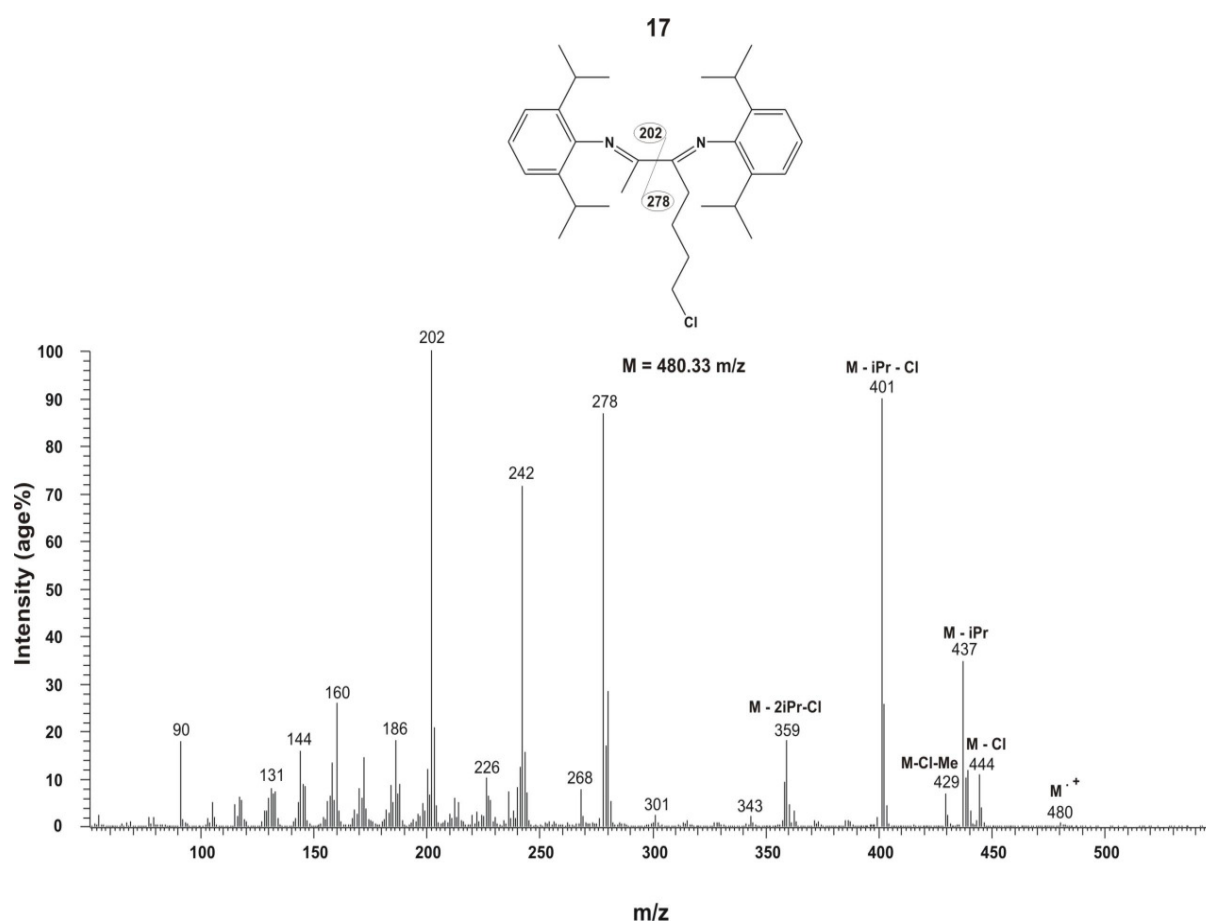
The compounds **15** – **17** containing  $\alpha$ -diimine moieties bearing chloro-alkyl groups at the backbone of the ligand structures were synthesized via metalating the appropriate  $\alpha$ -diimine compound **1**, **2**, or **3** by a 1:1 mixture of *n*-butyllithium (*n*-BuLi) and tetramethylethylenediamine (TMEDA). The resulting lithium salts were then reacted with 1-bromo-3-chloropropane to afford the corresponding products **15**, **16**, or **17** as shown in Scheme 61.



Scheme 61. Synthesis of the  $\alpha$ -diimine compounds 15-17.

Compounds **15** - **17** were characterized by GC-MS,  $^1\text{H}$  NMR, and  $^{13}\text{C}$  NMR spectroscopy (see the appendices for the full analysis data). The mass and NMR spectra of compound **17** will be discussed as example.

The mass spectrum of compound **17** (see Scheme 62) showed the molecular ion peak at  $m/z = 480$  with a weak intensity of 1% relative to the base peak. The loss of a chloro group results in a fragment with an intensity of 12% at  $m/z = 444$  while the further loss of a methyl group gives the peak at  $m/z = 429$  with an intensity of 9%.

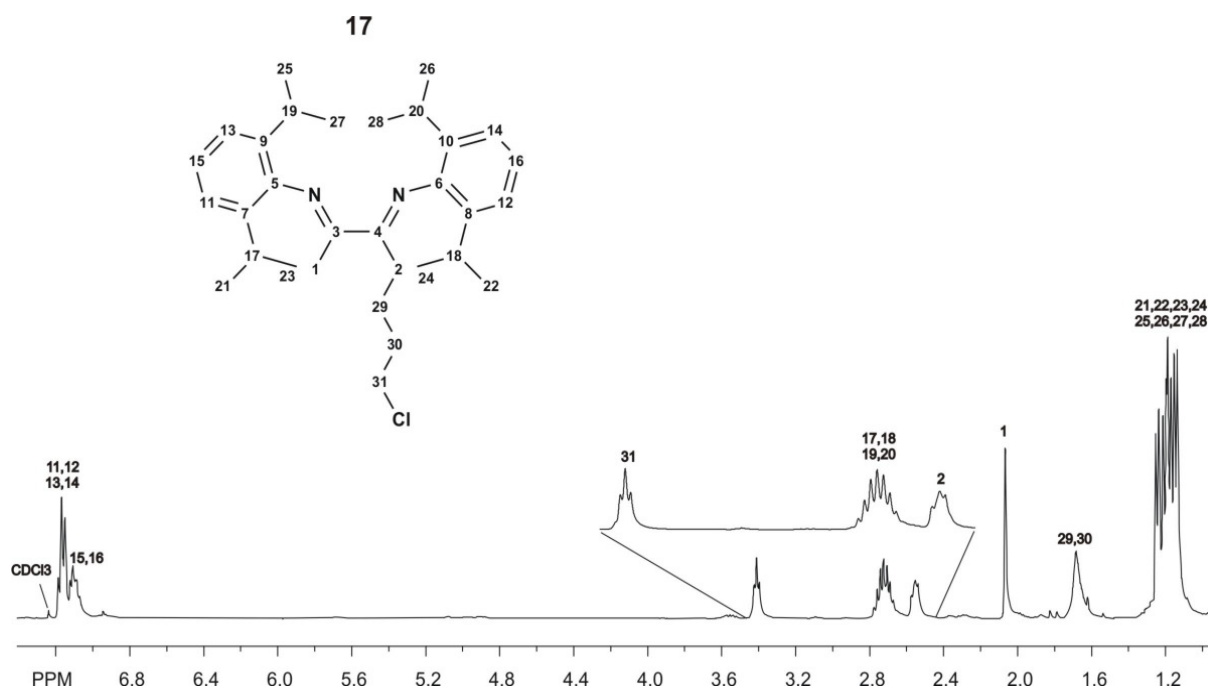


**Scheme 62. Mass spectrum of the  $\alpha$ -diimine compound **17**.**

The mass peak appearing at  $m/z = 437$  with an intensity of 36% is assigned to the dissociation of an isopropyl group while the further loss of a chloro group gives the mass peak at  $m/z = 401$  with an intensity of 91%. The dissociation of two isopropyl groups along with a chloro ligand leads to a fragment affording the mass peak at  $m/z = 359$  with an

intensity of 18%. The fragmentation of the diimine compound generates two imine moieties where the one bearing the chloropropyl group appears at  $m/z = 278$  with an intensity of 87% and the other produces the base peak at  $m/z = 202$ . The mass peak arising at  $m/z = 242$  with an intensity of 75% is attributed to the loss of a chloro ligand from the imine moiety bearing the chloropropyl group.

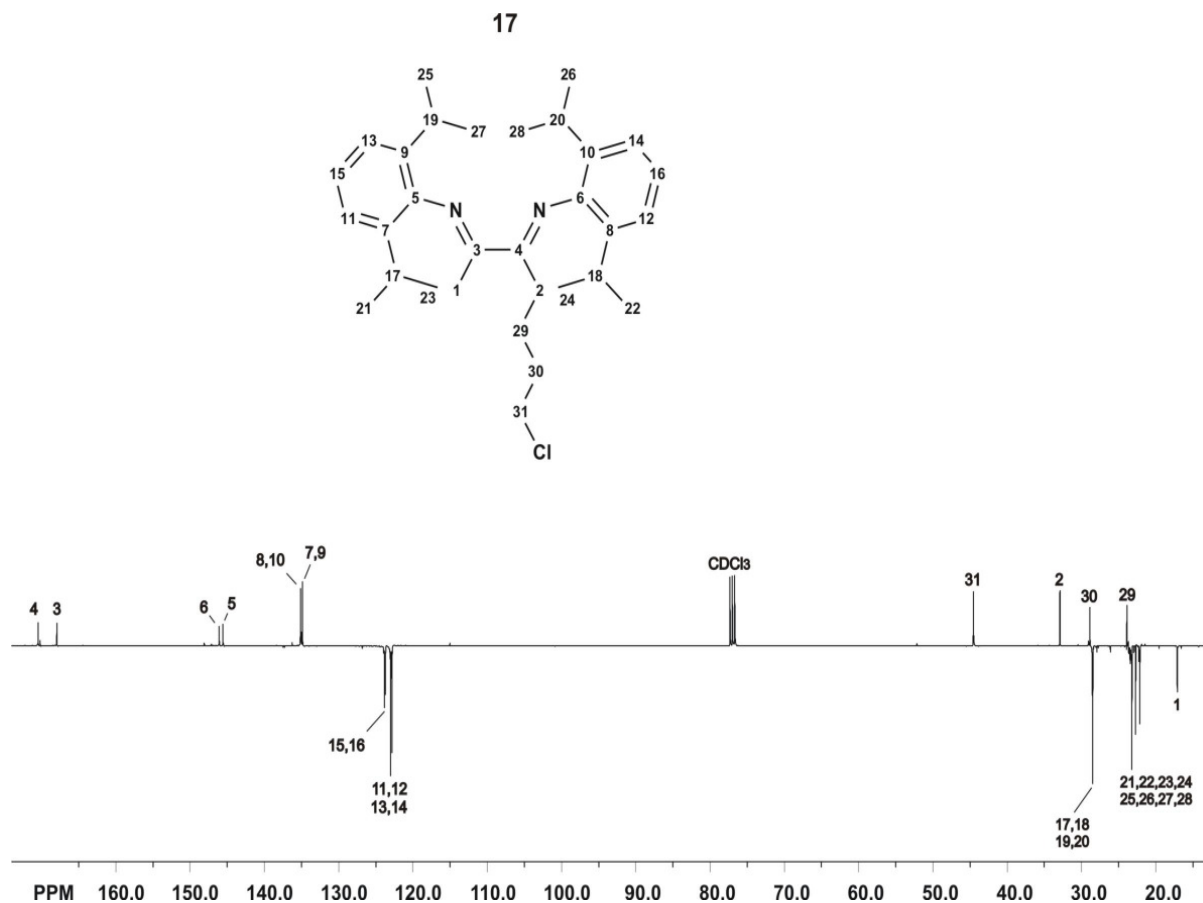
The  $^1\text{H}$  NMR spectrum of compound **17** (see Scheme 63) shows a multiplet at  $\delta = 7.20\text{--}7.14$  ppm which is assigned to the protons of the aromatic CH groups 11, 12, 13, and 14 while the other aromatic CH groups produce the signal at  $\delta = 7.11$  ppm. The methylene group binding the chloro ligand gives the proton NMR signal at  $\delta = 3.41$  ppm while the septet signal at  $\delta = 2.72$  ppm is assigned to the CH groups of the isopropyl functions.



**Scheme 63.**  $^1\text{H}$  NMR spectrum of the  $\alpha$ -diimine compound **17**.

The signal appearing at  $\delta = 2.55$  ppm is produced by the protons of the methylene group 2 while the methyl group at the backbone of the compound structure yields the singlet signal at  $\delta = 2.07$  ppm. The broad signal at  $\delta = 1.68$  ppm is attributed to the methylene groups 29 and 30 while the methyl groups belonging to the isopropyl functions produce the four doublets at  $\delta = 1.25, 1.22, 1.19,$  and  $1.14$  ppm.

The  $^{13}\text{C}$  NMR spectrum of compound **17** (see Scheme 64) shows the signal of the imine carbon connected to the chloropropyl group at  $\delta = 170.5$  ppm which is higher by 2.5 ppm than the other imine carbon atom at  $\delta = 168.0$  ppm. The signals belonging to the quaternary carbon atoms of the aromatic ring systems appear at  $\delta = 146.1$ , 145.6, 135.2, and 134.9 ppm, while the signals at  $\delta = 123.8$ , 123.7, 123, and 122.8 ppm can be assigned to the aromatic CH groups.

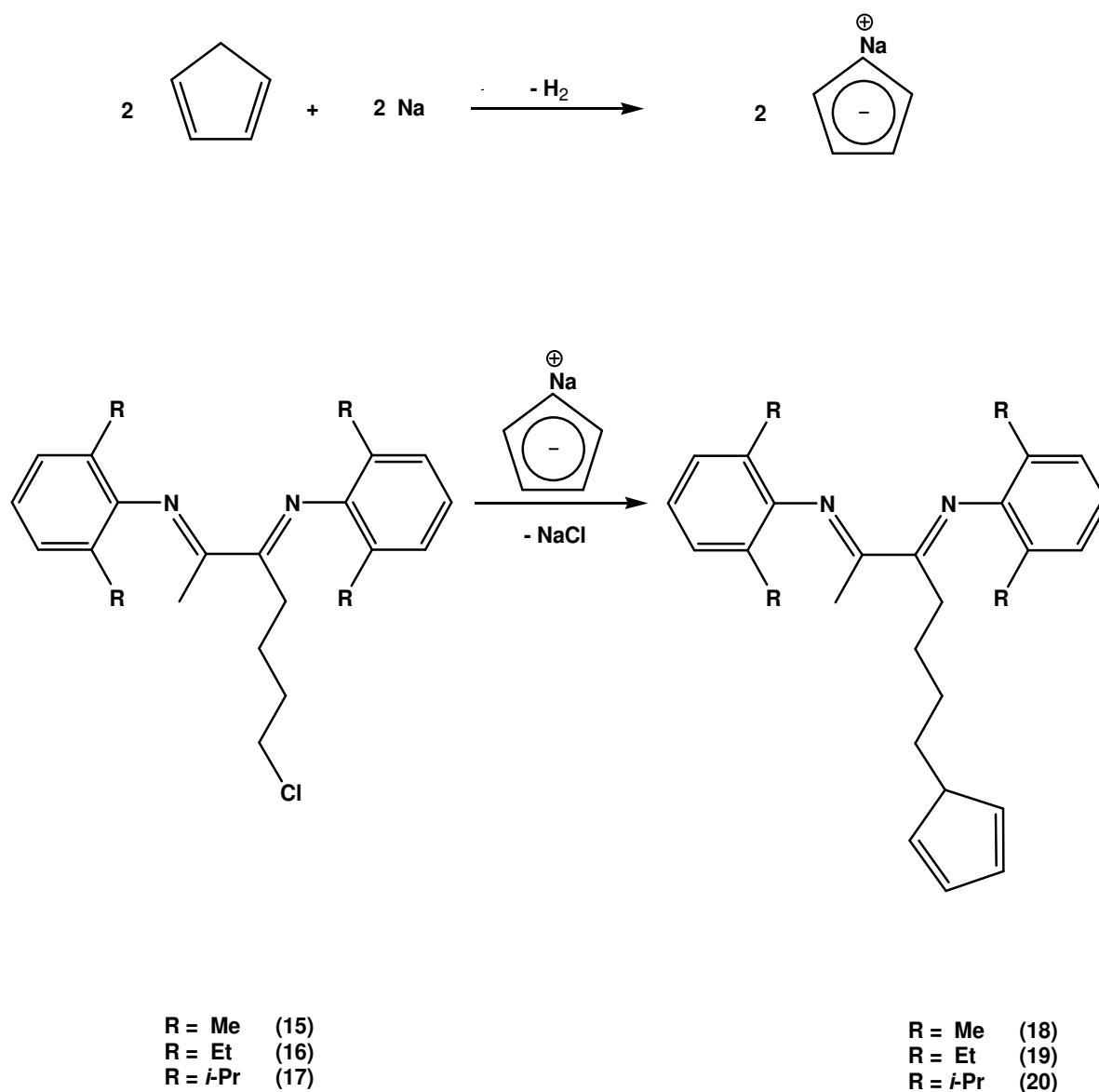


**Scheme 64.**  $^{13}\text{C}$  NMR spectrum of the  $\alpha$ -diimine compound **17**.

The methylene group binding the chloro ligand gives the signal at  $\delta = 44.6$  ppm while the methylene groups 2, 30 and 29 can be assigned to the signals at  $\delta = 32.9$ , 28.9 and 23.9 ppm. The carbon atoms of the CH groups of the isopropyl functions generate two signals which overlap at  $\delta = 28.5$  ppm while the signals at  $\delta = 23.2$ , 22.7, 22.2 and 22.1 ppm are assigned to the methyl groups of the isopropyl functions. The carbon atom of the methyl group at the backbone of the compound structure yields the resonance signal at  $\delta = 17.1$  ppm.

## 2.3.2.2 Synthesis and characterization of compounds 18-20

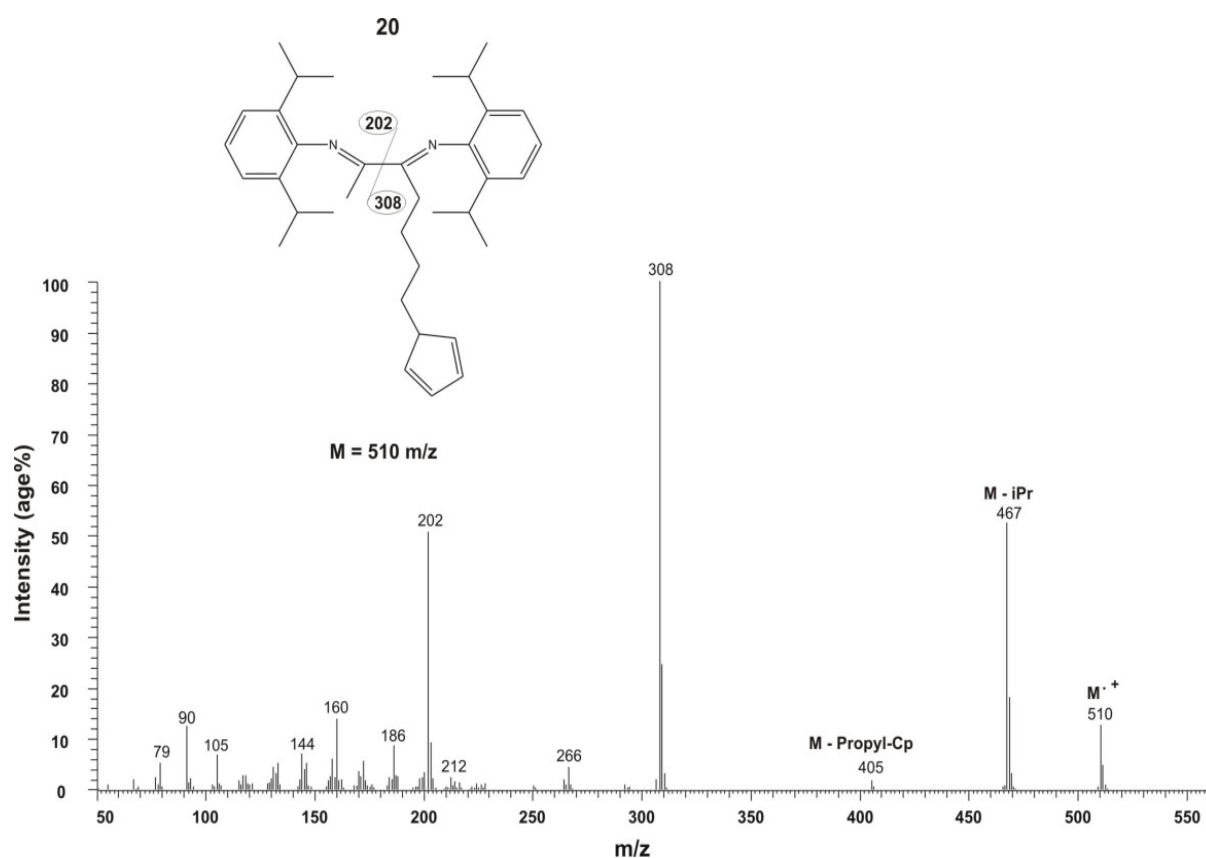
The compounds **18** – **20** consist of  $\alpha$ -diimine moieties combined with cyclopentadienyl ligands via butyl group. These compounds were synthesized by reacting the appropriate  $\alpha$ -diimine compound **15**, **16**, or **17** with sodium cyclopentadienide (NaCp) to afford the corresponding product **18**, **19**, or **20**. The synthesis steps are shown in Scheme 65.



**Scheme 65.** Synthesis of the  $\alpha$ -diimine compounds **18-20** bearing butylcyclopentadienyl groups at their backbones.

The compounds **18** - **20** were characterized via GC-MS,  $^1\text{H}$  NMR, and  $^{13}\text{C}$  NMR spectroscopy (see the appendices for the full analysis data). The mass and NMR spectra of compound **20** will be discussed as example.

The mass spectrum of compound **20** (see Scheme 66) shows the peak of the molecular ion at  $m/z = 510$  with an intensity of 15% relative to the base peak. The fragment appearing at  $m/z = 467$  with an intensity of 56% results from the dissociation of an isopropyl group from the molecule **20**. The loss of a propylcyclopentadienyl group which is attached to the backbone of the compound framework gives the peak at  $m/z = 405$  with an intensity of 2%.

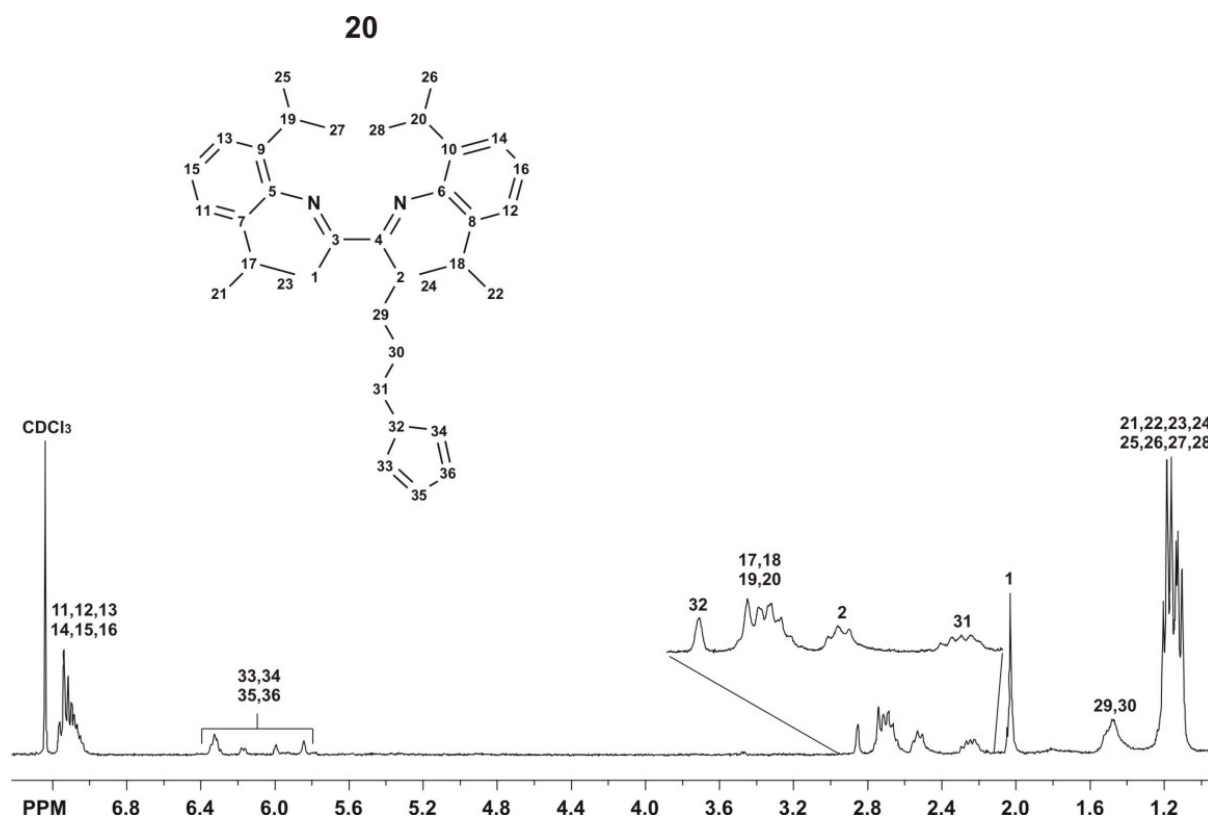


**Scheme 66. Mass spectrum of the  $\alpha$ -diimine compound **20**.**

The fragmentation of the diimine compound generates two imine moieties where the one bearing the propylcyclopentadienyl group produces the base peak at  $m/z = 308$  while the unsubstituted counterpart appears at  $m/z = 202$  with an intensity of 52%. Further dissociation of the imine moiety bearing a propylcyclopentadienyl group yields the mass peak at  $m/z = 266$  with an intensity of 5% which is attributed to the loss of an isopropyl group while the further

fragmentation of the other imine moiety affords the mass peaks at  $m/z = 186$  and  $160$  with the intensities of 9% and 14% which arise from the loss of a methyl and an isopropyl group.

The  $^1\text{H}$  NMR spectrum of compound **20** (see Scheme 67) shows a signal at  $\delta = 7.12$  ppm which is assigned to the protons of the CH groups belonging to the aryl rings. The aromatic CH groups of the cyclopentadienyl moiety (33, 34, 35, 36) produce the signals at  $\delta = 6.33$ , 6.17, 6.00, and 5.85 ppm while the aliphatic one yields the signal at  $\delta = 2.86$  ppm.

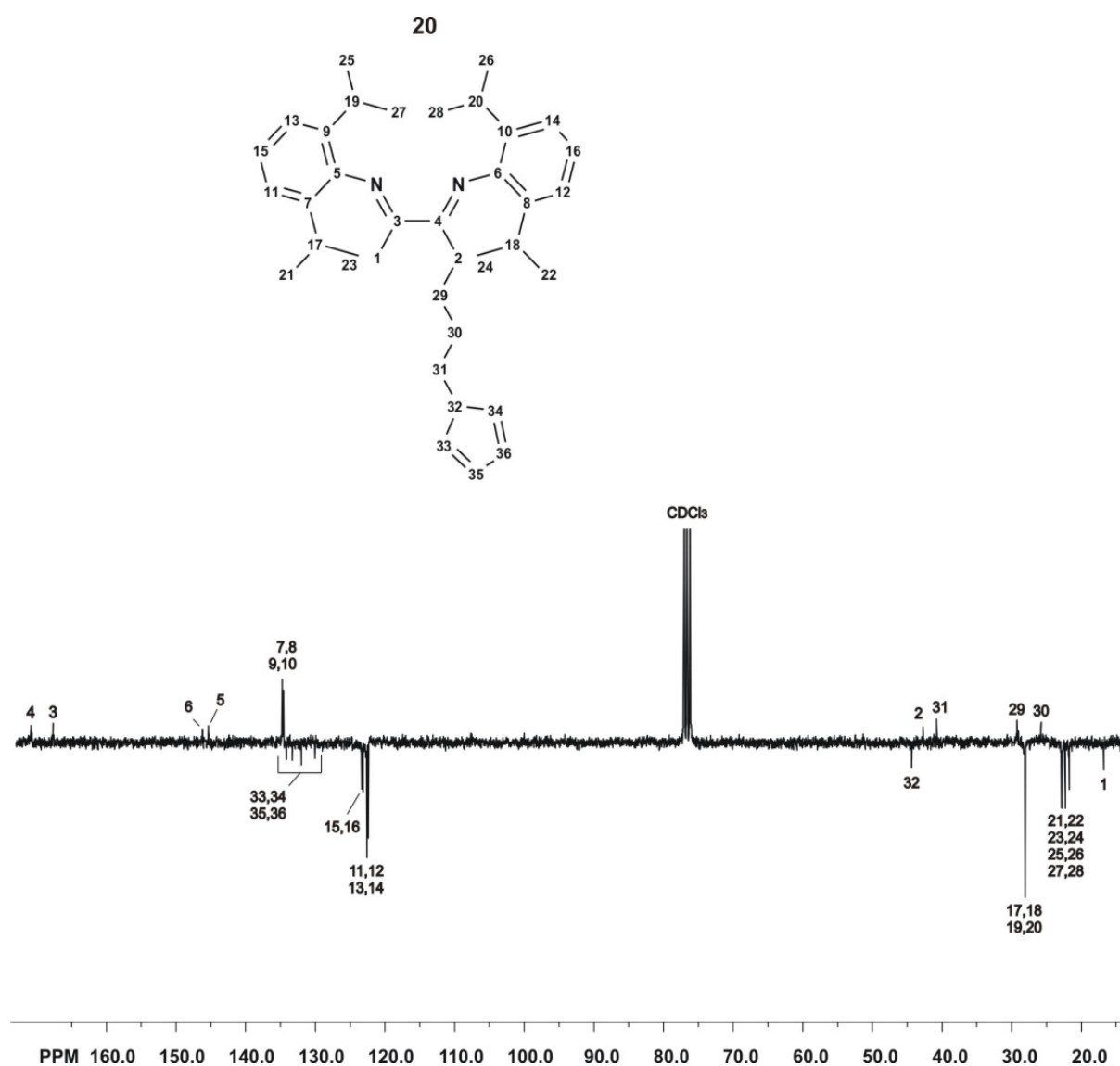


**Scheme 67.**  $^1\text{H}$  NMR spectrum of the  $\alpha$ -diimine compound **20**.

The CH groups of the isopropyl functions afford the signal at  $\delta = 2.70$  ppm. The signal at  $\delta = 2.53$  ppm is assigned to the methylene group bearing the propylcyclopentadienyl moiety while the methylene group binding the cyclopentadienyl ligand gives the signal at  $\delta = 2.25$  ppm which is lower by 1.16 ppm than the signal of the analogous methylene group binding to chloro ligand in the starting compound **17**. The signal appearing at  $\delta = 2.03$  ppm is produced by the protons of the methyl group at the backbone of the compound while the methylene groups 29 and 30 yield the multiplet at  $\delta = 1.48$  ppm. The four overlapping signals at  $\delta =$

1.25, 1.19, 1.15 and 1.12 ppm are attributed to the methyl groups belonging to the isopropyl functions.

The  $^{13}\text{C}$  NMR spectrum of compound **20** (see Scheme 68) shows the signal of the imine carbon atom bearing the propylcyclopentadienyl group at  $\delta = 171.2$  ppm which is higher by 3.2 ppm than the other imine carbon atom at  $\delta = 168$  ppm. The signals belonging to the quaternary carbon atoms of the aromatic ring systems (6) and (5) appear at  $\delta = 146.2$  and 145.7 ppm while the other quaternary carbon atoms (7, 8, 9, 10) arise at  $\delta = 135.2$  and 135.0 ppm.



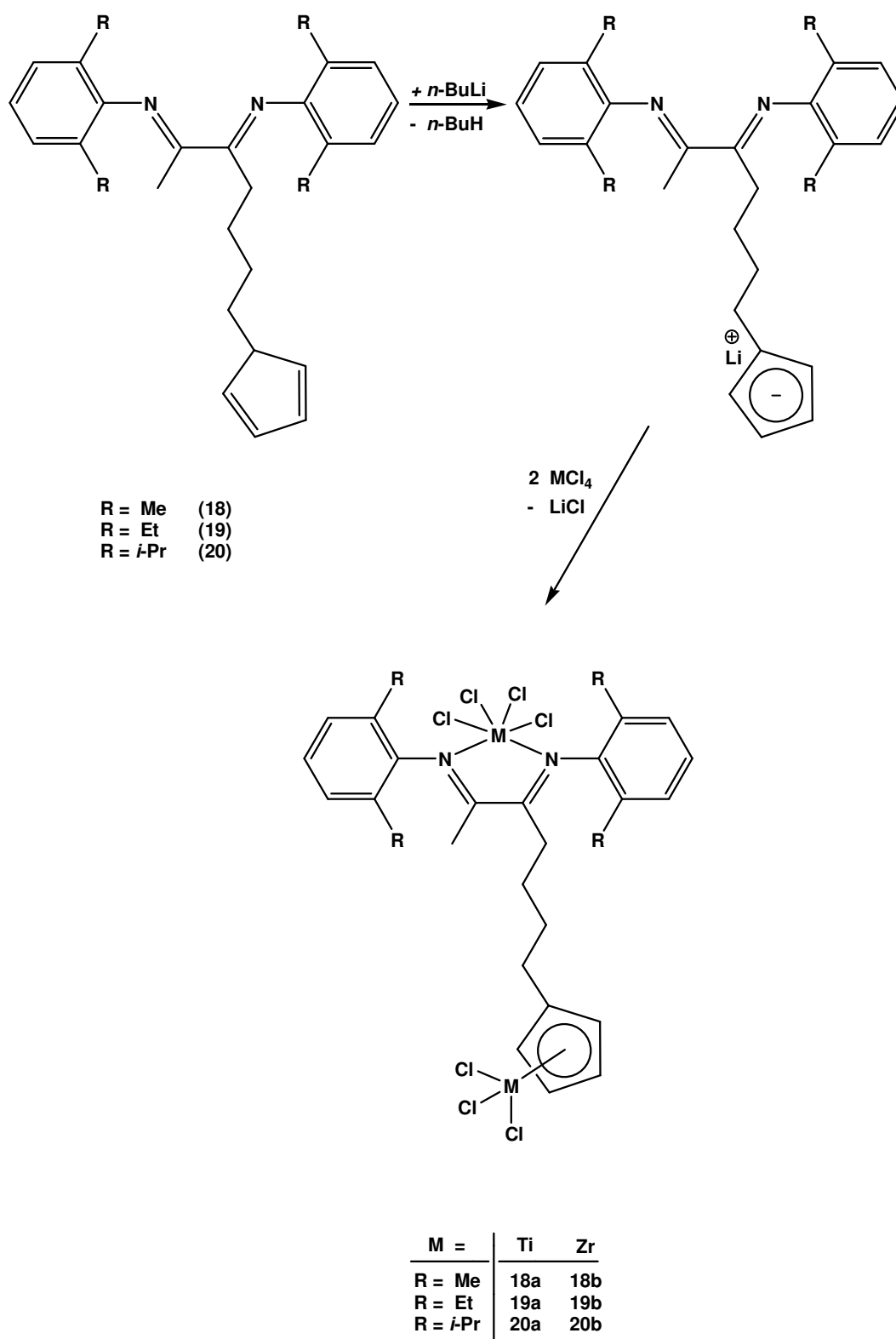
Scheme 68.  $^{13}\text{C}$  NMR spectrum of the  $\alpha$ -diimine compound **20**.

The carbon atoms belonging to the aromatic CH groups of the cyclopentadienyl moiety produce the signals at  $\delta = 134.5, 133.7, 132.4,$  and  $130.4$  ppm. The signals at  $\delta = 123.7$  and  $123.6$  ppm are attributed to the aromatic CH groups 15 and 16 while the aromatic CH groups (11, 12, 13, 14) yield the signals at  $\delta = 123.0$  and  $122.8$  ppm. The carbon atom of the aliphatic CH group of the cyclopentadienyl moiety affords the signal at  $\delta = 44.7$  ppm while the signal at  $\delta = 43.1$  ppm arises from the methylene group connected to the propylcyclopentadienyl moiety. The methylene group bearing the cyclopentadienyl ligand gives the signal at  $\delta = 41.2$  ppm which is lower by 3.4 ppm than the analogous methylene group binding the chloro ligand of the starting compound **17**. The signal at  $\delta = 29.6$  ppm is assigned to the methylene group 29 while the methylene group 30 produces the signal at  $\delta = 26.2$  ppm. Two signals overlapping at  $\delta = 28.4$  ppm result from the CH groups of the isopropyl functions while the methyl groups of these functions generate the signals at  $\delta = 23.2, 23.1, 22.7,$  and  $22.1$  ppm. The carbon atom of the methyl group at the backbone of the compound structure yields the resonance signal at  $\delta = 17.2$  ppm.

### 2.3.3 Synthesis and characterization of dinuclear complexes

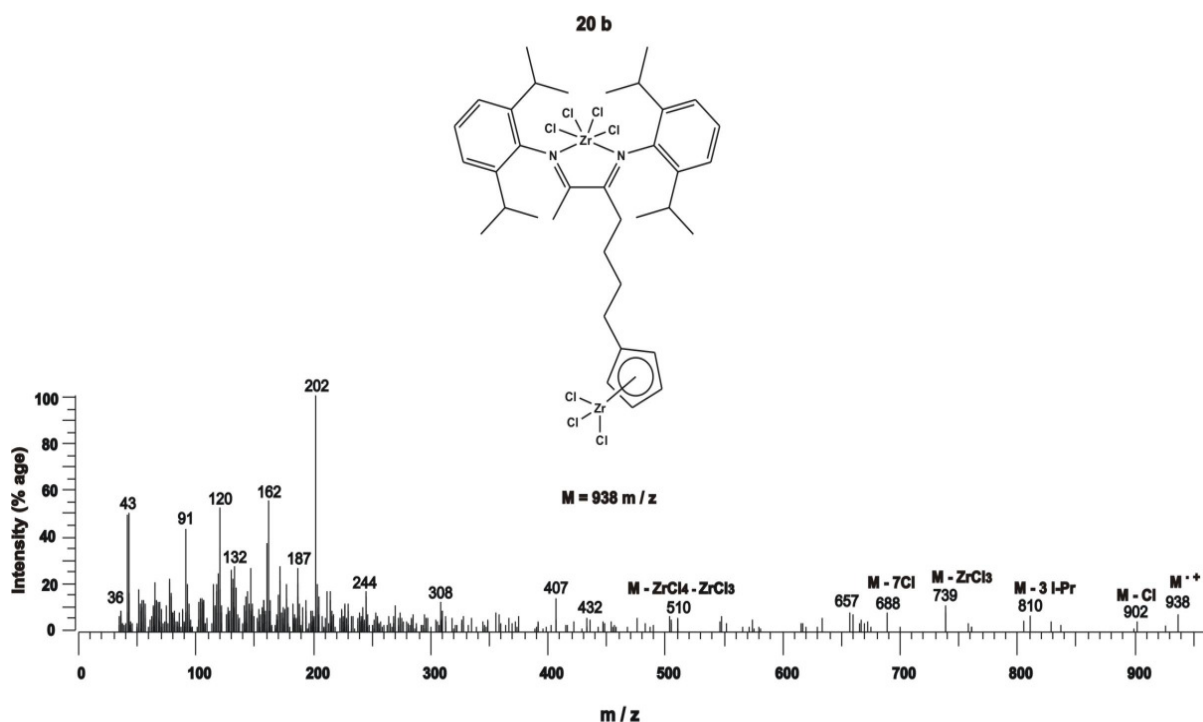
The synthesized compounds **18 - 20** consist of  $\alpha$ -diimine moieties bearing different ortho substituents at their aryl rings and cyclopentadienyl groups. These compounds are significant ligand systems for new dinuclear precursors. Each of the cyclopentadiene and  $\alpha$ -diimine moieties can coordinate an early transition metal salt. This is an easy approach of preparing a dinuclear complex by reacting one of these ligand systems **18 - 20** with only one metal salt. Furthermore, the dinuclear catalysts of these ligands are tunable to control the molecular weight of the produced polyethylene via changing the bulk of the ortho substituents at the aryl rings of the ligand frameworks. Herein, six new dinuclear precursors using these ligand systems were synthesized as will be described next.

The appropriate  $\alpha$ -diimine compound bearing a cyclopentadienyl group (**18**, **19**, or **20**) was reacted with *n*-butyllithium (*n*-BuLi). The resulting lithium salt was then mixed with two equivalents of titanium tetrachloride (TiCl<sub>4</sub>) or zirconium tetrachloride (ZrCl<sub>4</sub>). The corresponding dinuclear complexes (**18a,b**; **19a,b**; or **20a,b**) were prepared from this mixture by salt elimination reaction. The synthesis steps of the resulting complexes are shown in Scheme 69.

Scheme 69. Synthesis of the dinuclear complexes *18a,b*; *19a,b*; and *20a,b*.

The dinuclear complexes **18a,b**; **19a,b**; and **20a,b** were characterized via mass spectroscopy and elemental analysis (see the appendices for the full analysis data). The mass spectrum of complex **20b** will be discussed as example.

The mass spectrum of complex **20b** (see Scheme 70), shows the peak of the molecular ion at  $m/z = 938$  with an intensity of 9% relative to the base peak. The dissociation of a chloro substituent results in a peak with an intensity of 5% at  $m/z = 902$  while the peak at  $m/z = 810$  with an intensity of 8% is assigned to the loss of three isopropyl groups. The peak appearing at  $m/z = 739$  with the intensities 13% is produced by the dissociation of zirconium trichloride while the further loss of the other metal center (the zirconium tetrachloride) yields the ligand peak at  $m/z = 510$  with an intensity of 7%.

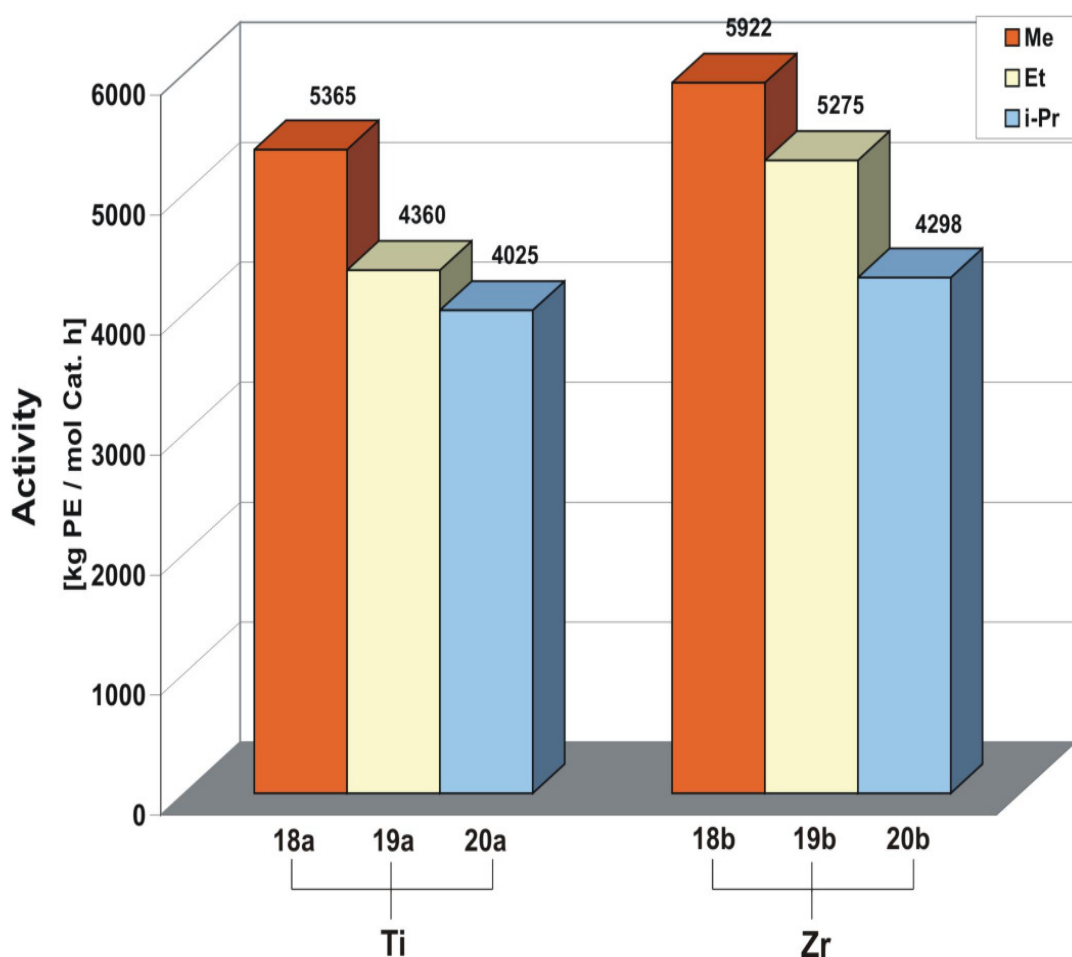


**Scheme 70. Mass spectrum of the  $\alpha$ -diimine compound **20b**.**

The dissociation of all chloro substituents from the metal centers affords the mass peak at  $m/z = 688$  with an intensity of 10% while the fragmentation of the diimine ligand generates two imine moieties where the one bearing the propylcyclopentadienyl group appears at  $m/z = 308$  with an intensity of 12% and the other part produces the base peak at  $m/z = 202$ .

### 2.3.4 Polymerization experiments with the dinuclear precursors *18a,b*; *19a,b*; and *20a,b*

The dinuclear complexes **18a,b**; **19a,b**; and **20a,b** were suspended in toluene and activated with methylaluminoxane (MAO), the M:Al ratio was 1:1500. The catalysts were transferred to a 1 l Büchi laboratory autoclave under inert atmosphere and tested for the polymerization of ethylene (in 250 ml of *n*-pentane, 10 bar ethylene, and a polymerization temperature of 65° C). The results of the ethylene polymerizations are illustrated in Scheme 71.



Scheme 71. The polymerization activities of the dinuclear complexes *18a,b*; *19a,b*; and *20a,b*.

In consequence of the similar half sandwich metallocene complexes attached to the dinuclear precursors **18a,b**; **19a,b**; and **20a,b**, the polymerization activities of the dinuclear catalysts are expected to show a dependence on the variant metal centers of the  $\alpha$ -diimine moiety and the size of the ortho substituents at the aryl rings of the catalysts structures.

The dinuclear catalysts **18b**, **19b**, and **20b** bearing zirconium centers showed higher ethylene polymerization activities than the analogous titanium catalysts **18a**, **19a**, and **20a**. This can be assigned to the better separation between the cationic active species of the catalysts and the anionic MAO species in the zirconium catalysts than in titanium ones.

The ethylene polymerization activities of both titanium and zirconium dinuclear catalysts demonstrated an obvious dependence on the size of the ortho substituents at the arene moieties. Among the dinuclear catalysts with the same metal centers, the catalysts bearing isopropyl substituents at the aryl rings (**20a**, **20b**) showed the lowest polymerization activities while the catalysts having methyl substituents (**18a**, **18b**) resulted in the highest activities. In general, the ethylene polymerization results reveal that the bulkier the substituents, the lower the polymerization activity. These results are compatible with the chain running mechanism which suggests that the bulky substituents can hinder the monomers from reaching the active catalytic centers due to their interaction with the axial coordination sites of the metal centers resulting in lower activities.

For comparison, the half sandwich complexes, cyclopentadienyltitanium trichloride **A** and cyclopentadienylzirconium trichloride **B** were activated with methylaluminoxane (MAO), the M:Al ratio was 1:1500. The activated complexes were tested for the polymerization of ethylene using the same polymerization conditions applied to the dinuclear catalysts **18a,b**; **19a,b**; and **20a,b**.

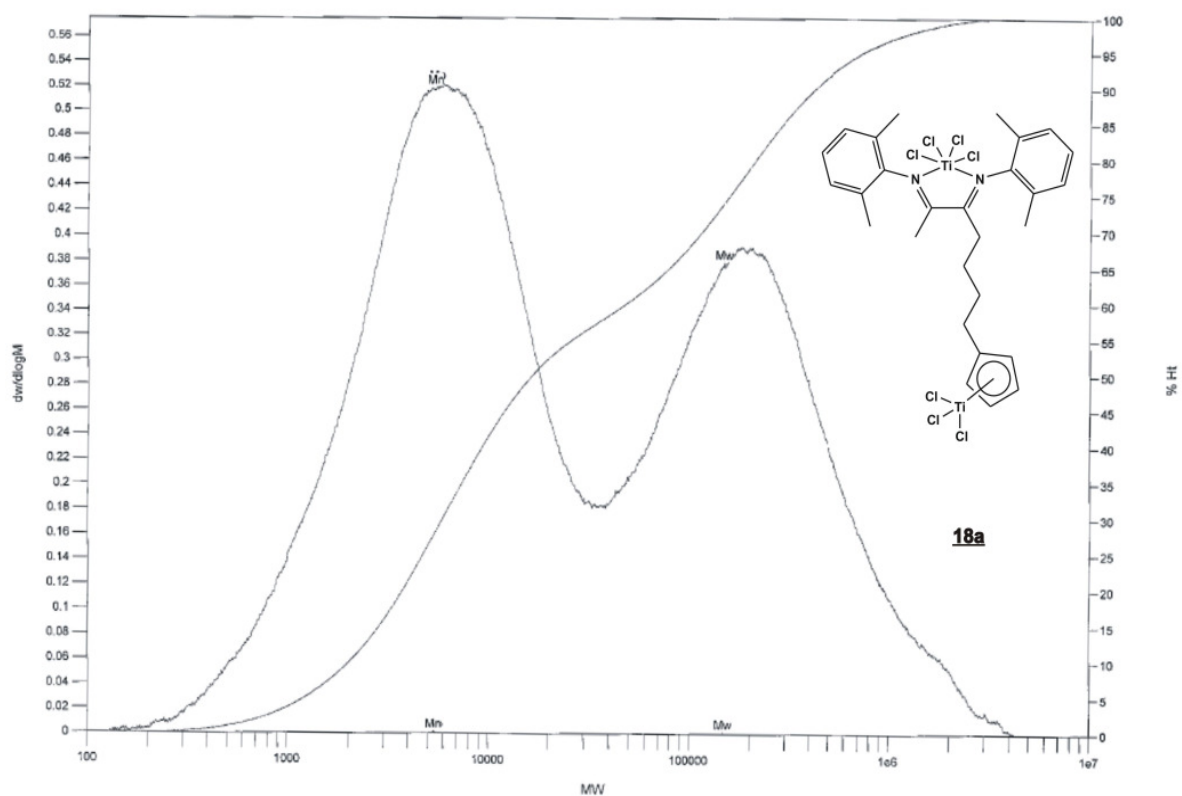
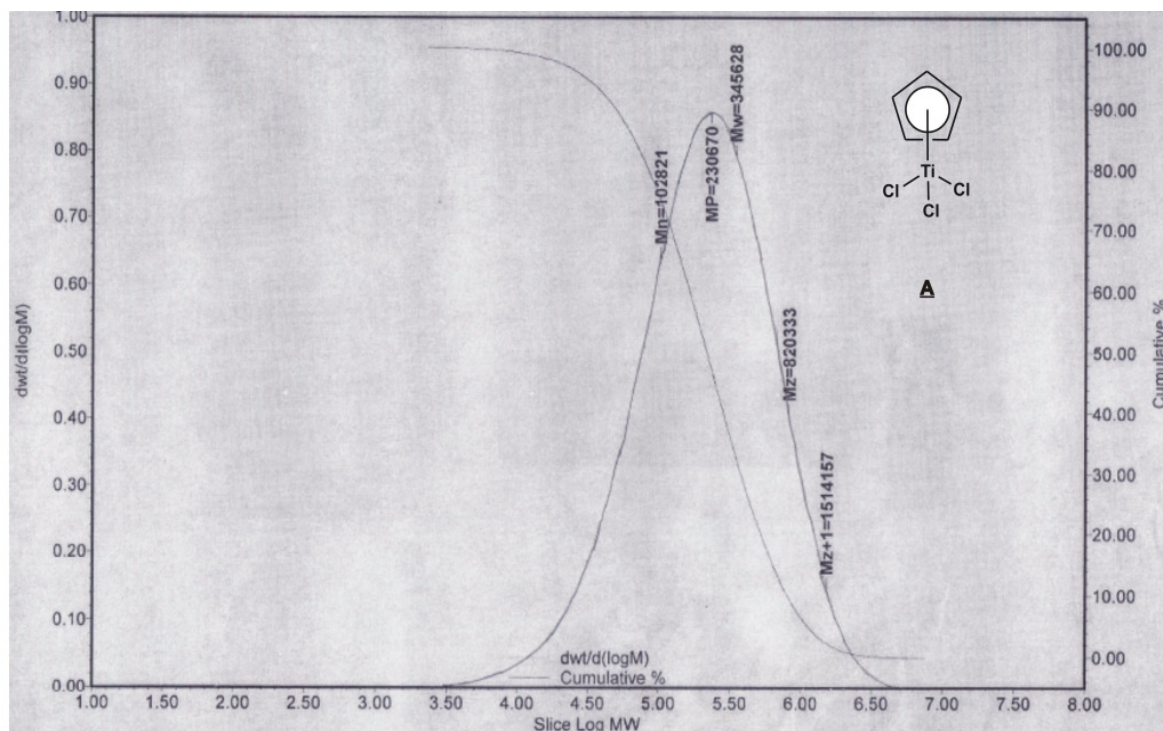
The ethylene polymerization activity of catalyst **A** was 6750 kg *PE* / mol *Cat* while the activity of catalyst **B** was 8130 kg *PE* / mol *Cat*. These activities are lowered when the half sandwich complexes were coupled with  $\alpha$ -diimine moieties to afford the dinuclear catalysts **18a,b**; **19a,b**; and **20a,b**. The coupling increases the steric hindrance around the active zirconium or titanium sites and prevents the ethylene molecules from reaching these sites leading to a reduced activity.

Samples of the polyethylenes produced with the dinuclear catalysts **18a,b** and **19a,b** and the half sandwich catalysts **A** and **B** were analyzed by gel permeation chromatography (GPC). The aim of this analysis is to test the bimodality of these dinuclear precursors. The results of GPC are summarized in Table 6.

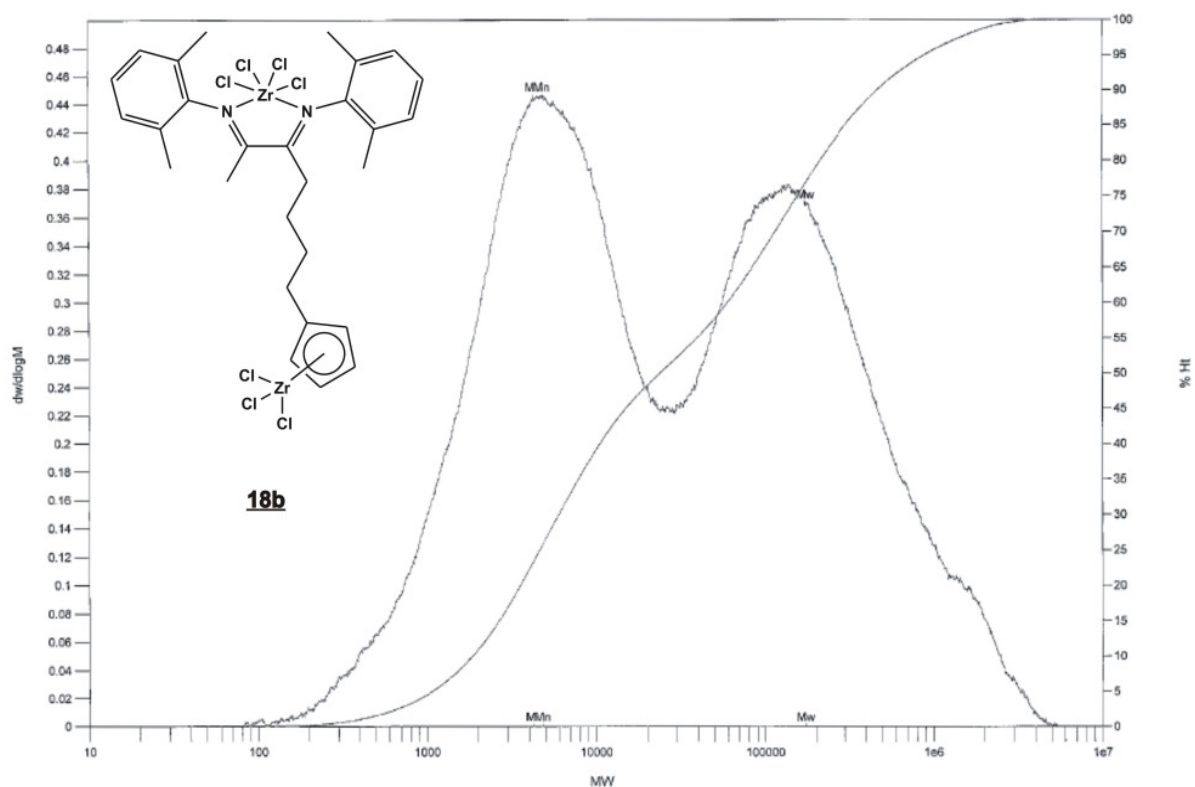
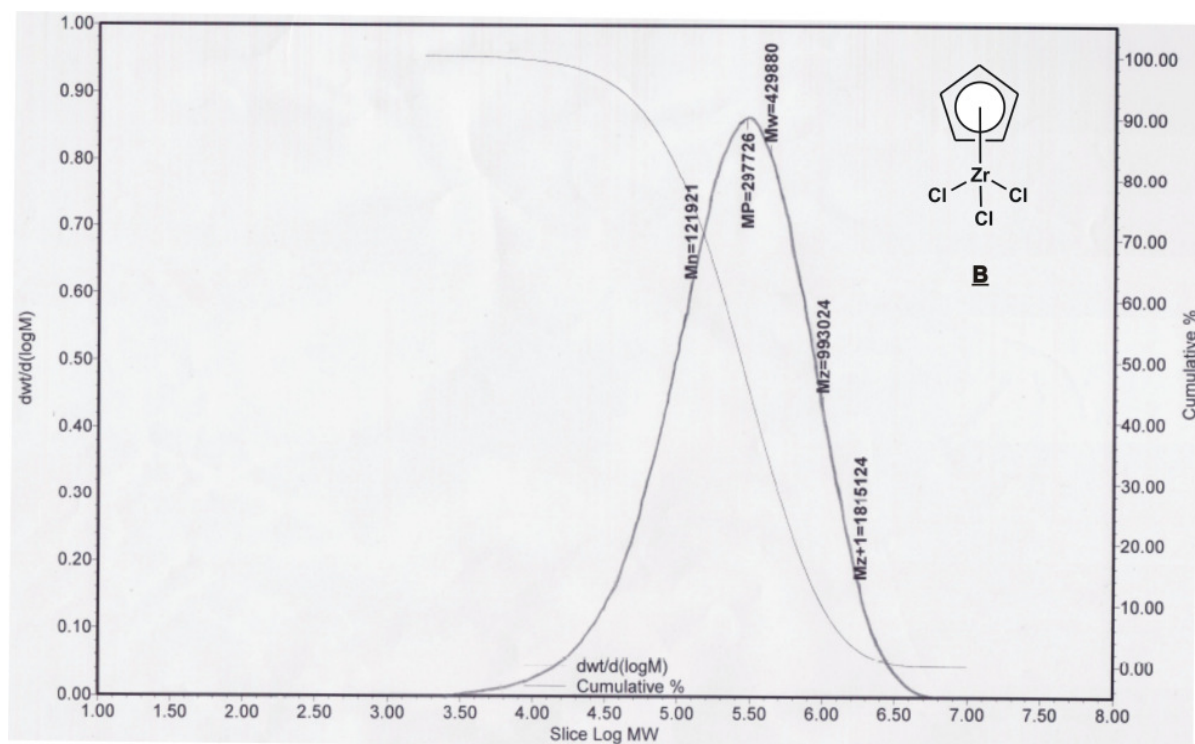
**Table 6. GPC results of the polyethylenes produced by the dinuclear catalysts 18a,b and 19a,b and the half sandwich catalysts A and B.**

<b>Complex Number</b>	<b>Mw (g/mol)</b>	<b>Mn (g/mol)</b>	<b>MWD</b>
<b>18a</b>	<b>148100</b>	<b>5361</b>	<b>27.62</b>
<b>18b</b>	<b>172914</b>	<b>4800</b>	<b>36.02</b>
<b>19a</b>	<b>396920</b>	<b>23657</b>	<b>16.78</b>
<b>19b</b>	<b>407573</b>	<b>8026</b>	<b>50.78</b>
<b>A</b>	<b>345628</b>	<b>102821</b>	<b>3.36</b>
<b>B</b>	<b>429880</b>	<b>121921</b>	<b>3.53</b>

The GPC results of polyethylenes produced with the dinuclear catalysts **18a,b** and **19a,b** displayed the desired broad or bimodal molecular weight distributions. These results can be assigned to the different active sites of the dinuclear catalysts. The molecular weights of the polyethylenes obtained with the half sandwich catalysts **A** and **B** are 345628 and 429880 g/mol. Therefore, the higher molecular weight fraction is estimated to be yielded by the catalyst **A** or **B** while the metal center of the  $\alpha$ -diimine unit affords the lower fraction. The GPC spectra of polyethylenes produced with the dinuclear catalysts **18a** (see Scheme 72) and **18b** (see Scheme 73) will be discussed as examples and will be compared with the GPC spectra of polyethylenes produced with the mononuclear catalysts **A** and **B**.



Scheme 72. GPC spectra of the polyethylenes produced with the mononuclear catalyst **A** (top) and the dinuclear catalyst **18a** (bottom).



Scheme 73. GPC spectra of the polyethylenes produced with the mononuclear catalyst **B** (top) and the dinuclear catalyst **18b** (bottom).

The GPC spectra of the polyethylenes produced with the half sandwich catalysts **A** and **B** exhibit narrow molecular weight distributions with  $MWD = 3.36$  and  $3.53$  while their dinuclear catalysts **18a,b** afford polyethylenes with bimodal molecular weight distributions of  $MWD = 27.62$  and  $36.02$ .

## 3. Experimental Part

### 3.1 General

All experimental work was routinely carried out using Schlenk technique. Dried and purified argon was used as inert gas. *n*-Pentane, *n*-hexane, diethyl ether, toluene and tetrahydrofuran were purified by distillation over Na/K alloy. Diethyl ether was additionally distilled over lithium aluminum hydride. Methylene chloride was dried with phosphorus pentoxide and calcium hydride. Methanol and ethanol were dried over molecular sieves. Deuterated solvents ( $\text{CDCl}_3$ ,  $\text{CD}_2\text{Cl}_2$ ) for NMR spectroscopy were purchased from Euriso-Top and stored over molecular sieves (3 Å). Methylalumoxane (30% in toluene) was purchased from Crompton (Bergkamen) and Albemarle (Baton Rouge, USA/Louvain, La Neuve, Belgium). Ethylene (3.0) and argon (4.8/5.0) were supplied by Rießner Company (Lichtenfels). 4-Allyl-2,6-diisopropylaniline was prepared according to the literature<sup>[108]</sup> All other starting materials were commercially available and used without further purification.

### 3.2 Measurement methods

#### 3.2.1 NMR spectroscopy

NMR spectra were recorded with Bruker ARX (250 MHz), Varian Inova (300 MHz) or Varian Inova (400 MHz) spectrometers. The samples were prepared under inert atmosphere (argon) and routinely recorded at 25°C. The chemical shifts in the  $^1\text{H}$  NMR spectra are referred to the residual proton signal of the solvent ( $\delta = 7.24$  ppm for  $\text{CDCl}_3$ ,  $\delta = 5.32$  ppm for  $\text{CD}_2\text{Cl}_2$ ) and in  $^{13}\text{C}$  NMR spectra to the solvent signal ( $\delta = 77.0$  ppm for  $\text{CDCl}_3$ ,  $\delta = 53.5$  ppm for  $\text{CD}_2\text{Cl}_2$ ).

#### 3.2.2 Mass spectrometry

Mass spectra were routinely recorded at the Zentrale Analytik of the University of Bayreuth with a VARIAN MAT CH-7 instrument (direct inlet, EI,  $E = 70$  eV) and a VARIAN MAT 8500 spectrometer.

### 3.2.3 GC/MS

GC/MS spectra were recorded with a FOCUS Thermo gas chromatograph in combination with a DSQ mass detector. A 30m HP-5 fused silica column (internal diameter 0.32 mm, film ( $d_f = 0.25 \mu\text{m}$ ), and flow 1 ml/min) was used and helium (4.6) was applied as carrier gas. The routinely performed temperature program started at 50°C and held this temperature for 2 min. After a heating phase of twelve minutes (20° C/min, final temperature was 290°C), the end temperature was held for 30 min (plateau phase).

At the Zentrale Analytik of the University of Bayreuth, GC/MS spectra were routinely recorded with a HP5890 gas chromatograph in combination with a MAT 95 mass detector.

### 3.2.4 Gel permeation chromatography (GPC)

GPC measurements were routinely performed by the analytical department at Saudi Basic Industries Corporation (SABIC) in Riyadh, Saudi Arabia.

### 3.2.5 Elemental analysis

The analyses were performed with a Vario EL III CHN instrument. Therefore, 4–6 mg of the complex was weighed into a standard tin pan. The tin pan was carefully closed and introduced into the auto sampler of the instrument. The raw values of the carbon, hydrogen, and nitrogen contents were multiplied with calibration factors (calibration compound: acetamide).

### 3.2.6 Crystal structure analysis

X-ray crystal structure analyses were performed by using a STOE-IPDS II diffractometer equipped with an Oxford Cryostream low-temperature unit.

Crystal data:

**C<sub>31</sub>H<sub>44</sub>N<sub>2</sub> (6)**: yellow prism crystallized from methanol; orthorhombic; space group is  $P2(1)2(1)2$ ;  $a = 19.014(4) \text{ \AA}$ ;  $b = 23.571(5) \text{ \AA}$ ;  $c = 6.2853(13) \text{ \AA}$ ;  $\alpha, \beta, \text{ and } \gamma = 90^\circ$ ;  $V = 2816.9(10) \text{ \AA}^3$ ;  $Z = 4$ ;  $d_{(\text{calc})} = 1.049 \text{ g/cm}^3$ ; wavelength = 0.71073 Å; Absorption coefficient = 0.06 mm<sup>-1</sup>;  $F(000) = 976$ ; reflections collected 13013; independent reflections 5198; Goodness-of-fit = 0.97; R indices ( $R1 = 0.0447, wR2 = 0.1054$ ).

**C<sub>32</sub>H<sub>46</sub>Cl<sub>4</sub>N<sub>2</sub>Pd (6g)**: orange prism crystallized from methylene chloride; triclinic; space group is *P*-1; *a* = 8.8350(6) Å; *b* = 10.5840(8) Å; *c* = 18.9310(13) Å;  $\alpha$  = 80.81°;  $\beta$  = 84.76°;  $\gamma$  = 86.89°; *V* = 1738.8(2) Å<sup>3</sup>; *Z* = 2; *d*<sub>(calc)</sub> = 1.350 g/cm<sup>3</sup>; wavelength = 0.71069 Å; Absorption coefficient = 0.86 mm<sup>-1</sup>; *F*(000) = 732; reflections collected 23280; independent reflections 6549; Goodness-of-fit = 0.94; *R* indices (*R*1 = 0.0358, *wR*2 = 0.0859).

**C<sub>68</sub>H<sub>96</sub>Br<sub>4</sub>N<sub>4</sub>Ni<sub>2</sub> (8)**: brown needle crystallized from methylene chloride; triclinic; space group is *P*-1; *a* = 13.0160(7) Å; *b* = 15.7980(9) Å; *c* = 18.3480(11) Å;  $\alpha$  = 94.41°;  $\beta$  = 108.59°;  $\gamma$  = 97.45°; *V* = 3517.6(3) Å<sup>3</sup>; *Z* = 2; *d*<sub>(calc)</sub> = 1.328 g/cm<sup>3</sup>; wavelength = 0.71069 Å; Absorption coefficient = 2.846 mm<sup>-1</sup>; *F*(000) = 1456; reflections collected 13251; independent reflections 7408; Goodness-of-fit = 1.049; *R* indices (*R*1 = 0.0607, *wR*2 = 0.1327).

### 3.3 Synthesis procedures

#### 3.3.1 General synthesis of the $\alpha$ -diimine compounds **1-3** and **7**

To a mixture of 10 g (116 mmol) of 2,3-butanedione and 50 ml of methanol in a 250 ml round-bottom flask, 238 mmol of the appropriate aniline was added. The mixture was stirred for five minutes followed by the addition of 12.28g (267 mmol) of formic acid. The stirring of the reaction mixture at room temperature resulted in the formation of a yellow precipitate within ten minutes and the reaction mixture was left to stir for 18 h to reach the maximum yield. The resulting yellow solid was collected by filtration then washed with 60 ml of methanol and dried under vacuum. For purification, the products were recrystallized from methanol to afford yellow crystals. Yields: **1**, 79%; **2**, 85%; **3**, 87%; **7**, 82%. All compounds were characterized by GC/MS and NMR spectroscopy.

#### 3.3.2 General synthesis of the $\alpha$ -diimine compounds bearing allyl groups (**4-6**)

A mixture of 3.15 ml (21 mmol) of tetramethylethylenediamine (TMEDA) and 13.13 ml (21 mmol) of *n*-butyllithium (1.6 M in *n*-hexane) was prepared in a pressure-equalizing dropping funnel containing 40 ml *n*-pentane. This mixture was added drop-wise to a stirred solution of 20 mmol of the appropriate  $\alpha$ -diimine compound (**1**, **2**, or **3**) in 100 ml of pentane. Immediately a color change of the solution from yellow to orange was observed. The reaction mixture was stirred overnight. The next step was the addition of 4 equiv. of allyl bromide (80

mmol, 7 ml) and refluxing the reaction mixture overnight. Later, the refluxing was stopped and the reaction mixture was allowed to cool down to room temperature. Removal of the solvent and the excess of allyl bromide by evaporation resulted in a viscous yellow liquid which was dissolved in n-pentane and filtered over sodium sulphate and silica. The solvent was removed and the resulting yellow powder was recrystallized from methanol at room temperature to afford the products as yellow crystals. Yields: **4**, 75%; **5**, 73%; **6**, 80%. All compounds were characterized by GC/MS and NMR spectroscopy. Compound **6** gave single crystals that were suitable for an X-ray analysis.

### 3.3.3 General synthesis of the complexes of $\alpha$ -diimines bearing allyl groups (**4a-g**, **5a-g**, **6a-g** and **8**)

The metal salts titanium tetrachloride ( $\text{TiCl}_4$ ), zirconium tetrachloride ( $\text{ZrCl}_4$ ), vanadium trichloride ( $\text{VCl}_3$ ), chromium trichloride ( $\text{CrCl}_3$ ), iron trichloride ( $\text{FeCl}_3$ ), dibromo(1,2-dimethoxyethane)nickel(II) ( $\text{NiBr}_2\cdot\text{DME}$ ), or dichloro (1,5-cyclooctadiene)palladium(II) ( $\text{PdCl}_2\cdot\text{COD}$ ) were used. 3 mmol of the desired metal salt was added to 4 mmol of the respective  $\alpha$ -diimine ligand bearing allyl groups (**4**, **5**, **6**, or **7**) dissolved in 150 ml THF. Diethyl ether was used instead of THF for the synthesis of the titanium and iron complexes. The mixture was stirred for 18 h at room temperature. For purification, the volume of the solvent was reduced in vacuo and the complexes were precipitated by adding pentane. After washing several times with n-pentane until the solvent stayed colorless, the products were dried in vacuo. The complexes were obtained as powders. The yields were 55-90%. All compounds were characterized by MS and elemental analysis. Complexes **6g** and **8** gave single crystals that were suitable for an X-ray analysis.

### 3.3.4 Synthesis of bis(cyclopentadienyl)methyl silane (**9L**)

Methyldichlorosilane (8.62 g, 75 mmol) in 80 ml of diethyl ether was cooled to  $-78^\circ\text{C}$  and to this mixture sodium cyclopentadienide (13.2 g, 150mmol) dissolved in 100 ml tetrahydrofuran was slowly added over a period of 3 h. The solution was left to warm to room temperature with continuous stirring. The suspension was filtered and the solvents of the filtered solution were removed under reduced pressure to afford the final product  $\text{MeSiH}(\text{CpH})_2$  as viscous clear yellow oil (12.3 g, 92%), a mixture of three stereoisomers. The product was used without purification in the next reaction.

### 3.3.5 Synthesis of the complex $(C_5H_4-SiHMe-C_5H_4)ZrCl_2$ (**9C**)

100 mmol of  $(C_5H_5-SiHMe-C_5H_5)$  was dissolved in 200 ml diethylether and mixed with 200 mmol of n-butyllithium (1.6 M in n-hexane) at  $-78^\circ C$ . After warming up to room temperature, the mixture was stirred for 4 h. Subsequently, at  $-78^\circ C$ , 2.33 g (100 mmol) zirconium tetrachloride were added and stirred for 12 h at room temperature. Then, the solvent was evaporated and the residue was extracted with dichloromethane and the solution was filtered over sodium sulfate. The solution was reduced in volume and the product was precipitated by adding n-pentane. The yield was 86%. The complex was characterized by MS and elemental analysis.

### 3.3.6 General synthesis procedure for the dinuclear precursors **10-14** via hydrosilylation reactions

The appropriate  $\alpha$ -diimine complex (2 mmol) bearing an allyl group (**6a**, **6b**, **6c**, **6f**, or **6g**) was mixed with 2 mmol of  $(C_5H_4-SiHMe-C_5H_4)ZrCl_2$  in 100 ml toluene. The mixture was stirred and then a few drops of Karstadt's catalyst, platinum(0)-1,3-divinyl-1,1,3,3-tetramethyldisiloxane (0.1 M in xylene), were added. The reaction mixture was stirred at room temperature for 40 h. The mixture was then filtered through a glass frit and the resulting solid was washed several times with toluene and dried in vacuo to afford the dinuclear precursors. The yields were 40-90%. All precursors were characterized via MS and elemental analysis.

### 3.3.7 General synthesis procedure for the $\alpha$ -diimine compounds bearing chloropropyl groups (**15-17**)

A mixture of 3.3 ml (22 mmol) of tetramethylethylenediamine (TMEDA) and 13.75 ml (22 mmol) of n-butyllithium (1.6 M in n-hexane) was prepared in a pressure-equalizing dropping funnel containing 40 ml n-pentane. This mixture was added drop-wise to a stirred solution of 22 mmol of the appropriate  $\alpha$ -diimine compound (**1**, **2**, or **3**) in 100 ml of n-pentane. Immediately the color of the solution changed from yellow to orange. The reaction mixture was stirred overnight. The next step was the addition of 2 equiv. of 1-bromo-3-chloropropane (44 mmol, 4.36 ml) and refluxing the reaction mixture for 24 h. Later, the refluxing was stopped and the reaction mixture was allowed to cool down to room temperature. Removal of the solvent and an excess of 1-bromo-3-chloropropane by evaporation resulted in a viscous yellow liquid which was dissolved in n-pentane and filtered over sodium sulphate. The

solvent was removed and the resulting yellow thick liquid was purified by column chromatography on silica gel using n-hexane as eluant. The products were obtained after evaporating the solvents as viscous yellow liquid. Yields: **15**, 72%; **16**, 77%; **17**, 74%. All compounds were characterized by GC/MS and NMR spectroscopy.

### *3.3.8 General synthesis of the $\alpha$ -diimine compounds bearing cyclopentadienyl groups (**18-20**)*

An amount of 3.52 g of sodium cyclopentadienide (40 mmol) was added to 40 mmol of the appropriate  $\alpha$ -diimine compound bearing a chloropropyl group (**15**, **16**, or **17**) in 100 ml of THF. The reaction mixture was stirred at 60°C for 36 h. The heating was stopped allowing the mixture to cool down to room temperature and the solvent was evaporated followed by the addition of n-pentane to the residue and filtering the resulting solution over sodium sulphate. The solvent was removed to afford the products as golden viscous liquids which were used in the next reactions without further purification. Yields: **18**, 75%; **19**, 73%; **20**, 82%. All compounds were characterized by GC/MS and NMR spectroscopy.

### *3.3.9 General synthesis of the dinuclear precursors (**18<sub>a,b</sub>**, **19<sub>a,b</sub>**, and **20<sub>a,b</sub>**)*

5 mmol of n-butyllithium (1.6 M in n-hexane) was drop-wise added to 5 mmol of the appropriate  $\alpha$ -diimine compound bearing a cyclopentadienyl group (**18**, **19**, or **20**) which was dissolved in 100 ml diethyl ether at -78°C. After warming up to room temperature, the mixture was stirred for 6 h. Subsequently, at -78°C, 10 mmol of titanium tetrachloride or zirconium tetrachloride was added and the mixture was stirred for 36 h at room temperature. Then, the solvent was evaporated and the residue was extracted with dichloromethane and the solution was filtered over sodium sulfate. The solution was reduced in volume and the products were precipitated by adding n-pentane. The yields were 70-85%. The compounds were characterized by MS and elemental analysis.

### *3.4 Polymerization of ethylene in the 1 l Büchi autoclave*

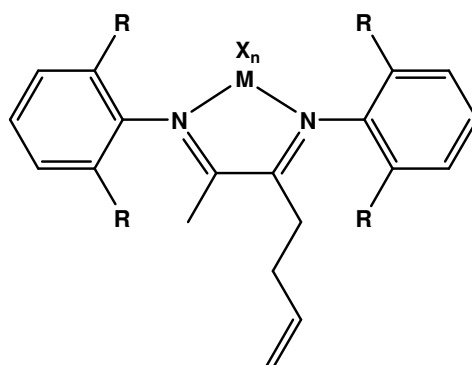
An amount of 1–5 mg of the desired complex was suspended in 5ml of toluene. Methylalumoxane (30% in toluene, M:Al = 1:1500) was added resulting in an immediate color change. The mixture was added to a 1 l Schlenk flask filled with 250 ml n-pentane. This mixture was transferred to a 1 l Büchi laboratory autoclave under inert atmosphere and thermostated at 65°C or 50°C. An ethylene pressure of 10 bar was applied for 1 h. After

releasing the pressure, the polymer was filtered over a frit, washed with diluted hydrochloric acid, water, and acetone, and finally dried in vacuo.

## 4. Summary

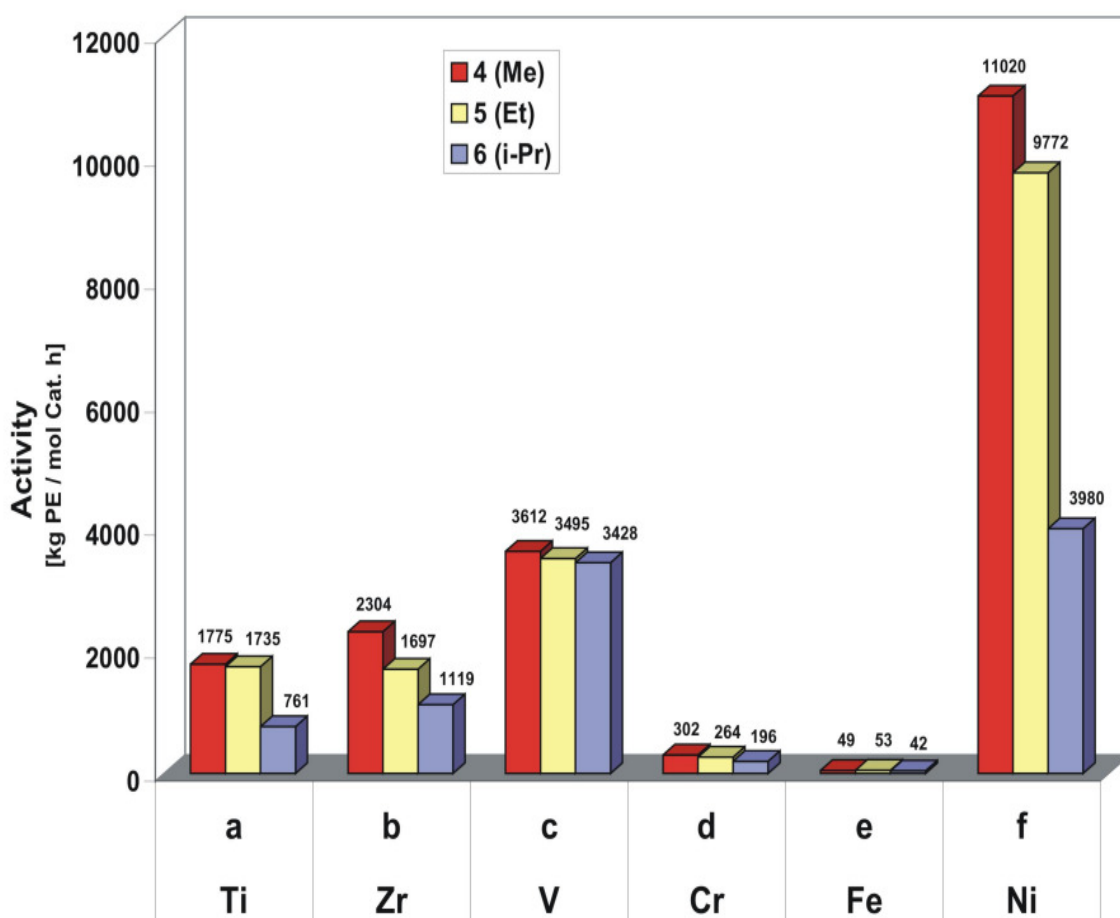
It was the goal of this project to synthesize dinuclear catalysts that provide two different active sites for the oligomerization and polymerization of  $\alpha$ -olefins, especially ethylene. The plan of synthesis involves precursors consisting of a diimine moiety coordinated to a late or early transition metal and a metallocene or half sandwich moiety. In order to achieve these goals, some  $\alpha$ -diimine compounds were functionalized with allyl or alkyl halide groups and then coupled with a metallocene or a half sandwich complex.

Three different  $\alpha$ -diimine compounds were synthesized and characterized by GC-MS,  $^1\text{H}$  NMR, and  $^{13}\text{C}$  NMR spectroscopy. These compounds are bearing allyl functions at their backbones and different ortho substituents at the arene moieties of their frameworks. 21 different complexes were prepared using these compounds and they were characterized by mass spectroscopy and elemental analysis. These complexes were activated with methylalumoxane (MAO) and tested for the catalytic polymerization of ethylene.



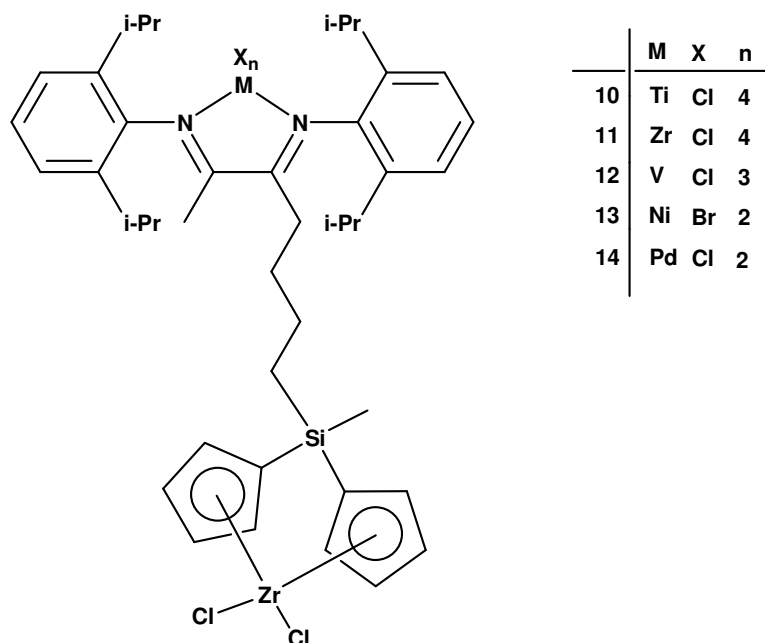
$\text{MX}_n =$	$\text{TiCl}_4$	$\text{ZrCl}_4$	$\text{VCl}_3$	$\text{CrCl}_3$	$\text{FeCl}_3$	$\text{NiBr}_2$	$\text{PdCl}_2$
$\text{R} = \text{Me}$	<b>4a</b>	<b>4b</b>	<b>4c</b>	<b>4d</b>	<b>4e</b>	<b>4f</b>	<b>4g</b>
$\text{R} = \text{Et}$	<b>5a</b>	<b>5b</b>	<b>5c</b>	<b>5d</b>	<b>5e</b>	<b>5f</b>	<b>5g</b>
$\text{R} = i\text{-Pr}$	<b>6a</b>	<b>6b</b>	<b>6c</b>	<b>6d</b>	<b>6e</b>	<b>6f</b>	<b>6g</b>

The ethylene polymerization results revealed that the bulkier the substituents at the aryl rings of the catalyst structure, the lower the polymerization activity. These results are compatible with the chain running mechanism which suggests that bulky substituents can hinder the monomers from reaching the active catalytic centers due to their interaction with the axial coordination sites of the metal centers. The palladium catalysts showed no polymerization activity as distinguished behavior. That may attribute to the allyl functions attached to the backbone of the catalyst structures which can interact with the active sites of the palladium catalysts resulting in blocking the active sites and deactivating the catalyst.



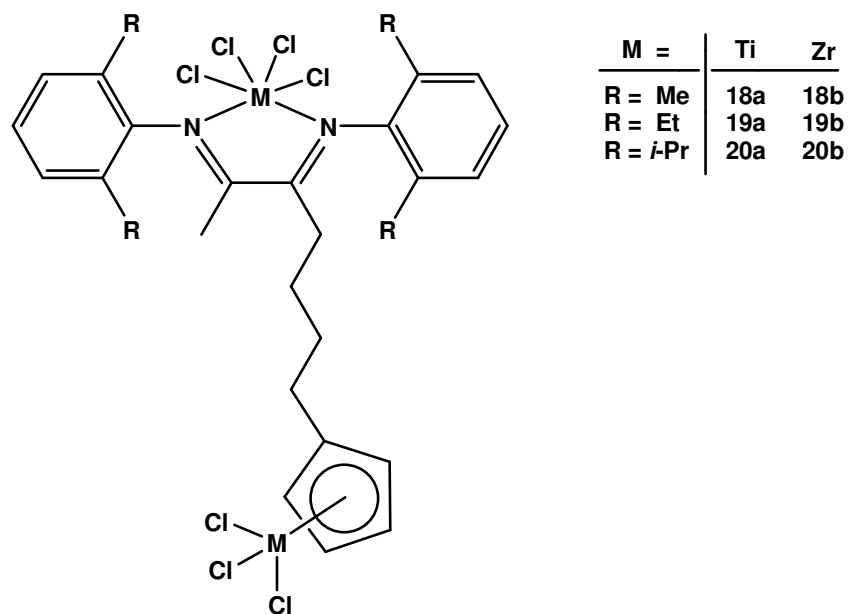
Five  $\alpha$ -diimine complexes bearing allyl groups were coupled with a bridged zirconocene complex possessing a hydride silane moiety via hydrosilylation reaction in the presence of Karstedt's catalyst to afford five new dinuclear precursors.

These dinuclear precursors were activated with methylalumoxane (MAO) and tested for the polymerization of ethylene.



The bridged silyl zirconocene moiety is the same for all these dinuclear complexes. Therefore, the ethylene polymerization activities of their catalysts showed a dependence on the variant metal centers of the  $\alpha$ -diimine moiety. The trend of polymerization activities was: Ni > Pd > V > Zr > Ti. The produced polyethylenes were analyzed via gel permeation chromatography (GPC). The GPC results showed broad molecular weight distributions due to the dual sites of these catalysts. The GPC spectrum of polyethylene produced with the dinuclear catalyst **13** was discussed as an example and compared with the GPC spectrum of polyethylene produced with its mononuclear catalyst **6f**.

Six novel dinuclear precursors consisting of  $\alpha$ -diimine moieties connected to half sandwich metallocene complexes were prepared and characterized via mass spectroscopy and elemental analysis. These dinuclear precursors were activated with methylalumoxane (MAO) and tested for the polymerization of ethylene.

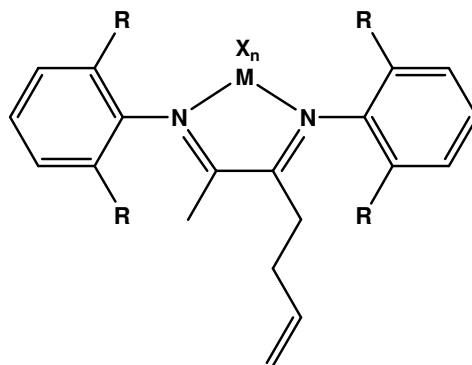


The ethylene polymerization activities of these dinuclear catalysts demonstrated a dependence on the size of the ortho substituents at the aryl rings of the catalysts structures. The results of ethylene polymerization agreed with the chain running mechanism: the bulkier the substituents the lower the polymerization activities. The results of gel permeation chromatography (GPC) of polyethylene produced by these catalysts exhibited bimodal molecular weight distributions. These results can be assigned to the different active sites of the dinuclear catalysts. The GPC spectra of polyethylenes produced with the dinuclear catalysts **18a,b** were discussed as examples.

## 5. Zusammenfassung

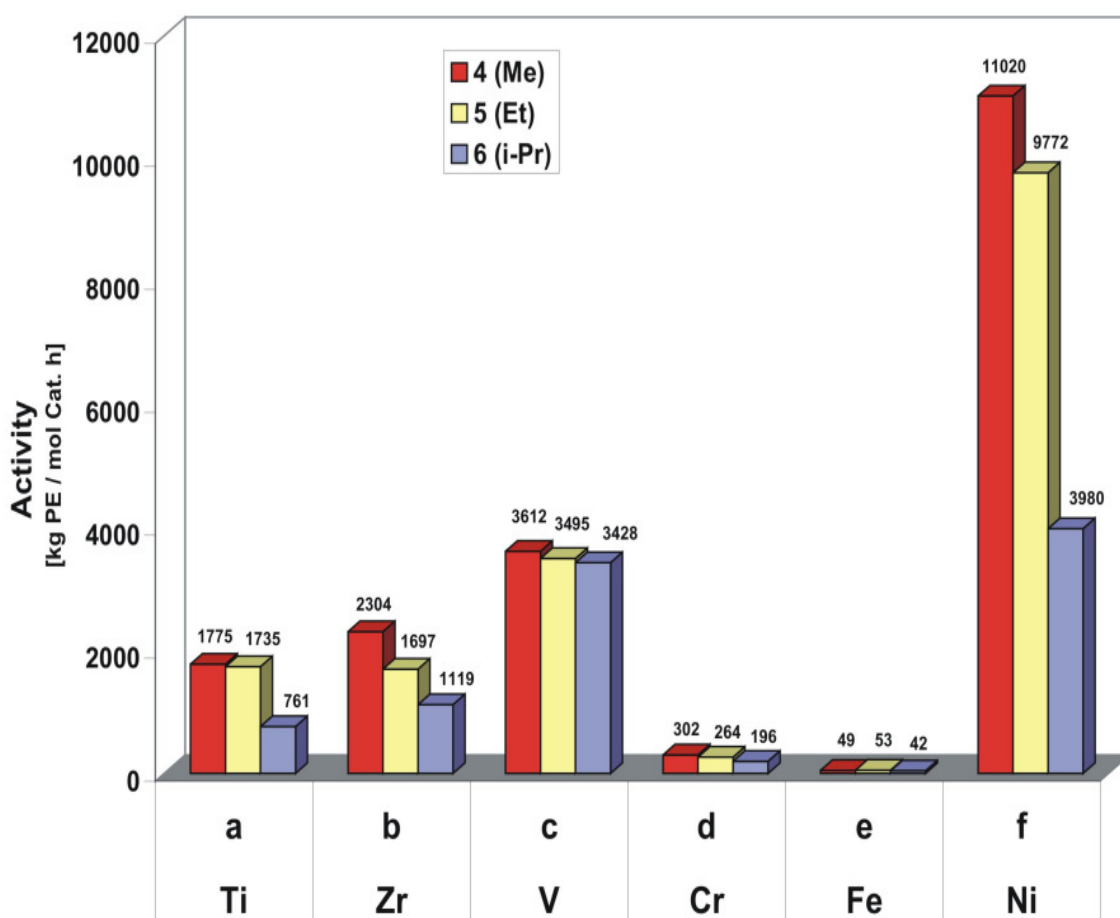
Ziel dieser Arbeit war es zweikernige Komplexe mit zwei unterschiedlichen aktiven Zentren darzustellen und deren Einsatz für die Oligomerisation und Polymerisation von Ethen zu untersuchen. Für die Komplexsynthese wurden zwei verschiedene Katalysatorvorstufen verknüpft. Die eine enthielt ein mit Alkyl- Alkylhalogeniden funktionalisiertes Diiminfragment mit einem späten oder frühen Übergangsmetall, die andere bestand aus einer Metallocen- oder Halbsandwichereinheit.

Es wurden drei verschiedene  $\alpha$ -Diimin-Verbindungen dargestellt und mittels GC-MS,  $^1\text{H}$ -NMR und  $^{13}\text{C}$ -NMR Spektroskopie charakterisiert. Diese organischen Ligandvorstufen besitzen Allylfunktionen am Grundgerüst und verschiedene ortho-substituierte Anilinfragmente. 21 verschiedene Komplexe wurden daraus synthetisiert und mit Hilfe der Massen-spektroskopie und C, H, N-Elementaranalyse charakterisiert. Nach Aktivierung mit Methylaluminoxan (MAO) wurden diese Komplexe hinsichtlich ihrer katalytischen Aktivität bei der Polymerisation von Ethen untersucht.



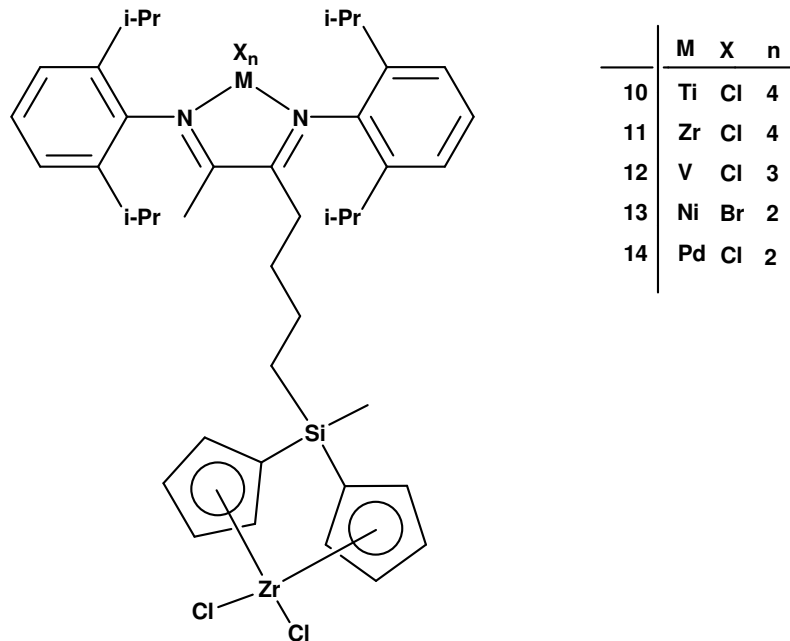
$\text{MX}_n =$	$\text{TiCl}_4$	$\text{ZrCl}_4$	$\text{VCl}_3$	$\text{CrCl}_3$	$\text{FeCl}_3$	$\text{NiBr}_2$	$\text{PdCl}_2$
$\text{R} = \text{Me}$	<b>4a</b>	<b>4b</b>	<b>4c</b>	<b>4d</b>	<b>4e</b>	<b>4f</b>	<b>4g</b>
$\text{R} = \text{Et}$	<b>5a</b>	<b>5b</b>	<b>5c</b>	<b>5d</b>	<b>5e</b>	<b>5f</b>	<b>5g</b>
$\text{R} = i\text{-Pr}$	<b>6a</b>	<b>6b</b>	<b>6c</b>	<b>6d</b>	<b>6e</b>	<b>6f</b>	<b>6g</b>

Die Aktivitäten der Katalysatoren zeigten, dass eine sterische Zunahme der Größe des Substituenten am Arylring mit einer Abnahme der Aktivitäten einherging. Diese Ergebnisse sind mit dem „chain running mechanism“ erklärbar, welcher besagt, dass sterisch anspruchsvolle Substituenten das Monomer an dessen Wechselwirkung mit dem aktiven Metallzentrum, aufgrund der axial koordinierenden Zentren, hindern können. Die Palladium-Katalysatoren zeigten keine katalytische Aktivität bei den Polymerisationsreaktionen. Der Grund dafür sind die Allylgruppen am Grundgerüst des Katalysators. Diese können mit den aktiven Zentren des Palladium Katalysators wechselwirken und sie besetzen. Dadurch kommt es zu einer Deaktivierung des Katalysators.



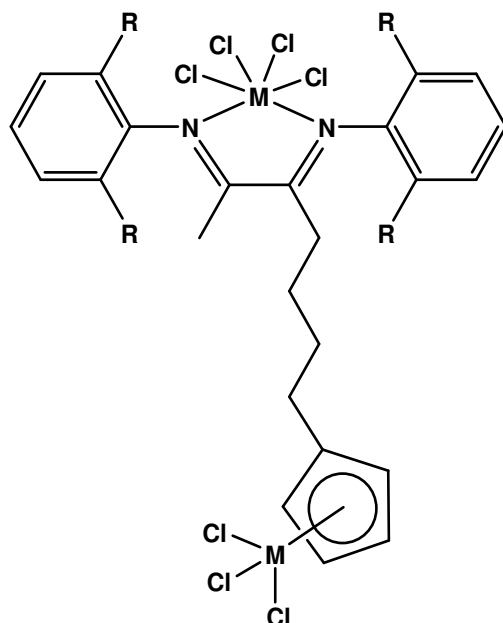
Fünf  $\alpha$ -Diimin-Komplexe mit Allylgruppen wurden durch Hydrosilylierungsreaktionen mit einem verbrückten Zirconocen-Komplex verbunden. Dabei wurde die Allylgruppe mit der Silanfunktion des Zirconocen-Komplexes in Gegenwart eines Karstedt-Katalysators umgesetzt, wodurch fünf neue zweikernige Katalysator-Vorstufen entstanden. Nach der

Aktivierung mit Methylaluminoxan wurden diese Komplexe hinsichtlich ihrer katalytischen Aktivität bei der Polymerisation von Ethen untersucht.



Die verbrückte Zirconoceneinheit ist für alle zweikernigen Komplexe nicht variiert worden. Die Aktivitäten der Polymerisationsreaktionen zeigten folgende Abhängigkeit von der Art des Zentralmetalls der Diimineinheit: Ni > Pd > V > Zr > Ti. Die GPC-Analysen des erhaltenen Polyethylens wiesen breite Molekulargewichtsverteilungen ( $M_n$ ) auf, was den zwei unterschiedlichen aktiven Zentren der Katalysatoren entspricht.

Sechs neue zweikernige Katalysatorvorstufen mit einer  $\alpha$ -Diimin-Einheit, gebunden an einen Metallocen Halbsandwich-Komplex, wurden funktionalisiert. Sie wurden durch Massenspektroskopie und C, H, N-Elementaranalyse charakterisiert. Nach der Aktivierung mit Methylaluminoxan wurden auch diese Komplexe hinsichtlich ihrer katalytischen Aktivität bei der Polymerisation von Ethen untersucht.



M =	Ti	Zr
R = Me	18a	18b
R = Et	19a	19b
R = <i>i</i> -Pr	20a	20b

Die Aktivitäten der Polymerisationsreaktionen dieser zweikernigen Katalysatoren zeigten eine Abhängigkeit von der Größe der ortho-Substituenten (R) des Arylrings. Auch hier stimmten die Ergebnisse mit dem „chain running mechanism“ überein: Größere Substituenten bedingten ein Erniedrigung der Aktivitäten der Polymerisationskatalysatoren. Die Ergebnisse der GPC-Analysen der hergestellten Polyethylene wiesen eine bimodale Molekulargewichtsverteilung auf. Dies kann den beiden aktiven Zentren der zweikernigen Komplexe zugeschrieben werden. Die GPC-Spektren der mit den zweikernigen Katalysatoren **18a** und **b** hergestellten Polyethylene wurden als Beispiele diskutiert.

## 6. References

- [1] H. Staudinger, *Ber. Dtsch. Chem. Ges.* **1920**, 53, 107.
- [2] H. Staudinger, H. Fritsch, *Helv. Chim. Acta* **1922**, 5, 785.
- [3] H. Staudinger, *Ber. Dtsch. Chem. Ges.* **1924**, 57, 1203.
- [4] H. Staudinger, *Ber. Dtsch. Chem. Ges.* **1926**, 59, 3019.
- [5] [http://nobelprize.org/nobel\\_prizes/chemistry/laureates/1953](http://nobelprize.org/nobel_prizes/chemistry/laureates/1953)
- [6] Neufeldt, *Chronik der Chemie 1800-1980*, VCH, Weinheim, **1987**.
- [7] Strube, *Geschichte der Chemie*, Dtsch. Verl. der Wissenschaften, Berlin, **1986**.
- [8] R. B. Seymour, T. Cheng, *History of Polyolefins*, **1986**, Riedel Publ. Co., New York.
- [9] J. P. Hogan, R. L. Banks, *Belg. Pat. 530617*, **1955**; *U. S. 2825721*, **1958**.
- [10] K. S. Whiteley, T. G. Heggs in Ullmann's Encyclopedia of Industrial Chemistry, (Ed.: B. Elvers, S. Hawkin, M. Ravencroft, G. Schulz), Vol. 5, **1992**.
- [11] K. Ziegler, H. Gellert, H. Kühlhorn, H. Martin, K. Meyer, K. Nagel, H. Sauer, K. Zosel, *Angew. Chem.* **1952**, 64, 323.
- [12] K. Ziegler, E. Holzkamp, H. Breil, H. Martin, *Angew. Chem.* **1955**, 67, 541.
- [13] G. Natta, *Angew. Chem.* **1956**, 68, 393.
- [14] K. Ziegler, *Angew. Chem.* **1964**, 76, 545.
- [15] G. Natta, *Angew. Chem.* **1964**, 76, 553.
- [16] D. S. Breslow, N. R. Newburg, *J. Am. Chem. Soc.* **1957**, 79, 5072.
- [17] G. Natta, P. Pino, G. Mazzanti, U. Giannini, *J. Am. Chem. Soc.* **1957**, 79, 2975.
- [18] H. Sinn, W. Kaminsky, H. J. Vollmer, *Angew. Chem.* **1980**, 92, 396.
- [19] H. Sinn, W. Kaminsky, *Adv. Organomet. Chem.* **1980**, 99, 18.
- [20] J. L. Atwood, D. C. Hrcir, R. D. Priester, R. D. Rogers, *Organometallics* **1983**, 2, 985.
- [21] S. Pasykiewicz, *Polyhedron* **1990**, 9, 429.
- [22] M. R. Mason, J. M. Smith, S. G. Bott, A. R. Barron, *J. Am. Chem. Soc.* **1993**, 115, 4971.
- [23] C. J. Harlan, M. R. Mason, A. R. Barron, *Organometallics* **1994**, 13, 2957.
- [24] C. J. Harlan, S. G. Bott, A. R. Barron, *J. Am. Chem. Soc.* **1995**, 117, 6465.
- [25] Y. Koide, S. G. Bott, A. R. Barron, *Organometallics* **1996**, 15, 5514.
- [26] E. P. Talsi, N. V. Semikolenova, V. N. Panchenko, A. P. Sobolev, D. E. Babushkin, A. A. Shubin, V. A. Zakharov, *J. Mol. Catal. A: Chem.* **1999**, 139, 131.
- [27] E. Zurek, T. Ziegler, *Organometallics* **2002**, 21, 83.
- [28] I.I. Zakharov, V.A. Zakharov, *Macromol. Theory Simul.* **2002**, 11, 352.

- [29] P. Cossee, *J. Catal.* **1964**, *3*, 80.
- [30] E.J. Arlman, *J. Catal.* **1964**, *3*, 89.
- [31] E.J. Arlman, P. Cossee, *J. Catal.* **1964**, *3*, 99.
- [32] F. Wild, L. Zsolnai, G. Huttner, H.-H. Brintzinger, *J. Organomet. Chem.* **1982**, *232*, 233.
- [33] F. Wild, M. Wasiucioneck, G. Huttner, H.-H. Brintzinger, *J. Organomet. Chem.* **1985**, *288*, 63.
- [34] J. A. Ewen, R. L. Jones, A. Razavi, J. D. Ferrara, *J. Am. Chem. Soc.* **1988**, *110*, 6255.
- [35] W. Kaminsky, *Catal. Today* **2000**, *62*, 23.
- [36] B. Peifer, W. Milius, H. G. Alt, *J. Organomet. Chem.* **1998**, *553*, 205.
- [37] L. K. Johnson, C. K. Killian, M. Brookhart, *J. Am. Chem. Soc.* **1995**, *117*, 6414.
- [38] L. K. Johnson, S. Mecking, M. Brookhart, *J. Am. Chem. Soc.* **1996**, *118*, 267.
- [39] C. Wang, A. Friedrich, T. R. Younkin, R. T. Li, R. H. Grubbs, A. Bansleben, M. W. Day, *Organometallics* **1998**, *17*, 3149.
- [40] T. R. Younkin, E. F. Connor, J. I. Henderson, S. K. Friedrich, R. H. Grubbs, D. A. Bansleben, *Science* **2000**, *287*, 460.
- [41] S. Matsui, Y. Tohi, M. Mitani, J. Saito, H. Makio, H. Tanaka, M. Nitabaru, T. Nakano, T. Fujita, *Chem. Lett.*, **1999**, 1065.
- [42] S. Matsui, M. Mitani, J. Saito, Y. Tohi, H. Makio, N. Matsukawa, Y. Takagi, K. Tsuru, M. Nitabaru, T. Nakano, H. Tanaka, N. Kashiwa, T. Fujita, *J. Am. Chem. Soc.* **2001**, *123*, 6847.
- [43] H. Makio, N. Kashiwa, T. Fujita, *Adv. Synth. Catal.* **2002**, *344*, 477.
- [44] G. J. P. Britovsek, V. C. Gibson, B. S. Kimberley, P. J. Maddox, S. J. McTavish, G. A. Solan, A. J. P. White, D. J. Williams, *Chem. Commun.* **1998**, 849.
- [45] G. J. P. Britovsek, V. C. Gibson, B. S. Kimberley, P. J. Maddox, S. J. McTavish, G. A. Solan, A. J. P. White, D. J. Williams, *J. Am. Chem. Soc.* **1999**, *121*, 8728.
- [46] G. J. P. Britovsek, V. C. Gibson, D. F. Wass, *Angew. Chem., Int. Ed.* **1999**, *37*, 428.
- [47] G. J. P. Britovsek, G. K. B. Clentsmith, V. C. Gibson, D. M. L. Goodgame, S. J. McTavish, Q. A. Pankhurst, *Catal. Commun.* **2002**, *3*, 207.
- [48] B. L. Small, M. Brookhart, *J. Am. Chem. Soc.* **1998**, *120*, 7143.
- [49] B. L. Small, M. Brookhart, A.M.A. Bennett, *J. Am. Chem. Soc.* **1998**, *120*, 4049.
- [50] B. L. Small, M. Brookhart, *Macromolecules* **1999**, *12*, 2120.
- [51] G. J. P. Britovsek, S. Mastroianni, G. A. Solan, S. P. D. Baugh, C. Redshaw, V. C. Gibson, A. J. P. White, D. J. Williams, M. R. J. Elsegood, *Chem. A Eur. J.* **2000**, *6*, 2221.

- [52] R. Schmidt, U. Hammon, S. Gottfried, M. B. Welch, H. G. Alt, *J. Appl. Polym. Sci.* **2003**, *88*, 476.
- [53] C. Görl, H. G. Alt, *J. Organomet. Chem.* **2007**, *692*, 4580.
- [54] F. A. R. Kaul, G. T. Puchta, H. Schneider, F. Bielert, D. Mihalios, W. A. Herrmann, *Organometallics* **2002**, *21*, 74.
- [55] C.-K. Liu, G.-X. Jin, H. Xuebao, *Acta Chimica Sinica* **2002**, *60*, 157.
- [56] M. Seitz, W. Milius, H. G. Alt, *J. Mol. Catal. A: Chem.* **2007**, *261*, 246.
- [57] C. Görl, H. G. Alt, *J. Mol. Catal. A: Chem.* **2007**, *273*, 118.
- [58] D. Zhang, G.-X. Jin, N. Hu, *Chem. Commun.* **2002**, 574.
- [59] D. Zhang, G.-X. Jin, N. Hu, *Eur. J. Inorg. Chem.* **2003**, 1570.
- [60] D. Zhang, G.-X. Jin, *Appl. Catal. A: General* **2004**, *26*, 85.
- [61] G.-X. Jin, D. Zhang, *J. Polym. Sci. A: Polym. Chem.* **2004**, *42*, 1018.
- [62] D. Zhang, G.-X. Jin, *Appl. Catal. A: General* **2004**, *262*, 13.
- [63] H. tom Dieck, M. Svoboda, T. Z. Grieser, *Z. Naturforsch* **1981**, *36b*, 832.
- [64] R. Van Asselt, C. J. Elsevier, W. J. J. Smeets, A. L. Spek, R. Benedix, *Recl. Trav. Chim. Pays-Bas* **1994**, *113*, 88.
- [65] G. Van Koten, K. Vrieze, *Adv. Organomet. Chem.* **1982**, *21*, 151.
- [66] C. M. Killian, D. J. Tempel, L. K. Johnson, M. Brookhart, *J. Am. Chem. Soc.* **1996**, *118*, 11664.
- [67] M. Brookhart, L. K. Johnson, C. M. Killian, S. Mecking, D. J. Tempel, *Polym. Prep., Am. Chem. Soc., Div. Polym. Chem.* **1996**, *37*, 254.
- [68] S. J. McLain, J. Feldman, E. F. McCord, K. H. Gardner, M. F. Teasley, E. B. Coughlin, K. J. Sweetman, L. K. Johnson, M. Brookhart, *Polym. Mater. Sci. Eng.* **1997**, *67*, 20.
- [69] R. L. Huff, S. A. Svejda, D. J. Tempel, M. D. Leatherman, L. K. Johnson, M. Brookhart, *Polym. Prep., Am. Chem. Soc., Div. Polym. Chem.* **2000**, *41*, 401.
- [70] M. Brookhart, L. K. Johnson, C. M. Killian, E. F. McCord, S. J. McLain, K. A. Kreutzer, S. D. Ittel, D. J. Tempel, US Patent Appl. US 5880241 **1999**.
- [71] S. A. Svejda, L. K. Johnson, M. Brookhart, *J. Am. Chem. Soc.* **1999**, *121*, 10634.
- [72] S. D. Ittel, L. K. Johnson, M. Brookhart, *Chem. Rev.* **2000**, *100*, 1169.
- [73] M. Brookhart, L. K. Johnson, C. M. Killian, S. A. Svejda, D. Gates, D. J. Tempel, R. L. Huff, M. D. Leatherman, *Macromol. Symp.* **2001**, *174*, 29.
- [74] T. V. Laine, M. Klinga, A. Maaninen, E. Aitola, M. Leskelä, *Acta Chem.Scand.* **1999**, *20*, 232.
- [75] M. Qian, M. Wang, B. Zhou, R. He, *Appl. Catal. A: General* **2001**, *209*, 11.

- [76] M. Sieger, M. Wanner, W. Kaim, D. J. Stufkens, T. L. Snoeck, S. Zálíš, *Inorg. Chem.* **2003**, *42*, 3340.
- [77] S. C. Bart, E. J. Hawrelak, A. K. Schmisser, E. Lobkovsky, P. J. Chirik, *Organometallics* **2004**, *23*, 237.
- [78] I. L. Fedushkin, N. M. Khvoynova, A. Yu. Baurin, G. K. Fukin, V. K. Cherkasov, M. P. Bubnov, *Inorg. Chem.* **2004**, *43*, 7807.
- [79] I. L. Fedushkin, V. A. Chudakovaa, A. A. Skatovaa, N. M. Khvoynovaa, Y. A. Kurskiia, T. A. Glukhova, G. K. Fukina, S. Dechertb, M. Hummert, H. Schumann, *Z. Anorg. Allg. Chem.* **2004**, *630*, 501.
- [80] V. Rosa, P. J. Gonzalez, T. Avilés, P. T. Gomes, R. Welter, A. C. Rizzi, M. C. G. Passeggi, C. D. Brondino, *Eur. J. Inorg. Chem.* **2006**, 4761.
- [81] V. Rosa, S. A. Carabineiro, T. Avilés, P. T. Gomes, R. Welter, J. M. Campos, M. R. Ribeiro, *J. Organomet. Chem.* **2008**, *693*, 769.
- [82] P. De Waele, B. A. Jazdzewski, J. Klosin, R. E. Murray, C. N. Theriault, P. C. Vosejka, *Organometallics* **2007**, *26*, 3896.
- [83] C. M. Killian, L. K. Johnson, M. Brookhart, *Organometallics* **1997**, *16*, 2005.
- [84] M. Helldörfer, J. Backhaus, W. Milius, H. G. Alt, *J. Mol. Catal. A: Chem.* **2003**, *193*, 59.
- [85] M. Helldörfer, W. Milius, H. G. Alt, *J. Mol. Catal. A: Chem.* **2003**, *197*, 1.
- [86] M. Helldörfer, J. Backhaus, H. G. Alt, *Inorganica Chimica Acta* **2003**, *351*, 34.
- [87] A. Köppl, H. G. Alt, *J. Mol. Catal. A: Chem.* **2000**, *154*, 45.
- [88] L. K. Johnson, M. Brookhart, *Macromolecules* **1998**, *31*, 6705.
- [89] S. A. Svejda, M. Brookhart, *Organometallics*, **1999**, *18*, 65.
- [90] D.P. Gates, S.A. Svejda, E. Onate, C.M. Killian, L.K. Johnson, P.S. White and M. Brookhart, *Macromolecules* **2000**, *33*, 2320.
- [91] T. Schleis, T.P. Spaniol, J. Okuda, J. Heinemann, R. Mülhaupt, *J. Organomet. Chem.* **1998**, *569*, 159.
- [92] M. Gasperini, F. Ragaini, S. Cenini, *Organometallics* **2002**, *21*, 2950.
- [93] M. Gasperini, F. Ragaini, *Organometallics* **2004**, *23*, 995.
- [94] B. K. Bahuleyan, G. W. SON, Dae-Won Park, C.-S. Ha, I. Kim, *J. Polym. Sci. A: Polym. Chem.* **2008**, *46*, 1066.
- [95] J. Liu, Y. Li, Y. Li, N. Hu, *J. Appl. Polym. Sci.* **2008**, *109*, 700.
- [96] M. Schmid, R. Eberhardt, M. Klinga, M. Leskelä, B. Rieger, *Organometallics* **2001**, *20*, 2321.
- [97] A. S. Ionkin, W. J. Marshall, *J. Organomet. Chem.* **2004**, *689*, 1057.

- [98] D. Pappalardo, M. Maueo, C. Pellecchia, *Macromol. Rapid Commun.* **1997**, *18*, 1017.
- [99] C. G. de Souza, R. F. de Souza, K. Bernardo-Gusmão, *Appl. Catal. A: General* **2007**, *325*, 87.
- [100] M. Helldörfer, H. G. Alt, *J. Appl. Polym. Sci.* **2003**, *89*, 1356.
- [101] D. P. Gates, S. A. Svejda, E. Oñate, C. M. Killian, L. K. Johnson, P. S. White, M. Brookhart, *Macromolecules* **2000**, *33*, 2320.
- [102] F. AlObaidia, Z. Yea, S. Zhu, *Polymer* **2004**, *45*, 6823.
- [103] L. C. Simon, H. Patel, J. B. P. Soares, R. F. de Souza, *Macromol. Chem. Phys.* **2001**, *202*, 3237.
- [104] P. P.-Pflügl, M. Brookhart, *Macromolecules* **2002**, *35*, 6074.
- [105] Z. Ye, H. Alsyouri, S. Zhu, Y. S. Lin, *Polymer* **2003**, *44*, 969.
- [106] F. AlObaidi, Z. Ye, S. Zhu, *Macromol. Chem. Phys.* **2003**, *204*, 1653.
- [107] Y.-G. Li, L. Pan, Z.-J. Zheng, Y.-S. Li, *J. Mol. Catal. A: Chem.* **2008**, *287*, 57.
- [108] M. Elliott, N. F. Janes, *J. Chem. Soc. C* **1967**, 1780.
- [109] L. Deng, T. Woo, L. Cavallo, P. M. Margl, T. Ziegler, *J. Am. Chem. Soc.* **1997**, *119*, 6177.
- [110] L. Deng, P.M. Margl, T. Ziegler, *J. Am. Chem. Soc.* **1997**, *119*, 1094.
- [111] M. Schilling, R. Bal, C. Görl, H. G. Alt, *Polymer* **2007**, *48*, 7461.
- [112] F. Lindenberg, T. Shribman, J. Sieler, E. H.-Hawkins, M. S. Eisen, *J. Organomet. Chem.* **1996**, *515*, 19.
- [113] S. K. Noh, S. Kim, J. Kim, D. H. Lee, K. B. Yoon, H. B. Lee, S. W. Lee, W. S. Huh, *J. Polym. Sci. Part A: Polym. Chem.* **1997**, *35*, 3717–3728.
- [114] B. Bosch, G. Erker, R. Fröhlich, *Inorg. Chim. Acta* **1998**, *270*, 446.
- [115] S. K. Noh, J. Kim, J. Jung, C. S. Ra, D. H. Lee, H. B. Lee, S. W. Lee, W. S. Huh, *J. Organomet. Chem.* **1999**, *580*, 90–97.
- [116] F. F. Mota, R. S. Mauler, R. F. de Souza, O. L. Casagrande, *Macromol. Chem. Phys.* **2001**, *202*, 1016.
- [117] D. Reardon, J. Guan, S. Gambarotta, G. P. A. Yap, *Organometallics* **2002**, *21*, 4390.
- [118] J. H. Brownie, M. C. Baird, L. N. Zakharov, A. L. Rheingold, *Organometallics* **2003**, *22*, 33.
- [119] S. K. Noh, Y. Yang, W. S. Lyoo, *J. Appl. Polym. Sci.* **2003**, *90*, 2469.
- [120] S. K. Noh, J. Lee, D. H. Lee, *J. Organomet. Chem.* **2003**, *667*, 53–60.
- [121] S. K. Noh, M. Lee, D. H. Kum, W. S. Lyoo, D. H. Lee, *J. Polym. Sci. Part A: Polym. Chem.* **2004**, *42*, 1712–1723.

- [122] M. Deppner, R. Burger, H. G. Alt, *J. Organomet. Chem.* **2004**, 689, 1194.
- [123] E. C. E. Rosenthal, H. Cui, K. C. H. Lange, S. Dechert, *Eur. J. Inorg. Chem.* **2004**, 4681.
- [124] S. Jie, D. Zhang, T. Zhang, W.-H. Sun, J. Chen, Q. Ren, D. Liu, G. Zheng, W. Chen, *J. Organomet. Chem.* **2005**, 690, 1739.
- [125] Z. Wei, H. Al-Shammari, S. Palackal, A. Abu-Raqabah, US2005203260 A1 **2005**.
- [126] J. Kuwabara, D. Takeuchi, K. Osakada, *Organometallics* **2005**, 24, 2705.
- [127] D. A. Pennington, P. N. Horton, M. B. Hursthouse, M. Bochmann, S. J. Lancaster, *Polyhedron* **2005**, 24, 151.
- [128] J.-P. Taquet, O. Siri, P. Braunstein, *Inorg. Chem.* **2006**, 45, 4668.
- [129] F. Lin, J. Sun, X. Liu, W. Lang, X. Xiao, *J. Appl. Polym. Sci.* **2006**, 101, 3317.
- [130] J. C. Chadwick, R. Huang, N. Kukalyekar, S. Rastogi, *Macromol. Symp.* **2007**, 260, 154.
- [131] C. Görl, H. G. Alt, *J. Organomet. Chem.* **2007**, 692, 5727.
- [132] H. Zou, S. Hu, H. Huang, F. Zhu, Q. Wu, *Europ. Polym. J.* **2007**, 43, 3882.
- [133] S. K. Kim, H. K. Kim, M. H. Lee, S. W. Yoon, Y. Han, S. Park, J. Lee, Y. Do, *Eur. J. Inorg. Chem.* **2007**, 537.
- [134] T. D. Tilley, In *The Chemistry of Organic Silicon Compounds*; Patai, S., Rappoport, Z., Eds.; John Wiley & Sons Ltd.: New York, **1989**, p 1415.
- [135] I. Ojima, In *The Chemistry of Organic Silicon Compounds*; Patai, S., Rappoport, Z., Eds.; John Wiley & Sons Ltd.: New York, **1989**, p 1479.
- [136] K. Ohsima, In *Advances in Metal-Organic Chemistry*; Liebeskind, L. S., Ed.; JAI Press Ltd.: London, **1991**, 2, 101.
- [137] B. Marciniec, H. Maciejewski, W. Duczmal, R. Fiedorow, D. Kityński, *Appl. Organomet. Chem.* **2003**, 17, 127.
- [138] I. E. Markó, S. Stérin, O. Buisine, G. Berthon, G. Michaud, B. Tinant, J.-P. Declercq *Adv. Synth. Catal.* **2004**, 346, 1429.
- [139] J. L. Speier, J. A. Webster, G. H. Barnes, *J. Am. Chem. Soc.* **1957**, 79, 974.
- [140] J. C. Saam, J. L. Speier *J. Am. Chem. Soc.* **1958**, 80, 4104.
- [141] J. W. Ryan, J. L. Speier, *J. Am. Chem. Soc.* **1964**, 86, 895.
- [142] J. L. Speier, *Adv. Organomet. Chem.* **1979**, 17, 407.
- [143] B. D. Karstedt, (General Electric), US 3715334, **1973**.
- [144] P. B. Hitchcock, M. F. Lappert, N. J. W. Warhurst, *Angew. Chem. Int. Ed. Engl.* **1991**, 30, 438.

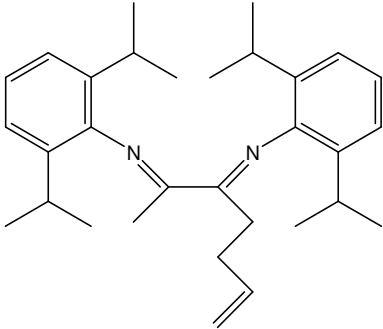
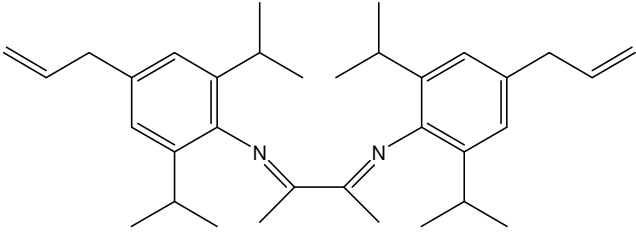
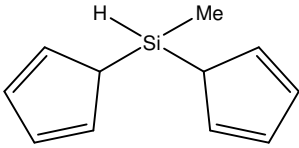
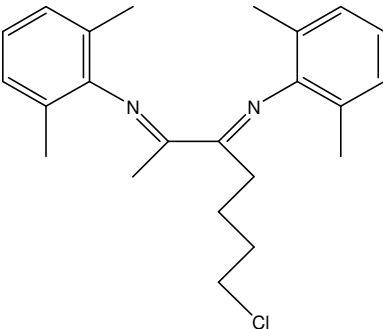
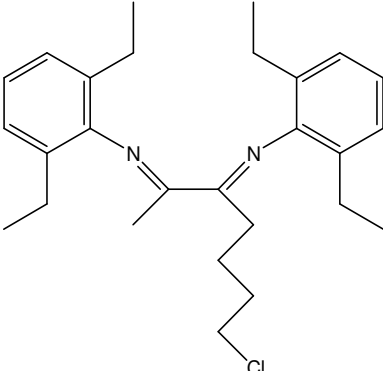
- 
- [145] A. J. Chalk, J. F. Harrod, *J. Am. Chem. Soc.* **1965**, *87*, 16.
- [146] J. F. Harrod, A. J. Chalk, In *Organic Synthesis via Metal Carbonyls*; Wender, I., Pino, P., Eds.; John Wiley & Sons Ltd.: New York **1977**, *2*, 673.
- [147] J. Stein, L. N. Lewis, K. A. Smith, K. X. Lettko, *J. Inorg. and Organom. Polym.* **1991**, *1*, 325.
- [148] S. Sakaki, N. Mizoe, M. Sugimoto, *Organometallics* **1998**, *17*, 2510.
- [149] M. A. Schroeder, M. S. Wrighton, *J. Organomet. Chem.* **1977**, *128*, 345.
- [150] C. L. Reichel, M. S. Wrighton, *Inorg. Chem.* **1980**, *19*, 3858.
- [151] A. Milan, E. Towns, P. M. Maitlis, *J. Chem. Soc., Chem. Commun.* **1981**, 673.
- [152] A. Milan, M.-J. Fernandez, P. Bentz, P. M. Maitlis, *J. Mol. Catal.* **1984**, *26*, 89.
- [153] I. Ojima, M. Yatabe, T. Fuchikami, *J. Organomet. Chem.* **1984**, *260*, 335.
- [154] C. L. Randolph, M. S. Wrighton, *J. Am. Chem. Soc.* **1986**, *108*, 3366.
- [155] H. G. Alt, R. Ernst, I. K. Böhmer, *J. Organomet. Chem.* **2002**, *658*, 259.
- [156] H. G. Alt, R. Ernst, *Inorg. Chim. Acta* **2003**, *350*, 1.
- [157] H. G. Alt, R. Ernst, I. K. Böhmer, *J. Mol. Catal. A: Chem.* **2003**, *191*, 177.
- [158] H. G. Alt, R. Ernst, *J. Mol. Catal. A: Chem.* **2003**, *195*, 11.
- [159] M. Schilling, C. Görl, H. G. Alt, *J. Appl. Polym. Sci.* **2008**, *109*, 3344.

## 7. Appendices

## Appendix A: Mass spectra

Table A1: Mass spectra of organic compounds

Nr.	Structure	Retention time [s]	Mass spectra [ $m/z$ (%)]
1		740	292( $M^+$ ), 277(24), 172(1), 146(100), 105(30)
2		796	348( $M^+$ ), 333(1), 319(91), 200(1), 174(100), 105(30)
3		804	404( $M^+$ ,0.8), 361(70), 212(1), 202(100), 160(23)
4		792	332( $M^+$ ,24), 317(36), 212(1), 186(100), 146(65), 105(38)
5		834	388( $M^+$ ,4), 359(50), 240(1), 214(100), 174(81), 105(87)

Nr.	Structure	Retention time [s]	Mass spectra [ $m/z$ (%)]
6		836	444( $M^+$ ,28), 429.3(1), 401(76), 242(100), 202(56), 186(22)
7		892	484( $M^+$ ,1), 441(38), 242(100), 200(12), 186(18), 158(13)
9L		416	174( $M^+$ , 8), 109(100), 93(42), 81(25)
15		859	368( $M^+$ ,1) 353(36), 317(100), 222(67), 146(94), 105(50)
16		897	424( $M^+$ ), 395(2), 388(26), 359(100), 306(18), 214(94), 174(64), 105(20)

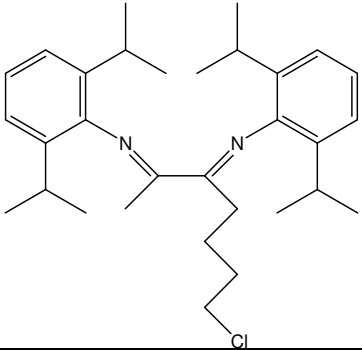
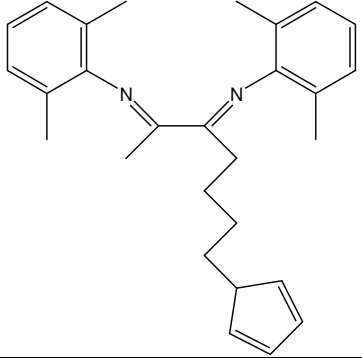
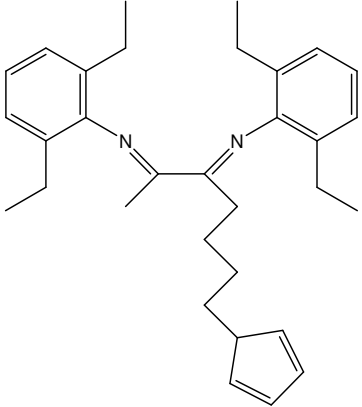
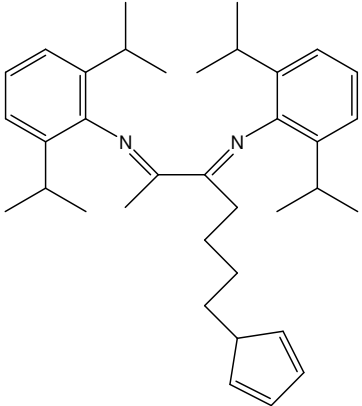
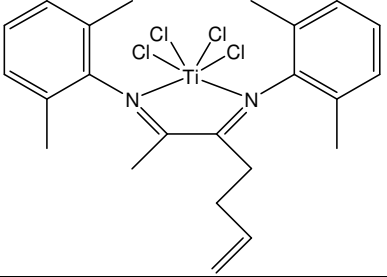
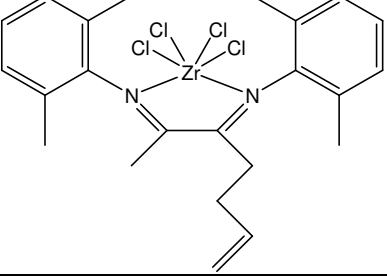
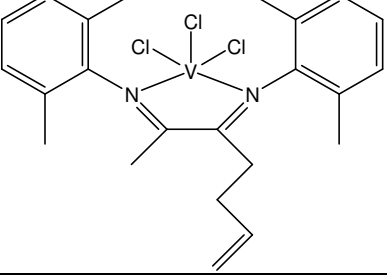
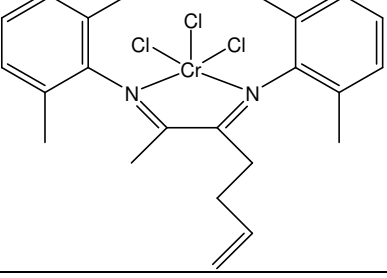
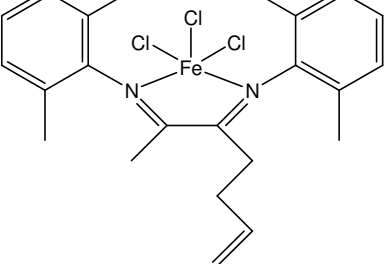
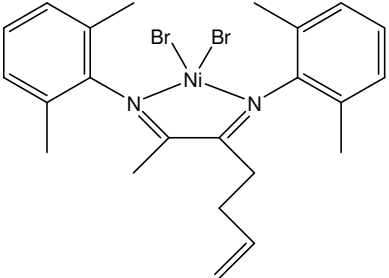
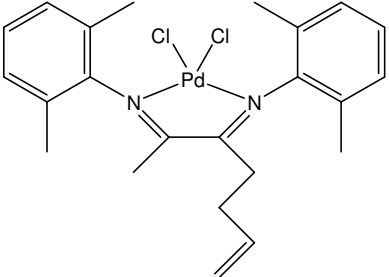
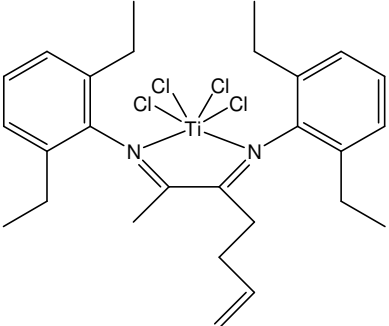
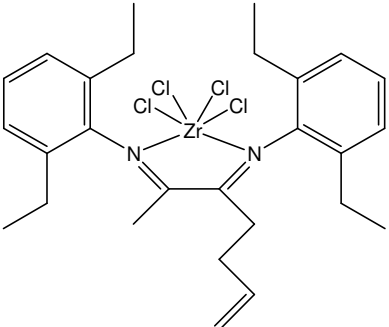
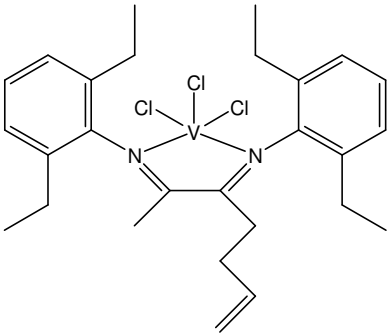
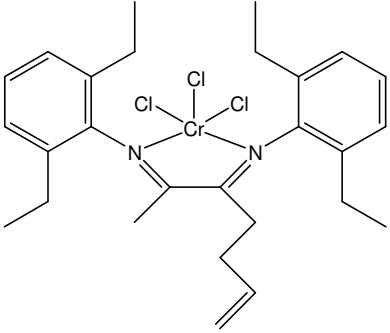
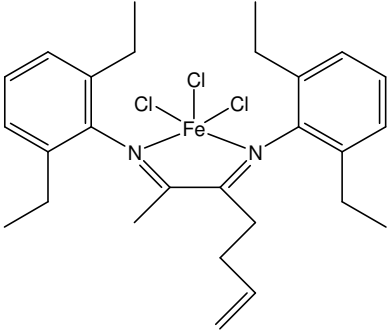
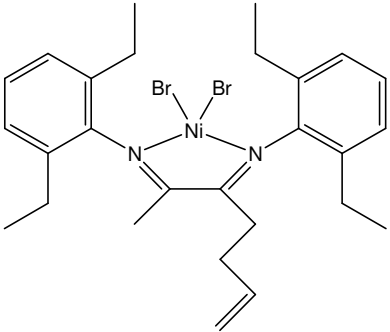
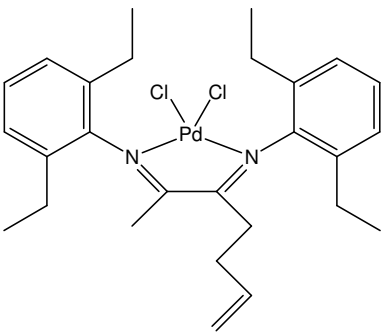
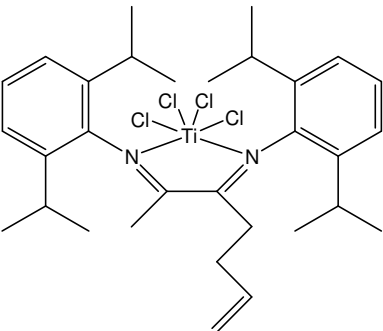
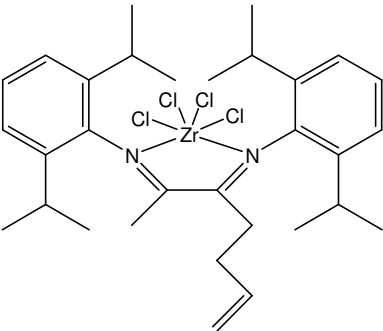
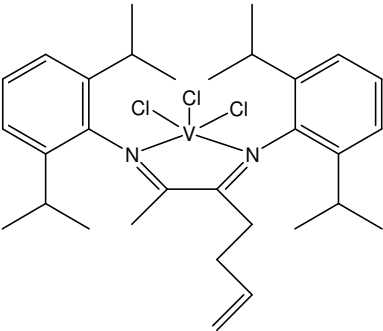
Nr.	Structure	Retention time [s]	Mass spectra [ $m/z$ (%)]
17		896	480( $M^+$ ,1), 444(12), 437(36), 429(9), 401(91), 359(18), 278(87), 242(75), 202(100), 160(26)
18		927	398( $M^+$ ,28), 383(32), 293(8), 252(100), 236(6), 146(64), 105(58)
19		976	454( $M^+$ ,12), 425(100), 349(3), 280(53), 250(4), 174(42), 105(39)
20		974	510( $M^+$ ,15), 467(56), 405(2), 308(100), 266(5), 202(52), 186(9), 160(14)

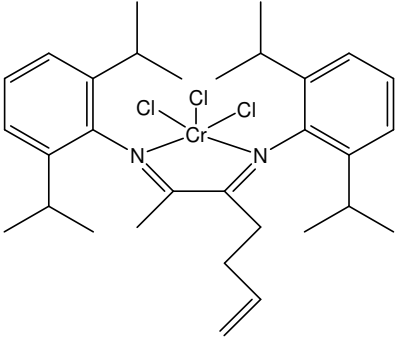
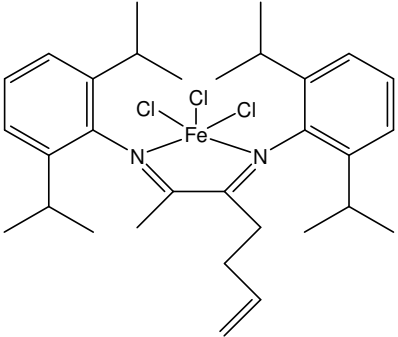
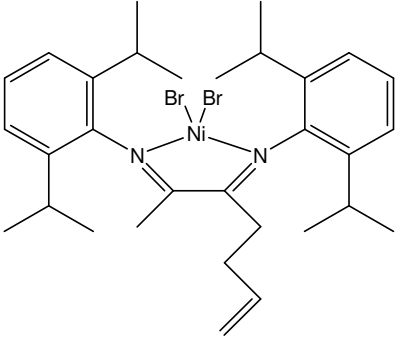
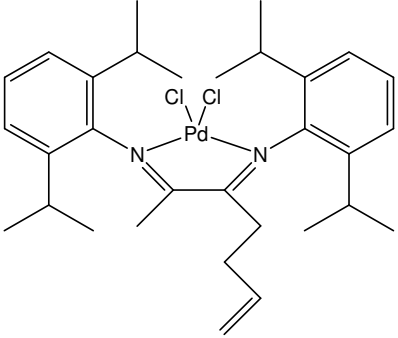
Table A2: Mass spectra of complexes

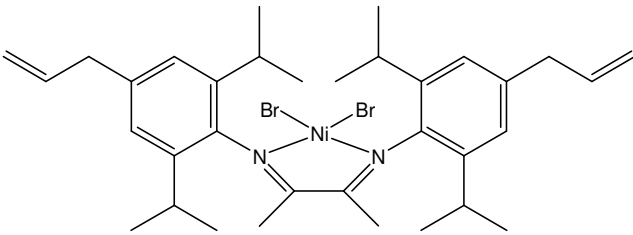
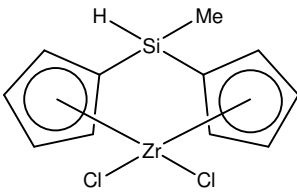
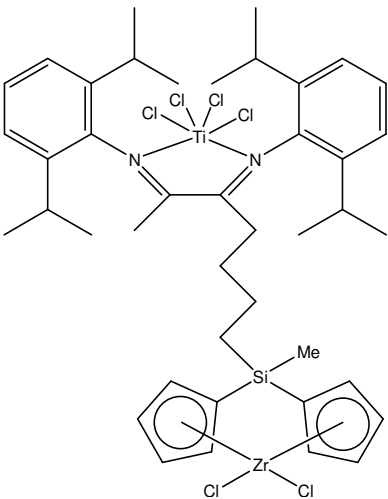
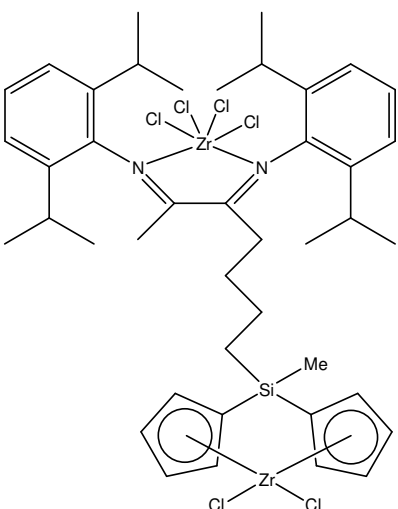
Nr.	Structure	Mass spectra [ $m/z$ (%)]
4a		522( $M^+$ , 10), 508(15), 488(12), 484(8), 449(22), 331(100), 318(58), 186(50), 146(53), 105(50)
4b		562( $M^+$ , 6), 528(4), 455(13), 332(65), 317(48), 229(27), 212(64), 121(100), 106(83)
4c		489( $M^+$ , 15), 472(11), 382(24), 332(47), 317(45), 213(80), 198(100), 157(32), 121(93), 106(40)
4d		488( $M^+$ , 8), 450(8), 359(20), 332(32), 317(30), 157(5), 122(15), 105(21)
4e		493( $M^+$ , 3), 460(2), 451(12), 435(5), 332(91), 317(35), 161(46), 121(95), 106(98), 77(100)

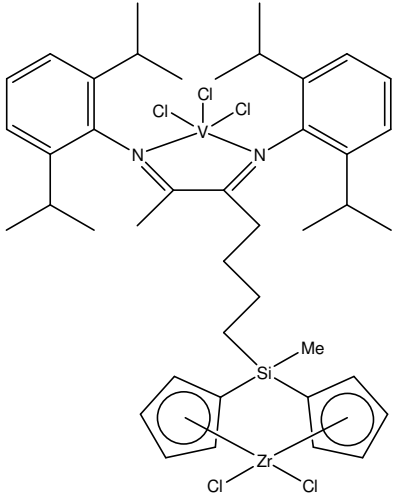
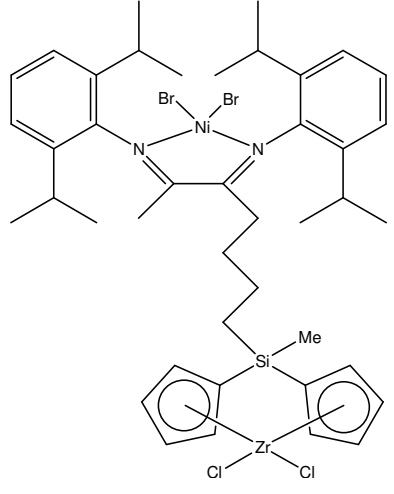
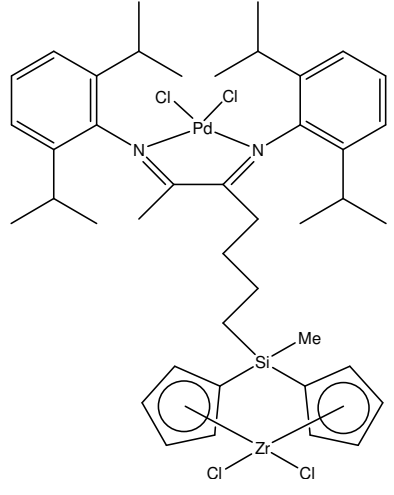
Nr.	Structure	Mass spectra [ $m/z$ (%)]
4f		550( $M^+$ ), 510(10), 470(32), 332(55), 318(34), 186(43), 146(57), 105(100)
4g		507( $M^+$ , 6), 470(5), 332(20), 317(20), 186(48), 146(64), 120(42)
5a		577( $M^+$ , 3), 543(4), 535(7), 495(2), 471(3), 388(100), 359(18), 240(32), 214(13), 190(16), 174(80), 134(65), 105(50)
5b		619( $M^+$ , 28), 589(31), 547, (15), 520(30), 478(10), 388(100), 231(40), 214(24), 174(32)

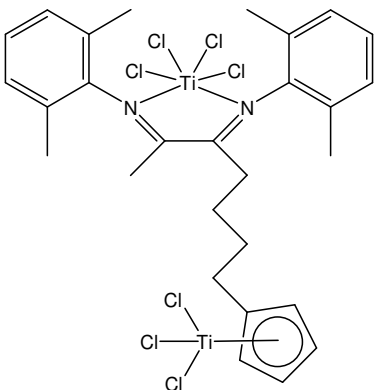
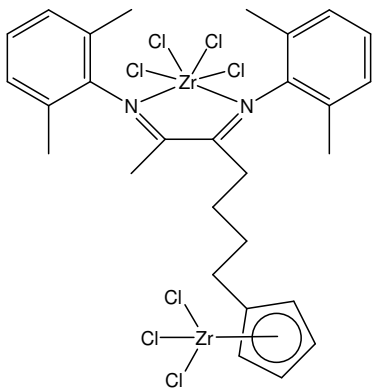
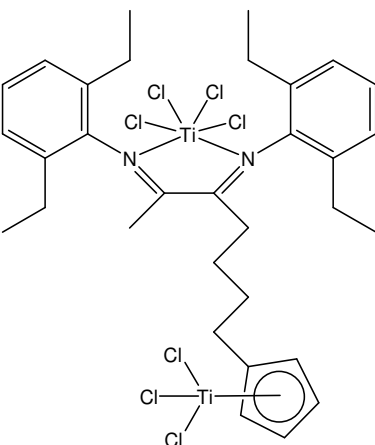
Nr.	Structure	Mass spectra [ $m/z$ (%)]
5c		544( $M^+$ , 2), 502(4), 479(6), 424(14), 402(12), 388(13), 241(42), 215(35), 174(50), 142(16), 134(76), 120(26), 106(28)
5d		545( $M^+$ , 6), 510(12), 504(18), 474(10), 425(25), 401(8), 388(18), 239(16), 213(80), 156(28), 144(100), 120(84)
5e		549( $M^+$ , 15), 535(22), 520(8), 508(15), 428(7), 388(100), 359(28), 240(44), 214(33), 174(65), 162(22), 120(20), 105(97)
5f		606( $M^+$ , 5), 565(12), 527(20), 486(14), 447(20), 388(16), 359(100), 214(92), 174(59), 158(18), 120(30), 105(74)

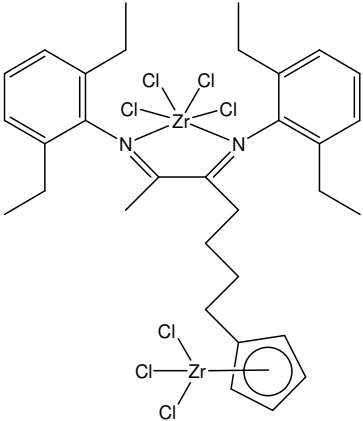
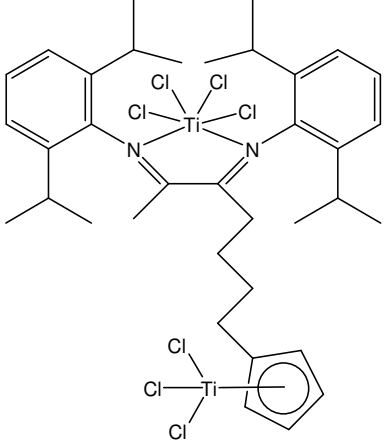
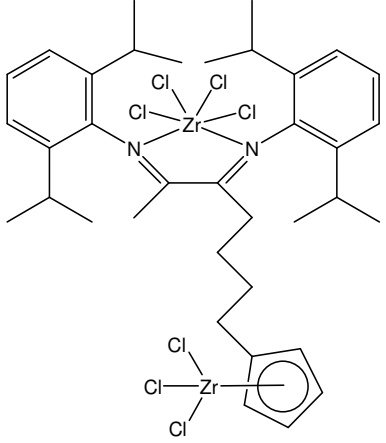
Nr.	Structure	Mass spectra [ $m/z$ (%)]
5g		565( $M^+$ , 2), 529(5), 526(10), 500(7), 388(45), 214(20), 174(6), 105(16)
6a		634( $M^+$ ), 598(13), 563(25), 544(14), 526(36), 519(8), 444(50), 401(40), 357(15), 277(28), 242(64), 202(80), 190(15), 186(100), 117(34)
6b		674( $M^+$ , 8), 643(6), 633(10), 586(3), 502(5), 444(100), 401(33), 242(46), 202(42), 186(37), 176(13)
6c		598( $M^+$ , 7), 567(13), 529(3), 512(10), 494(12), 443(20), 427(27), 352(30), 254(48), 226(72), 177(29), 156(10), 105(58)

Nr.	Structure	Mass spectra [ $m/z$ (%)]
<b>6d</b>		<p>601(<math>M^+</math>, 6), 566(10), 558(15), 515(6), 585(12), 445(10), 425(5), 177(6), 158(35), 120(19)</p>
<b>6e</b>		<p>605(<math>M^+</math>, 5), 570(10), 566(6), 562(12), 519(15), 488(20), 478(10), 444(38), 430(12), 401(13), 352(10), 252(44), 242(95), 201(84), 186(100), 177(93), 162(100), 130(35), 120(63)</p>
<b>6f</b>		<p>662(<math>M^+</math>, 10), 623(18), 619(15), 582(37), 578(52), 545(22), 502(45), 444(77), 399(38), 263(28), 242(73), 216(10), 202(100), 158(35), 120(26)</p>
<b>6g</b>		<p>621(<math>M^+</math>, 7), 587(20), 580(35), 544(32), 463(48), 444(58), 240(45), 202(100), 118(38)</p>

Nr.	Structure	Mass spectra [ $m/z$ (%)]
8		702( $M^+$ ), 643(10), 622(18), 485(9), 441(87), 242(100), 200(28), 186(82), 158(53)
9C		331( $M^+$ , 48), 317(18), 296(78), 259(23), 227(63), 192(15), 174(14), 162(25), 109(21)
10		966( $M^+$ ), 931(8), 922(15), 901(7), 878(25), 792(13), 618(22), 535(14), 444(100), 290(92), 238(38), 202(47), 186(35)
11		1008( $M^+$ ), 977(3), 973(5), 888(3), 848(8), 835(5), 796(3), 775(10), 717(5), 595(6), 531(9), 462(7), 444(25), 369(6), 325(7), 254(24), 202(100), 162(48)

Nr.	Structure	Mass spectra [ $m/z$ (%)]
12		934( $M^+$ ), 899(3), 802(5), 778(6), 774(10), 758(15), 751(16), 707(23), 672(20), 616(18), 509(29), 444(60), 364(42), 293(44), 252(48), 202(100)
13		996( $M^+$ ), 965(3), 937(2), 904(2), 837(2), 778(4), 762(7), 710(12), 512(9), 456(10), 444(53), 427(44), 388(24), 271(52), 202(54), 186(51)
14		955( $M^+$ , 5), 921(13), 884(16), 797(15), 779(20), 624(19), 445(35), 403(37), 467(18), 326(23), 269(34), 244(64), 202(76)

Nr.	Structure	Mass spectra [ $m/z$ (%)]
18a		738( $M^+$ , 7), 706(5), 588(5), 551(6), 486(14), 424(15), 316(10), 216(18), 188(48), 158(37), 146(100), 120(49), 105(93)
18b		827( $M^+$ , 3), 792(9), 721(7), 632(8), 597(4), 484(12), 442(9), 386(5), 345(7), 290(8), 214(16), 146(63), 121(100), 106(97)
19a		796( $M^+$ ), 761(12), 741(2), 710(4), 643(10), 606(6), 455(15), 434(7), 362(9), 308(10), 250(9), 216(15), 174(11), 134(24)

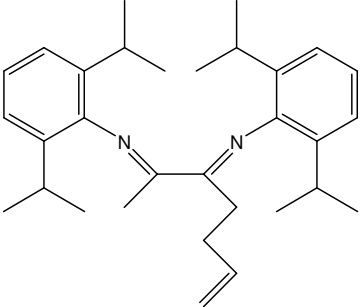
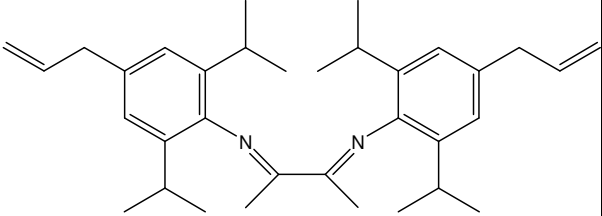
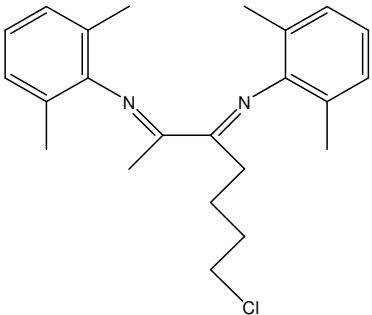
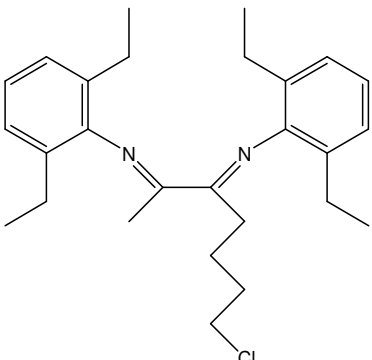
Nr.	Structure	Mass spectra [ $m/z$ (%)]
19b		<p>879(<math>M^+</math>, 4), 845(3), 809(8), 774(5), 763(7), 736(12), 689(4), 469(8), 454(20), 411(6), 359(17), 280(7), 242(10), 174(53), 149(63), 134(100), 120(35)</p>
20a		<p>854(<math>M^+</math>), 825(7), 784(4), 765(3), 748(7), 734(6), 697(7), 512(15), 462(19), 390(20), 244(24), 202(100), 162(100), 144(33), 120(39)</p>
20b		<p>938(<math>M^+</math>, 9), 902(5), 810(8), 739(13), 688(10), 510(7), 407(14), 308(12), 244(17), 202(100), 187(26), 162(55), 132(27), 120(52)</p>

## Appendix B: NMR spectra

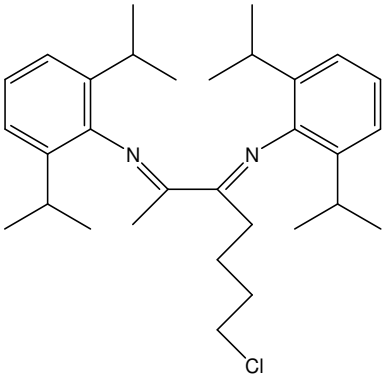
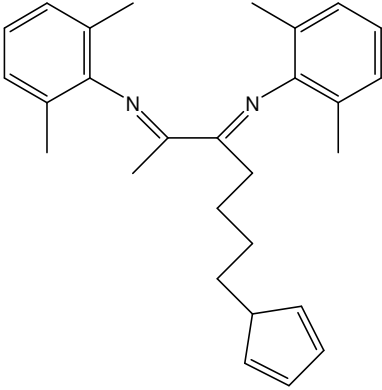
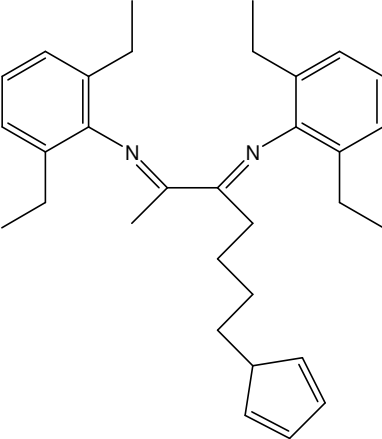
Table B1:  $^1\text{H}$ -NMR and  $^{13}\text{C}$ -NMR spectra of organic compounds

Nr.	Structure	$^1\text{H}$ -NMR [ppm] <sup>a)</sup>	$^{13}\text{C}$ -NMR [ppm] <sup>b)</sup>
1		7.5(d,4H), 6.92(t,2H), 2.02(s,12H), 1.98(s,6H).	Cq: 168, 148.3, 124.6 CH: 127.9, 123.2 CH <sub>2</sub> : - CH <sub>3</sub> : 17.8, 15.8
2		7.1(d,4H), 7.04(t,2H), 2.37(m,8H), 2.05(s,6H), 1.15(dd,12H).	Cq: 168, 147.5, 130.5 CH: 126.1, 123.5 CH <sub>2</sub> : 24.7 CH <sub>3</sub> : 16.2, 13.6
3		7.20(d,4H), 7.13(t,2H), 2.75(sep,4H), 2.10(s,6H), 1.22(d,12H), 1.18(d,12H).	Cq: 168, 146, 135 CH: 123.8, 123, 28.5 CH <sub>2</sub> : - CH <sub>3</sub> : 22.8, 16.8
4		7.06(d,4H), 6.93(t,2H), 5.65(m,1H), 4.89(dd,2H), 2.62(t,2H), 2.25(q,2H), 2.04(s,12H), 2.02(s,3H).	Cq: 171, 167.6, 148.2, 147.9, 126.8 CH: 137.5, 128.1, 123.4 CH <sub>2</sub> : 115.2, 30.9, 28.8 CH <sub>3</sub> : 18.3, 18.1, 16.2
5		7.1(d,4H), 7.02(t,2H), 5.65(m,1H), 4.88(dd,2H), 2.63(t,2H), 2.4(m,8H), 2.25(q,2H), 2.05(s,3H), 1.17(t,12H).	Cq: 170.5, 167.8, 147.4, 146.9, 130.3 CH: 137.5, 126.2, 125.8, 123.5 CH <sub>2</sub> : 115, 30.6, 28.7, 24.7 CH <sub>3</sub> : 16.8, 13.9, 13.4

a) 25 °C in chloroform-*d*<sub>1</sub>, rel. CHCl<sub>3</sub>,  $\delta$  = 7.24 ppmb) 25 °C in chloroform-*d*<sub>1</sub>, rel. CHCl<sub>3</sub>,  $\delta$  = 77.0 ppm

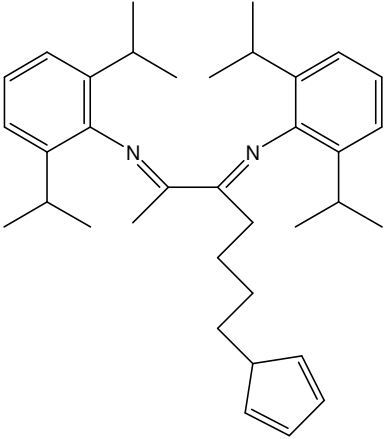
Nr.	Structure	<sup>1</sup> H-NMR [ppm] <sup>a)</sup>	<sup>13</sup> C-NMR [ppm] <sup>b)</sup>
6		7.16(m,6H), 5.7(m,1H), 4.95(dd,2H), 2.75(sep,4H), 2.65(t,2H), 2.27(q,2H), 2.05(s,3H), 1.2(m,24H).	Cq: 170.5, 168, 146.5, 145.5, 135.2, 134.8 CH: 137.5, 123.7, 123, 122.7, 28.5 CH <sub>2</sub> : 115, 30.5, 29 CH <sub>3</sub> : 23.3, 23.2, 22.7, 22.1, 17.1
7		6.95(s,4H), 6.01(m,2H), 5.10(dd,4H), 3.38(d,4H), 2.67(sep,4H), 2.04(s,6H), 1.17(d,12H), 1.14(d,12H)	Cq: 168.4, 144.3, 135 CH: 138, 123.2, 28.5 CH <sub>2</sub> : 115.3, 40.2 CH <sub>3</sub> : 22.8, 16.5
15		7.06(d,4H), 6.94(t,2H), 3.38(t,2H), 2.52(t,2H), 2.04(s,6H), 2.02(s,6H), 2.01(s,3H), 1.64(m,4H).	Cq: 170.8, 167.5, 148.4, 147.8, 124.6 CH: 128.5, 128, 123.3, 123.3 CH <sub>2</sub> : 44.4, 32.7, 28.3, 24.2 CH <sub>3</sub> : 18, 16.3
16		7.1(d,4H), 7.02(t,2H), 3.37(t,2H), 2.52(t,2H), 2.36(m,8H), 2.03(s,3H), 1.65(m,4H), 1.18(t,6H), 1.13(t,6H).	Cq: 170.4, 167.7, 147.4, 146.9, 130.6, 130.3 CH: 126.1, 125.9, 123.6, 123.5 CH <sub>2</sub> : 44.4, 32.8, 28.6, 24.8, 24 CH <sub>3</sub> : 16.7, 13.9, 13.4

a) 25 °C in chloroform-*d*<sub>1</sub>, rel. CHCl<sub>3</sub>, δ = 7.24 ppmb) 25 °C in chloroform-*d*<sub>1</sub>, rel. CHCl<sub>3</sub>, δ = 77.0 ppm

Nr.	Structure	<sup>1</sup> H-NMR [ppm] <sup>a)</sup>	<sup>13</sup> C-NMR [ppm] <sup>b)</sup>
17		7.20-7.14(m,4H), 7.11(t,2H), 3.41(t,2H), 2.72(sep,4H), 2.55(t,2H), 2.07(s,3H), 1.68(m,4H), 1.25(d,6H), 1.22(d,6H), 1.19(d,6H), 1.14(d,6H).	Cq: 170.5, 168, 146.1, 145.6, 135.2, 134.9 CH: 123.8, 123.7, 123, 122.8, 28.5 CH <sub>2</sub> : 44.6, 32.9, 28.9, 23.9 CH <sub>3</sub> : 23.2, 22.7, 22.2, 22.1, 17.1
18		7.05(d,4H), 6.92(t,2H), 6.34(m,1H), 6.18(m,1H), 5.98(m,1H), 5.83(m,1H), 2.86(m,1H), 2.52(t,2H), 2.23(q,2H), 2.03(s,3H), 2.01(s,6H), 2.00(s,6H), 1.46(m,4H).	Cq: 171.5, 167.5, 148.5, 148, 124.7, 124.6 CH: 134.6, 133.6, 132.3, 130.4, 128, 123.2, 44.7 CH <sub>2</sub> : 43.1, 41.2, 29.3, 26.4 CH <sub>3</sub> : 18, 16.3
19		7.10(d,4H), 7.01(t,2H), 6.34(m,1H), 6.18(m,1H), 5.98(m,1H), 5.84(m,1H), 2.86(m,1H), 2.52(t,2H), 2.35(q,8H), 2.22(q,2H), 2.02(s,3H), 1.46(m,4H), 1.16(t,6H), 1.13(t,6H).	Cq: 171.2, 167.7, 147.5, 147, 130.6, 130.4 CH: 134.6, 133.6, 132.3, 130.4, 126.1, 125.8, 123.5, 123.4, 44.7 CH <sub>2</sub> : 43.1, 41.2, 29.4, 26.3, 24.8, 24.7 CH <sub>3</sub> : 16.8, 13.8, 13.4

a) 25 °C in chloroform-*d*<sub>1</sub>, rel. CHCl<sub>3</sub>, δ = 7.24 ppm

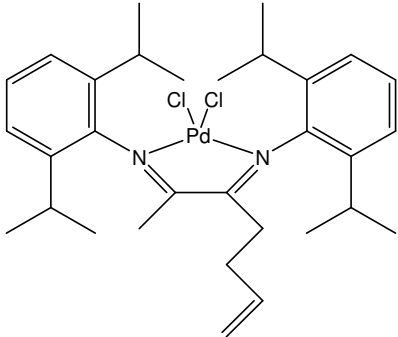
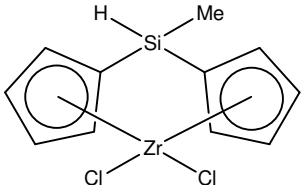
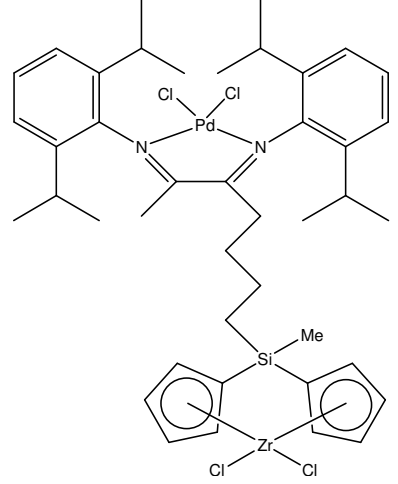
b) 25 °C in chloroform-*d*<sub>1</sub>, rel. CHCl<sub>3</sub>, δ = 77.0 ppm

Nr.	Structure	$^1\text{H-NMR}$ [ppm] <sup>a)</sup>	$^{13}\text{C-NMR}$ [ppm] <sup>b)</sup>
20		7.12(m,6H), 6.33(m,1H), 6.17(m,1H), 6.00(m,1H), 5.85(m,1H), 2.86(m,1H), 2.70(m,4H), 2.53(t,2H), 2.25(q,2H), 2.03(s,3H), 1.48(m,4H), 1.25(d,6H), 1.19(d,6H), 1.15(d,6H), 1.12(d,6H).	Cq: 171.2, 168, 146.2, 145.7, 135.2, 135 CH: 134.5, 133.7, 132.4, 130.4, 123.7, 123.6, 123.0, 122.8, 44.7, 28.4 CH <sub>2</sub> : 43.1, 41.2, 29.6, 26.2 CH <sub>3</sub> : 23.2, 23.1, 22.7, 22.1, 17.2

a) 25 °C in chloroform-*d*<sub>1</sub>, rel. CHCl<sub>3</sub>,  $\delta$  = 7.24 ppm

b) 25 °C in chloroform-*d*<sub>1</sub>, rel. CHCl<sub>3</sub>,  $\delta$  = 77.0 ppm

Table B2:  $^1\text{H-NMR}$  and  $^{13}\text{C-NMR}$  spectra of complexes

Nr.	Structure	$^1\text{H-NMR}$ [ppm] <sup>a)</sup>	$^{13}\text{C-NMR}$ [ppm] <sup>b)</sup>
6g		7.40(t,2H), 7.29(d,2H), 7.27(d,2H), 5.64(m,1H), 5.01(dd,2H), 3.10(sep,2H), 2.98(sep,2H), 2.54(t,2H), 2.21(q,2H), 2.13(s,3H), 1.54(d,6H), 1.47(d,6H), 1.29(d,6H), 1.23(d,6H).	Cq: 178.6, 174, 141.3, 140.9, 139.3 CH: 134.2, 129, 124, 29.5, 29.3 CH <sub>2</sub> : 117.3, 32.6, 31 CH <sub>3</sub> : 24.2, 23.5, 20.8
9C		6.8-6.4(m,4H), 6.1(d,4H), 5.16(s,1H), 0.1(s,3H).	Cq: 108 CH: 130, 128, 115, 114 CH <sub>2</sub> : - CH <sub>3</sub> : -2
14		7.4-7.2(m,6H), 7-6(br,8H), 3.1(m,4H), 2.35(br,t,2H), 2.1(s,3H), 1.7(m,2H), 1.5(m,12H), 1.3(m,12H), 0.9(m,4H), 0.1(s,3H).	n. a.

a) 25 °C in methylene chloride-*d*<sub>2</sub>, rel. CH<sub>2</sub>Cl<sub>2</sub>, δ = 5.32 ppmb) 25 °C in methylene chloride-*d*<sub>2</sub>, rel. CH<sub>2</sub>Cl<sub>2</sub>, δ = 53.5 ppm

## Appendix C: Elemental analysis

Table C1: Elemental analysis data of the complexes 4a-f

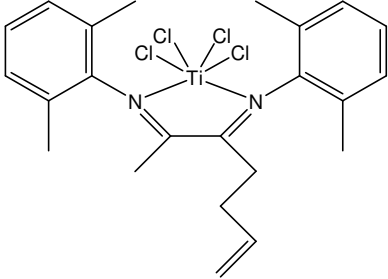
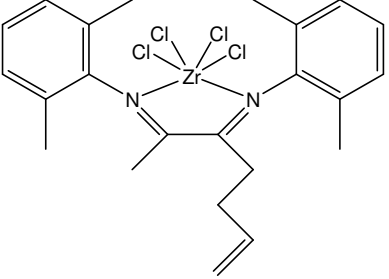
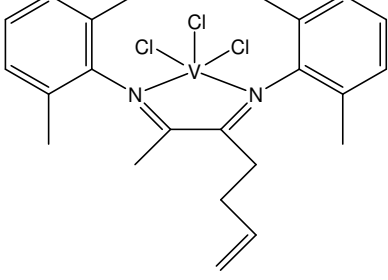
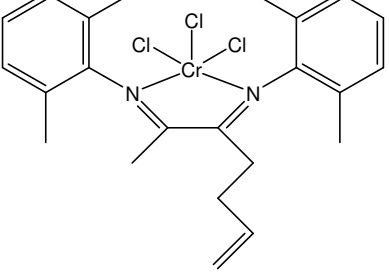
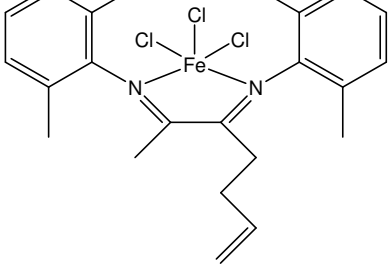
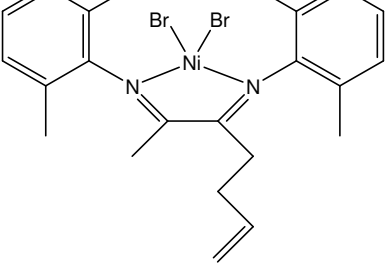
4a	4b
 <p>Measured: C, 53.04 ; H, 5.48 ; N, 4.98 Calculated: C, 52.90; H, 5.40; N, 5.36</p>	 <p>Measured: C, 48.52; H, 5.13; N, 5.04 Calculated: C, 48.85; H, 4.99; N, 4.95</p>
4c	4d
 <p>Measured: C, 55.85; H, 5.65; N, 5.85 Calculated: C, 56.40; H, 5.76; N, 5.72</p>	 <p>Measured: C, 57.17; H, 5.90; N, 5.48 Calculated: C, 56.28; H, 5.75; N, 5.71</p>
4e	4f
 <p>Measured: C, 54.83; H, 5.68; N, 5.20 Calculated: C, 55.84; H, 5.71; N, 5.66</p>	 <p>Measured: C, 48.47; H, 4.97; N, 4.82 Calculated: C, 50.14; H, 5.12; N, 5.08</p>

Table C2: Elemental analysis data of the complexes *4g* and *5a-e*

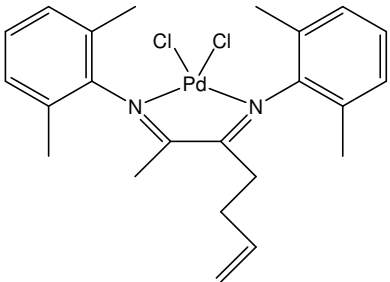
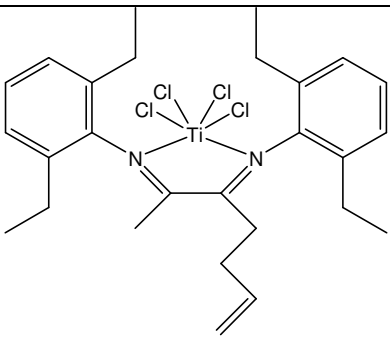
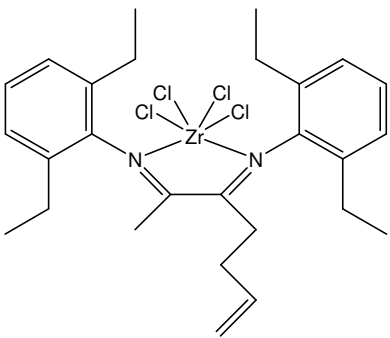
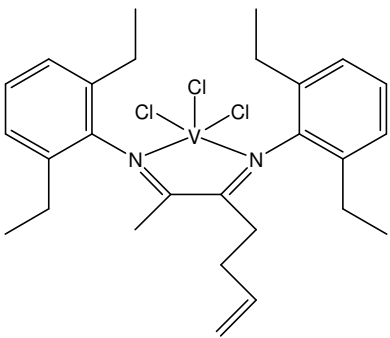
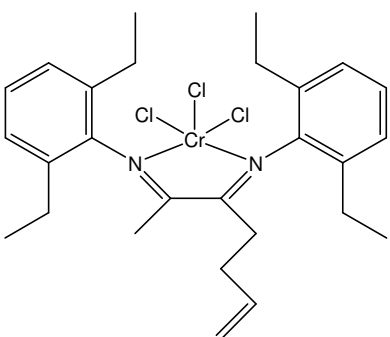
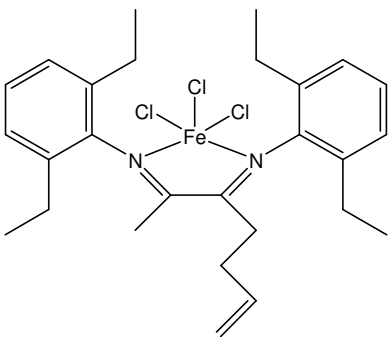
<b>4g</b>	<b>5a</b>
 <p>Measured: C, 52.63; H, 5.64; N, 5.25 Calculated: C, 54.19; H, 5.54; N, 5.49</p>	 <p>Measured: C, 56.39; H, 6.27; N, 4.69 Calculated: C, 56.08; H, 6.27; N, 4.84</p>
<b>5b</b>	<b>5c</b>
 <p>Measured: C, 55.42; H, 6.03; N, 4.37 Calculated: C, 52.17; H, 5.84; N, 4.51</p>	 <p>Measured: C, 62.52; H, 6.37; N, 5.31 Calculated: C, 59.41; H, 6.65; N, 5.13</p>
<b>5d</b>	<b>5e</b>
 <p>Measured: C, 61.45; H, 6.08; N, 5.30 Calculated: C, 59.29; H, 6.63; N, 5.12</p>	 <p>Measured: C, 57.50; H, 6.38; N, 5.02 Calculated: C, 58.88; H, 6.59; N, 5.09</p>

Table C3: Elemental analysis data of the complexes 5f, 5g, and 6a-d

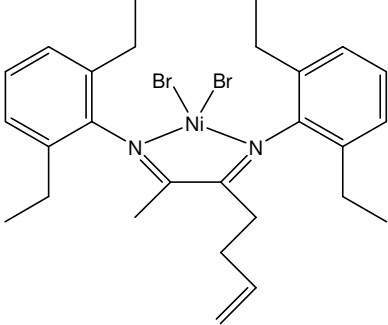
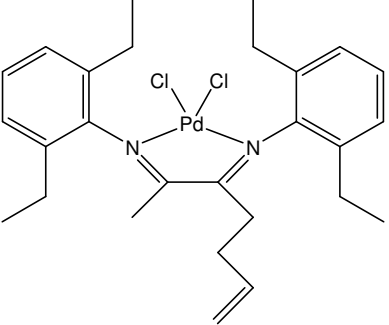
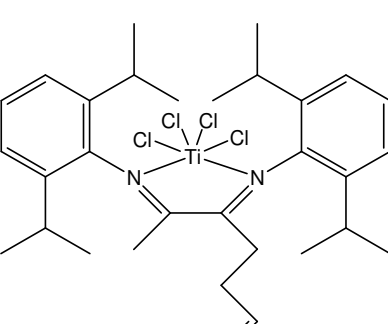
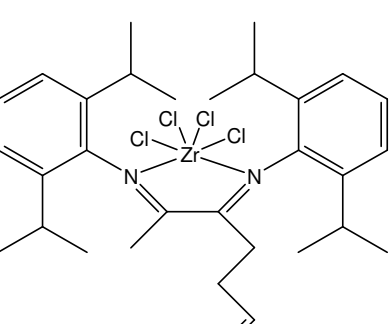
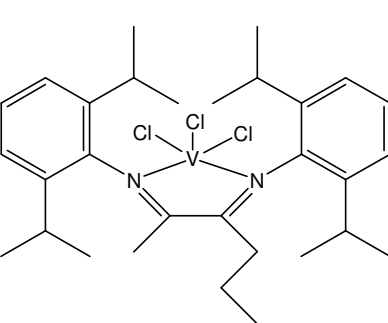
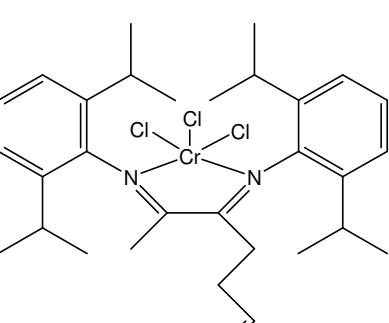
<b>5f</b>	<b>5g</b>
 <p>Measured: C, 56.35; H, 6.18; N, 4.61 Calculated: C, 55.42; H, 5.98; N, 4.61</p>	 <p>Measured: C, 56.84; H, 6.45; N, 4.86 Calculated: C, 57.30; H, 6.41; N, 4.95</p>
<b>6a</b>	<b>6b</b>
 <p>Measured: C, 58.79; H, 6.89; N, 4.15 Calculated: C, 58.69; H, 6.99; N, 4.42</p>	 <p>Measured: C, 55.07; H, 5.27; N, 4.03 Calculated: C, 54.94; H, 6.54; N, 4.13</p>
<b>6c</b>	<b>6d</b>
 <p>Measured: C, 59.83; H, 6.98; N, 4.80 Calculated: C, 61.85; H, 7.37; N, 4.65</p>	 <p>Measured: C, 59.29; H, 7.20; N, 4.45 Calculated: C, 61.74; H, 7.35; N, 4.65</p>

Table C4: Elemental analysis data of the complexes *6e-g*, *9C*, and *8*

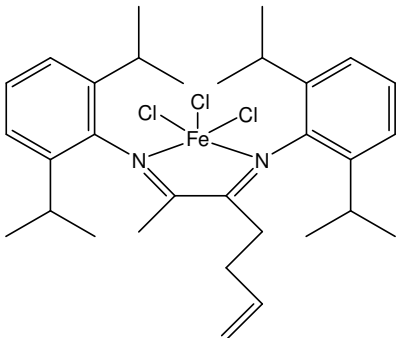
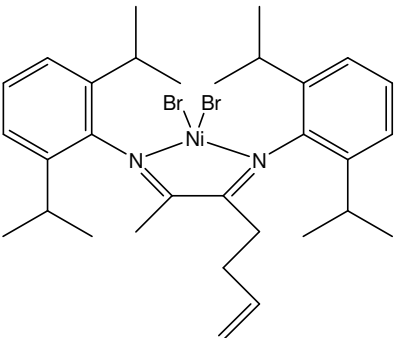
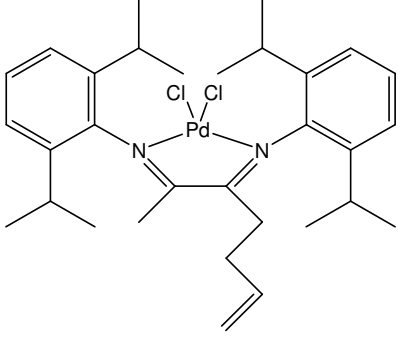
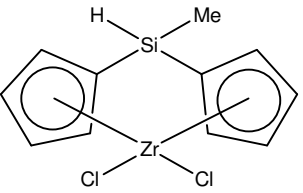
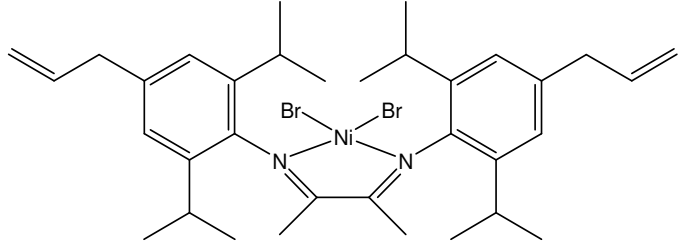
<b>6e</b>	<b>6f</b>
 <p>Measured: C, 59.58; H, 7.29; N, 4.26 Calculated: C, 61.35; H, 7.31; N, 4.62</p>	 <p>Measured: C, 55.63; H, 6.52; N, 4.01 Calculated: C, 56.14; H, 6.69; N, 4.22</p>
<b>6g</b>	<b>9C</b>
 <p>Measured: C, 60.18; H, 7.11; N, 4.38 Calculated: C, 59.86; H, 7.13; N, 4.50</p>	 <p>Measured: C, 38.76; H, 3.53; N, - Calculated: C, 39.51; H, 3.62; N, -</p>
<b>8</b>	
 <p>Measured: C, 57.41; H, 6.53; N, 3.96 Calculated: C, 58.07; H, 6.88; N, 3.98</p>	

Table C5: Elemental analysis data of the complexes 10-13

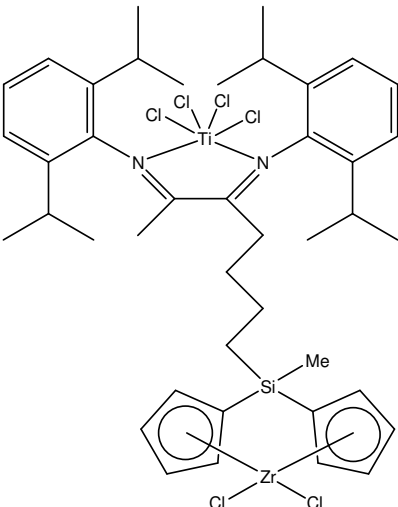
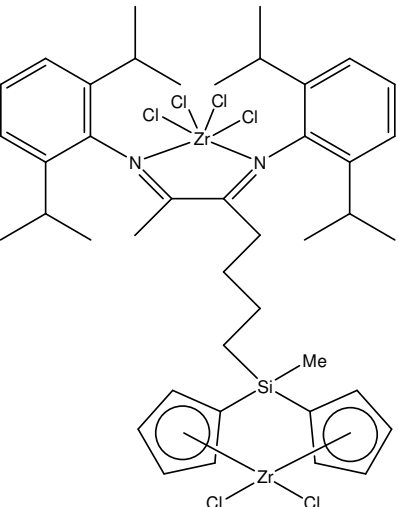
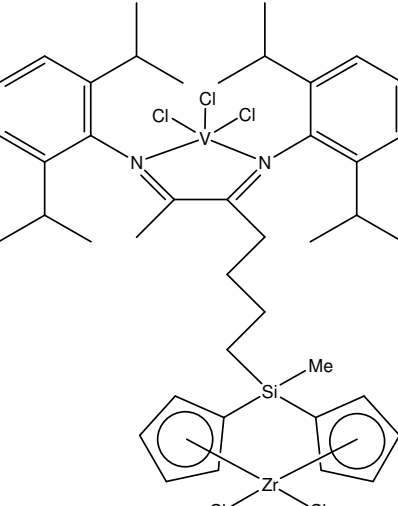
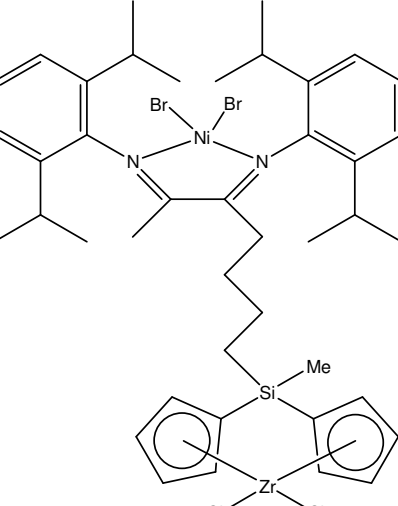
10	11
 <p>Measured: C, 49.15; H, 6.15; N, 2.92 Calculated: C, 52.07; H, 5.83; N, 2.89</p>	 <p>Measured: C, 48.15; H, 5.88; N, 2.80 Calculated: C, 49.84; H, 5.58; N, 2.77</p>
12	13
 <p>Measured: C, 53.16; H, 6.47; N, 2.95 Calculated: C, 53.87; H, 6.03; N, 2.99</p>	 <p>Measured: C, 49.97; H, 5.97; N, 2.58 Calculated: C, 50.57; H, 5.66; N, 2.81</p>

Table C6: Elemental analysis data of the complexes *14*, *18a*, *18b*, *19a*

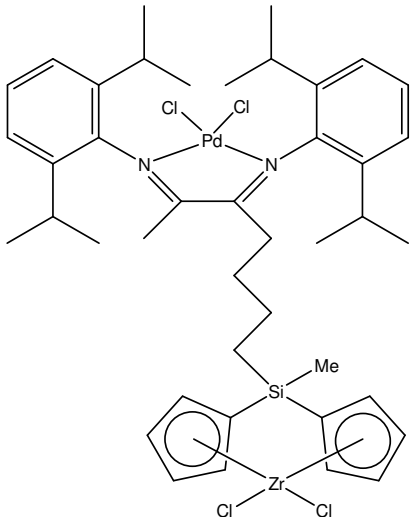
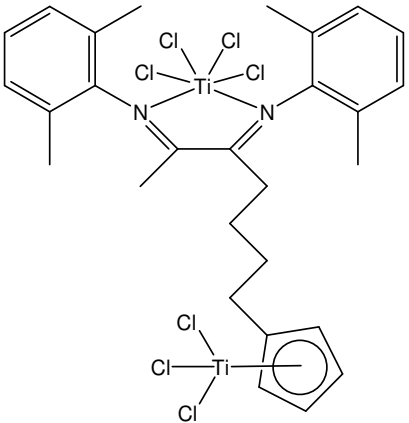
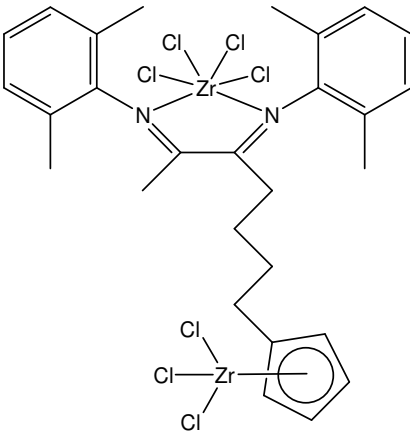
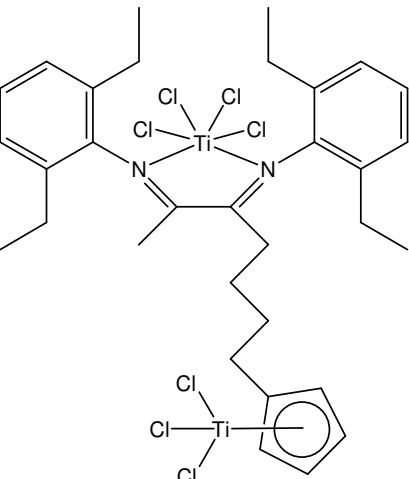
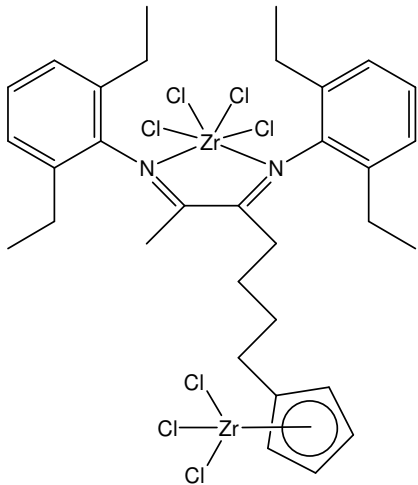
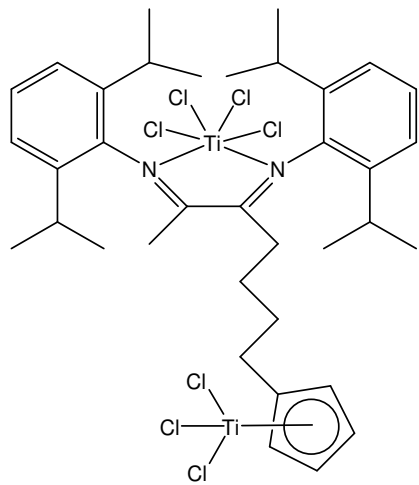
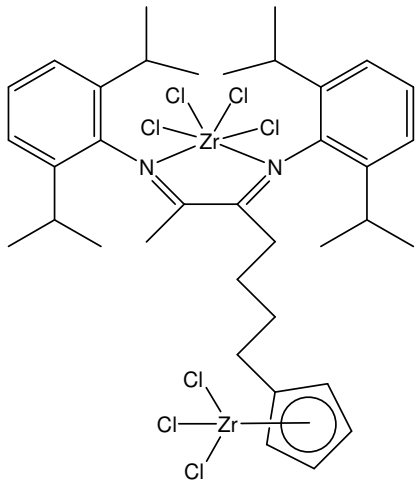
<b>14</b>	<b>18a</b>
 <p>Measured: C, 51.50; H, 6.29; N, 3.16 Calculated: C, 52.74; H, 5.90; N, 2.93</p>	 <p>Measured: C, 45.39; H, 4.47; N, 4.10 Calculated: C, 45.36; H, 4.49; N, 3.78</p>
<b>18b</b>	<b>19a</b>
 <p>Measured: C, 40.45; H, 4.01; N, 3.63 Calculated: C, 40.61; H, 4.02; N, 3.38</p>	 <p>Measured: C, 46.95; H, 5.01; N, 3.61 Calculated: C, 48.19; H, 5.18; N, 3.51</p>

Table C7: Elemental analysis data of the complexes *19b*, *20a*, and *20b*

<b>19b</b>	<b>20a</b>
 <p data-bbox="240 875 687 904">Measured: C, 42.53; H, 5.13; N, 3.16</p> <p data-bbox="240 943 687 972">Calculated: C, 43.46; H, 4.67; N, 3.17</p>	 <p data-bbox="810 875 1257 904">Measured: C, 48.54; H, 6.07; N, 3.35</p> <p data-bbox="810 943 1257 972">Calculated: C, 50.65; H, 5.79; N, 3.28</p>
<b>20b</b>	
 <p data-bbox="528 1659 975 1688">Measured: C, 44.31; H, 5.28; N, 2.76</p> <p data-bbox="528 1727 975 1756">Calculated: C, 45.98; H, 5.25; N, 2.98</p>	

**Appendix D: Crystal structure analysis****Table D1: Crystal data and structure refinement of compound 6.**

Empirical formula	C <sub>31</sub> H <sub>44</sub> N <sub>2</sub>	
Formula weight	444.68	
Temperature	133(2) K	
Wavelength	0.71073 Å	
Crystal system	Orthorhombic	
Space group	P2(1)2(1)2	
Unit cell dimensions	a = 19.014(4) Å	α = 90°
	b = 23.571(5) Å	β = 90°
	c = 6.2853(13) Å	γ = 90°
Volume	2816.9(10) Å <sup>3</sup>	
Z	4	
Density (calculated)	1.049 Mg/m <sup>3</sup>	
Absorption coefficient	0.06 mm <sup>-1</sup>	
F(000)	976	
Crystal size	0.63 x 0.38 x 0.29 mm <sup>3</sup>	
θ range for data collection	2.1 to 25.6°	
Index ranges	-19<h<23, -28<k<24, -7<l<7	
Reflections collected	13013	
Independent reflections	5198 [R(int) = 0.0304]	
Completeness to θ = 25.6°	99.3 %	
Absorption correction	None	
Refinement method	Full-matrix least-squares on F <sup>2</sup>	
Data / restraints / parameters	5198 / 0 / 299	
Goodness-of-fit on F <sup>2</sup>	0.97	
Final R indices [I > 2σ (I)]	R1 = 0.0447, wR2 = 0.1054	
R indices (all data)	R1 = 0.0582, wR2 = 0.1103	
Largest diff. peak and hole	0.36 and -0.21 e.Å <sup>-3</sup>	

**Table D2: Crystal data and structure refinement of complex 6g.**

Empirical formula	C <sub>32</sub> H <sub>46</sub> Cl <sub>4</sub> N <sub>2</sub> Pd	
Formula weight	706.91	
Temperature	133(2) K	
Wavelength	0.71069 Å	
Crystal system	Triclinic	
Space group	<i>P</i> -1	
Unit cell dimensions	a = 8.8350(6) Å	α = 80.81°
	b = 10.5840(8) Å	β = 84.76°
	c = 18.9310(13) Å	γ = 86.89°
Volume	1738.8(2) Å <sup>3</sup>	
Z	2	
Density (calculated)	1.350 Mg/m <sup>3</sup>	
Absorption coefficient	0.86 mm <sup>-1</sup>	
F(000)	732	
Crystal size	0.50 x 0.28 x 0.14 mm <sup>3</sup>	
θ range for data collection	2.0 to 25.7°	
Index ranges	-10<h<10, -12<k<12, -23<l<23	
Reflections collected	23280	
Independent reflections	6549 [R(int) = 0.043]	
Completeness to θ = 25.7°	98.9 %	
Absorption correction	None	
Refinement method	Full-matrix least-squares on F <sup>2</sup>	
Data / restraints / parameters	6549 / 0 / 390	
Goodness-of-fit on F <sup>2</sup>	0.94	
Final R indices [I > 2σ (I)]	R1 = 0.0358, wR2 = 0.0859	
R indices (all data)	R1 = 0.0480, wR2 = 0.0886	
Largest diff. peak and hole	1.18 and -0.97 e.Å <sup>-3</sup>	

**Table D3: Crystal data and structure refinement for complex 8.**

Empirical formula	$C_{68} H_{96} Br_4 N_4 Ni_2$
Formula weight	1406.55
Temperature	133(2) K
Wavelength	0.71069 Å
Crystal system	Triclinic
Space group	$P\bar{1}$
Unit cell dimensions	$a = 13.0160(7)$ Å $\alpha = 94.41^\circ$ $b = 15.7980(9)$ Å $\beta = 108.59^\circ$ $c = 18.3480(11)$ Å $\gamma = 97.45^\circ$
Volume	$3517.6(3)$ Å <sup>3</sup>
Z	2
Density (calculated)	1.328 Mg/m <sup>3</sup>
Absorption coefficient	2.846 mm <sup>-1</sup>
F(000)	1456
Crystal size	0.95 x 0.27 x 0.14 mm <sup>3</sup>
$\theta$ range for data collection	1.7 to 25.7°
Index ranges	-15 < h < 14, -19 < k < 19, 0 < l < 22
Reflections collected	13251
Independent reflections	7408 [R(int) = 0]
Completeness to $\theta = 25.7^\circ$	98.6 %
Absorption correction	Numerical
Refinement method	Full-matrix least-squares on F <sup>2</sup>
Data / restraints / parameters	7408 / 0 / 703
Goodness-of-fit on F <sup>2</sup>	1.049
Final R indices [I > 2 $\sigma$ (I)]	R1 = 0.0607, wR2 = 0.1327
R indices (all data)	R1 = 0.1134, wR2 = 0.1415
Largest diff. peak and hole	1.38 and -1.05 e.Å <sup>-3</sup>

## **Erklärung**

Hiermit erkläre ich, dass ich die Arbeit selbständig verfasst und keine anderen als die angegebenen Quellen und Hilfsmittel benutzt habe.

Ferner erkläre ich, dass ich nicht andersweitig mit oder ohne Erfolg versucht habe, eine Dissertation zu diesem oder gleichartigem Thema einzureichen oder mich der Doktorprüfung zu unterziehen.

Bayreuth, den 18. Februar 2009

Haif Alshammari